UNIVERSITY OF
KWAZULU-NATAL

HYPERSPHERES OF STATIC CHARGED FLUIDS IN STANDARD AND MODIFIED GRAVITY

LUSHEN MOODLY

Hyperspheres of Static Charged Fluids in Standard and Modified Gravity by

LUSHEN MOODLY

Submitted in fulfilment of the
requirements for the degree of
Master of Science
in the
School of Mathematical Sciences
University of KwaZulu-Natal

As the candidate's supervisor, I have approved this dissertation for submission

Prof S Hansraj	[redacted]	10 December 2019
Name	Signature	Date

Dedication

To my late grandmother

Mrs Nagamah Gounden (1934-2019)

with eternal love and appreciation.

Preface and Declaration

The research done in this dissertation is original work and has not been previously submitted to any other institution. Where reference to the work of other researchers was made, it has been duly acknowledged.

This project was completed under the supervision of Professor S. Hansraj.

Lushen Moodly

Acknowledgements

I offer my sincere thanks and appreciation to the following people and organisations for their contribution in helping me see this dissertation through to a purposeful end:

- My supervisor Professor Sudan Hansraj for his expert guidance, continuous support and unwavering assistance. You have inspired me with your passion and expertise in the field of relativity and mathematics. Thank you for your patience and understanding, you have helped pave the way for me as a young researcher. The knowledge you have imparted to me is invaluable and I will be eternally grateful.

- The staff at the School of Mathematics at the University of KwaZulu–Natal for their assistance and encouragement as well as the wonderful research opportunites and facilities I was provided with.

- The National Research Foundation (NRF) for the award of a masters bursary.

- My family and friends for their endless support and motivation throughout the duration of my studies.

Abstract

In this thesis we study the Einstein–Maxwell field equations for charged isotropic spheres initially with the imposition of the geometrical restriction of conformal flatness. We conduct a thorough analysis of these equations in order to verify the existence of conformally flat charged stars. We then prescribe well known metric potentials and examine the resulting dynamical quantities for physical viability. Thereafter, we abandon the conformal flatness case and examine the Karmarkar condition for spacetimes of embedding class 1. We use this technique to generate new exact solutions for a charged star and a cosmological fluid. The charged star solution was subject to extensive physical analysis and was shown to be comparable to a realistic star according to observational data. Finally, we consider 5–dimensional spacetimes in Einstein–Gauss–Bonnet (EGB) theory. We abandon charge and impose a strange star equation of state with anisotropic stresses. New exact models have been generated and compared with the 5–dimensional Einstein counterpart. We make use of the data obtained from the X–ray pulsar LMC X–4 to determine the value of the constants in our model and display the necessary qualitative features of such astrophysical objects.

Contents

Chapter 1

Introduction

General relativity, a modern theory of gravity proposed by Einstein in 1915, serves as a generalisation of special relativity which was proposed in 1905. This began when Einstein determined that the laws of physics are the same in all inertial reference frames and that the speed of light is constant in these frames. He subsequently spent ten years developing his theory by trying to include acceleration in his equations. By doing so he found that the three dimensions of space and one dimension of time were interwoven into a single four dimensional continuum known as spacetime. This culminated in him redefining gravity as a distortion in spacetime caused by massive objects as opposed to a force. This theory generalises the classical Newtonian approach, and has been confirmed by various tests over the years. Some predictions such as time dilatation were confirmed experimentally in the late 1930's. In addition gravitational lensing which was also determined experimentally, is now a tool used by astronomers to study what appeared to be hidden stars and galaxies that are obscured by other massive objects. Another exciting prediction of general relativity was gravitational waves which are ripples in spacetime caused by violent events in the universe. The Laser Interferometer Gravitational Wave Observatory (LIGO) detected the first gravitational wave in 2015 [1]. These experiments, among others,

served as strong support of the theory of general relativity.

This theory was also applied in many areas of cosmology. Although initially a Newtonian approach was favoured, the understanding of certain astronomical phenomena required the inclusion of relativistic effects. Einstein developed the field equations which were used to represent the behaviour of gravitational fields in response to matter or spacetime. Einstein's field equations in four dimensions are a system of ten non–linear partial differential equations in general. They can be modified to include charged fluids which results in the Einstein–Maxwell field equations. Because these are non–linear differential equations, it is quite difficult to obtain exact solutions. These exact solutions are important to develop astrophysical models and to test their physical relevance. A selection of important exact solutions that have been found are listed hereunder.

1. The Schwarzschild exterior solution [2] was one of the first exact solutions to the Einstein field equations. It describes the gravitational field outside a spherical, uncharged, static body. It is also a good model for the gravitational field of a slowly rotating body such as the planets or our Sun. The Jebsen–Birkhoff theorem [3] asserts that the Schwarzschild exterior solution is the unique vacuum metric for static and non–static spheres.

2. The Schwarzschild interior solution [4] describes the interior gravitational field of static spheres with constant density. These are called incompressible fluids. At the boundary of a star, the interior and exterior solutions match. It is a reasonable model for compact stars although it does suffer some pathologies like an infinite sound speed.

3. The Reissner–Nordstrom solution [5, 6] is a static solution to the Einstein–Maxwell field equations, which is applied in the exterior gravitational field of a

spherically symmetric, static, charged body. In the absence of charge, the Reissner–Nordstrom solution reduces to the Schwarzschild exterior solution.

4. The Vaidya shining star solution [7] models the exterior gravitational field of a radiating neutral sphere.

5. The Kerr solution [8] models the exterior gravitational field of a rotating body. If there is no angular momentum then the Kerr solution reduces to the Schwarzschild exterior solution. Introducing charge generates the Kerr–Newman exact solutions. However, we are yet to find an interior solution that will smoothly transition to the Kerr solution, so this is still an open problem since 1963.

In this work we endeavour to find new solutions, specifically for the case of a conformally flat spacetime. Conformal flatness is characterised by the vanishing of the Weyl tensor which imposes a restriction on the master field equation. There have been some conformally flat solutions reported recently by Banerjee and Santos [9] and Shi–Chang [10] but they do not satisfy the energy conditions. The work done by Xingxiang [11] also fails to satisfy the energy conditions but is otherwise physically reasonable. We aim to find unique solutions that are physically reasonable, in a systematic manner. Furthermore, we study spacetimes of embedding class 1 as well as anisotropic distributions in the context of the Einstein–Gauss–Bonnet higher curvature theory.

- In chapter 2 we discuss the mathematical framework for general relativity and derive the Einstein–Maxwell field equations. A brief account of Einstein–Gauss–Bonnet theory is considered that is relevant to later work.
- In chapter 3 we report on known models of conformally flat charged fluid spheres and we discover new exact models and analyse these for physical ap-

plicability.

- In chapter 4 we analyse charged stars of embedding class 1 and discover new models which are physically admissible.

- In chapter 5 we find new exact solutions in 5–D Einstein–Gauss–Bonnet with anisotropic stresses.

- Finally, in chapter 6 we make some concluding remarks on the achievements of this work.

Chapter 2

Mathematical Preliminaries

2.1 Introduction

In this chapter we consider the mathematical framework that is needed for our study, which includes aspects of differential geometry and surface theory. We nominate the spherically symmetric line element or the metric tensor and we then compute the required Christoffel symbols, Riemann tensor, Ricci tensor, Ricci scalar and Einstein tensor. We further calculate the Weyl conformal tensor components which are useful to determine whether solutions are conformally flat or not. Note that being tensorial, the Einstein field equations will remain the same in any coordinate system. We also list the Einstein–Maxwell field equations, and perform the necessary transformations to them in order to facilitate integration. Finally, we list a set of conditions against which models may be tested for physical reasonableness.

2.2 Differential geometry

Spacetime M is taken to be a 4–dimensional differentiable manifold endowed with a symmetric, nonsingular metric field $\mathbf{g}$ of signature ($-$ + + +) in four dimensions. As the metric tensor field is indefinite the manifold is pseudo–Riemannian. Points in M are labeled by the real coordinates $(x^a) = (x^0, x^1, x^2, x^3)$ where x^0 is timelike and x^1, x^2, x^3 are spacelike. The line element given by

$$ds^2 = g_{ab}dx^a dx^b \tag{2.1}$$

defines the invariant distance between neighbouring points of a curve in M. The fundamental theorem of Riemannian geometry guarantees the existence of a unique symmetric connection that preserves inner products under parallel transport. This is called the metric connection $\mathbf{\Gamma}$ or the Christoffel symbol of the second kind. The coefficients of the metric connection $\mathbf{\Gamma}$ are given by the Levi–Civita symbol

$$\Gamma^a{}_{bc} = \frac{1}{2}g^{ad}\left(g_{cd,b} + g_{db,c} - g_{bc,d}\right) \tag{2.2}$$

where commas denote partial differentiation. The quantity

$$R^a{}_{bcd} = \Gamma^a{}_{bd,c} - \Gamma^a{}_{bc,d} + \Gamma^a{}_{ec}\Gamma^e{}_{bd} - \Gamma^a{}_{ed}\Gamma^e{}_{bc} \tag{2.3}$$

is a $(1,3)$ tensor field and is called the Riemann tensor or the curvature tensor. Contracting the Riemann tensor (2.3)

$$\begin{aligned} R_{ab} &= R^c{}_{acb} \\ &= \Gamma^d{}_{ab,d} - \Gamma^d{}_{ad,b} + \Gamma^e{}_{ab}\Gamma^d{}_{ed} - \Gamma^e{}_{ad}\Gamma^d{}_{eb} \end{aligned} \tag{2.4}$$

generates the Ricci tensor R_{ab} . The Riemann tensor indicates the deviation from flatness and the vanishing of this tensor is indicative of a flat spacetime. On con-

tracting the Ricci tensor (2.4) we obtain

$$\begin{aligned} R &= g^{ab}R_{ab} \\ &= R^{a}{}_{a} \end{aligned} \tag{2.5}$$

where R is the Ricci scalar. The Einstein tensor $\mathbf{G}$ is constructed in terms of the Ricci tensor (2.4) and the Ricci scalar (2.5) as follows:

$$G^{ab} = R^{ab} - \frac{1}{2}Rg^{ab}. \tag{2.6}$$

The Einstein tensor has zero divergence,

$$G^{ab}{}_{;b} = 0 \tag{2.7}$$

a property referred to in the literature as the contracted Bianchi identity. As a consequence, the covariant divergence of energy momentum also vanishes and this provides a law of conservation of energy.

An arbitrary rank two tensor can be decomposed into its symmetric and anti–symmetric parts. Similarly the Riemann tensor (2.3) decomposes into the Weyl tensor (or conformal curvature tensor) and parts which involve the Ricci tensor and the curvature scalar. This decomposition is given by

$$\begin{aligned} R_{abcd} &= C_{abcd} - \frac{1}{6}R\left(g_{ac}g_{bd} - g_{ad}g_{bc}\right) \\ &+ \frac{1}{2}\left(g_{ac}R_{bd} - g_{bc}R_{ad} + g_{bd}R_{ac} - g_{ad}R_{bc}\right) \end{aligned} \tag{2.8}$$

where $\mathbf{C}$ is the Weyl tensor. The Weyl tensor is trace-free,

$$C^{ab}{}_{ad} = 0$$

and inherits all the symmetry properties of the curvature tensor (2.3). The vanishing of the Weyl tensor is an indication of conformal flatness. This suggests that the spacetime can be cast into a trivial functional scaling of the flat Minkowski spacetime. In addition, the Weyl tensor may be decomposed into an electric and magnetic part which is relevant to the study of gravitational waves.

The matter content is specified by the energy–momentum tensor $\mathbf{T}$ which is given by

$$T_{ab} = (\rho + p)u_a u_b + p g_{ab} + q_a u_b + q_b u_a + \pi_{ab} \tag{2.9}$$

for neutral matter. In the above, ρ is the energy density, p is the isotropic pressure, q_a is the heat flow vector and π_{ab} represents the stress tensor. These quantities are measured relative to a fluid four–velocity $\mathbf{u}$ ($u^a u_a = -1$). The heat flow vector and stress tensor satisfy the conditions $q^a u_a = 0$ and $\pi^{ab} u_b = 0$.

In the simpler case of a perfect fluid, which is the case for most cosmological and astrophysical models, the energy–momentum tensor (2.9) has the form

$$T_{ab} = (\mu + p)u_a u_b + p g_{ab}. \tag{2.10}$$

Einstein postulated that the equivalence of matter and geometry is expressible as the Einstein field equations, which are a system of up to 10 nonlinear partial differential equations

$$G_{ab} = \kappa T_{ab}. \tag{2.11}$$

We utilise geometric units where the speed of light and the coupling constant $\kappa = \frac{8\pi G}{c^4}$ are taken to be unity. Note that the field equations may be independently derived using the Euler–Lagrange dynamical equations.

2.3 Spacetime geometry

It is reasonable to assume that the interior of a spherically symmetric charged star is described by the line element

$$ds^2 = -e^{2\nu(r)}dt^2 + e^{2\lambda(r)}dr^2 + r^2\left(d\theta^2 + \sin^2\theta d\phi^2\right) \tag{2.12}$$

where the functions $\nu(r)$ and $\lambda(r)$ are gravitational potentials. Additionally we consider a co-moving fluid four–velocity field $u^a = e^{-\nu}\delta_0{}^a$.

For the line element (2.12), the Christoffel symbol components are given by

$$\Gamma^0_{01} = \nu' \qquad \Gamma^1_{00} = \nu' e^{2(\nu-\lambda)}$$

$$\Gamma^1_{11} = \lambda' \qquad \Gamma^2_{12} = \frac{1}{r}$$

$$\Gamma^1_{22} = -re^{-2\lambda} \qquad \Gamma^1_{33} = -re^{-2\lambda}\sin^2\theta$$

$$\Gamma^2_{33} = -\sin\theta\cos\theta \qquad \Gamma^3_{23} = \cot\theta$$

$$\Gamma^3_{13} = \frac{1}{r}\ .$$

From (2.4), the Ricci tensor components evaluate to

$$R_{00} = e^{2(\nu-\lambda)}\left(\nu'' + \nu'^2 - \nu'\lambda' + \frac{2\nu'}{r}\right) \tag{2.13}$$

$$R_{11} = -\left(\nu'' + \nu'^2 - \nu'\lambda' - \frac{2\lambda'}{r}\right) \tag{2.14}$$

$$R_{22} = 1 - e^{-2\lambda}\left(1 + r\left(\nu' - \lambda'\right)\right) \tag{2.15}$$

$$R_{33} = \sin^2\theta(1 - e^{-2\lambda}(1 + r(\nu' - \lambda'))). \tag{2.16}$$

Consequently, the Ricci scalar is calculated as

$$R = 2\left(\frac{1}{r^2} - e^{-2\lambda}\left(\nu'' + \nu'^2 - \nu'\lambda' + \frac{2\nu'}{r} - \frac{2\lambda'}{r} + \frac{1}{r^2}\right)\right). \tag{2.17}$$

The Einstein tensor may now be calculated in the form

$$G^{00} = e^{-2\nu}\frac{1}{r^2}\left(r\left(1 - e^{-2\lambda}\right)\right)' \tag{2.18}$$

$$G^{11} = e^{-2\lambda}\left(-\frac{1}{r^2}\left(1 - e^{-2\lambda}\right) + \frac{2\nu'}{r}e^{-2\lambda}\right) \tag{2.19}$$

$$G^{22} = \frac{e^{-2\lambda}}{r^2}\left(\nu'' + \nu'^2 + \frac{\nu'}{r} - \nu'\lambda' - \frac{\lambda'}{r}\right) \tag{2.20}$$

$$G^{33} = \frac{e^{-2\lambda}}{r^2\sin^2\theta}\left(\nu'' + \nu'^2 + \frac{\nu'}{r} - \nu'\lambda' - \frac{\lambda'}{r}\right). \tag{2.21}$$

The nonzero Weyl conformal tensor components are given by,

$$C_{r\theta r\theta} = \frac{1}{\sin^2\theta}C_{r\phi r\phi} = \frac{r^2}{2e^{2\nu}}C_{rtrt} = -\frac{e^{2\lambda}}{2r^2\sin^2\theta}C_{\theta\phi\theta\phi}$$

$$= -e^{2(\lambda-\nu)}C_{\theta t\theta t} = -\frac{e^{2(\lambda-\nu)}}{\sin^2\theta}C_{\phi t\phi t} = f(r) \tag{2.22}$$

where

$$f(r) = \frac{1}{6}\left(r\left(\lambda' - \nu'\right) - e^{2\lambda} + 1 + r^2\left(\nu'' + \nu'^2 - \nu'\lambda'\right)\right). \tag{2.23}$$

2.4 Einstein–Maxwell field equations

When the effects of an electromagnetic field are present, the field equations (2.11) must be supplemented with Maxwell's equations. The complete system of Einstein-Maxwell equations has the form

$$\begin{aligned} G_{ab} &= T_{ab} \\ &= M_{ab} + E_{ab} \end{aligned} \tag{2.24}$$

$$F_{ab;c} + F_{bc;a} + F_{ca;b} = 0 \tag{2.25}$$

$$F^{ab}{}_{;b} = J^a \tag{2.26}$$

where **T** is the total energy–momentum tensor, **M** is the (uncharged) energy–momentum tensor, **E** is the contribution of the electromagnetic field, **F** is the Faraday electromagnetic field tensor and **J** is the four–current density.

The electromagnetic contribution **E** to the total energy–momentum tensor is given by

$$E_{ab} = F_{ac}F_b{}^c - \frac{1}{4}g_{ab}F_{cd}F^{cd} \tag{2.27}$$

where **F** is skew–symmetric. The four–current density can be written as

$$J^a = \sigma u^a \tag{2.28}$$

where σ is the proper charge density. The electromagnetic field tensor **F** is defined in terms of the four–potential **A** by

$$F_{ab} = A_{b;a} - A_{a;b}. \tag{2.29}$$

The four–potential $\mathbf{A}$ is taken as

$$A_a = (\phi(r), 0, 0, 0)$$

and has the advantage of generating only one non–vanishing component, and its skew–symmetric counterpart, of the electromagnetic field tensor

$$F_{01} = -\phi'(r) \tag{2.30}$$

where we have utilised (2.29). The corresponding contravariant component has the form

$$F^{01} = e^{-2(\nu+\lambda)}\phi'(r) = e^{-(\nu+\lambda)}E(r)$$

where we have put

$$E(r) = e^{-(\nu+\lambda)}\phi'(r) \tag{2.31}$$

following Herrera and Ponce de Leon [12]. The quantity $E(r)$ is interpreted as the electrostatic field intensity. In general the Faraday tensor F_{ab} depends on the magnetic field as well, however gauge freedom allows us to suppress magnetic effects so that only the electric field is active.

With the help of (2.30) it can be verified that (2.25) is identically satisfied. The field equation (2.26) is identically satisfied for $a = 1, 2, 3$ but the condition

$$e^{-\lambda}\left(r^2E\right)' = r^2\sigma \tag{2.32}$$

is obtained for $a = 0$.

The Einstein–Maxwell field equations (2.24) may be expressed as the system

$$\left[r\left(1-e^{-2\lambda}\right)\right]' = r^2\rho + \frac{1}{2}r^2E^2 \tag{2.33}$$

$$-\left(1-e^{-2\lambda}\right) + 2\nu' r e^{-2\lambda} = pr^2 - \frac{1}{2}r^2E^2 \tag{2.34}$$

$$e^{-2\lambda}\left[\frac{r\nu'}{\nu} - \frac{r\lambda'}{\lambda} + r^2\left(\nu'' - \nu'\lambda' + \nu'^2\right)\right] = pr^2 + \frac{1}{2}E^2r^2 \tag{2.35}$$

$$\sigma^2 = \frac{4e^{-2\lambda}}{r^2}\left(r^2\dot{E} + E\right)^2 \tag{2.36}$$

for the static spherically symmetric spacetime (2.12), where the dot denotes differentiation with respect to the variable x. The conservation laws $T^{ab}{}_{;b} = 0$ reduce to the equation

$$p' + (\rho + p)\nu' = \frac{E}{r^2}\left[r^2E\right]' \tag{2.37}$$

which can be used in the place of one of the field equations in the system (2.33). However since (2.37) incorporates four physical quantities, it has limited use.

We employ the following transformation, which has been used by Durgapal and Bannerji [13], Durgapal and Fuloria [14] and Finch and Skea [15], to simplify the field equations. A new coordinate x and two metric functions $y(x)$ and $Z(x)$ defined as follows, $x = Cr^2$, $Z(x) = e^{-2\lambda(r)}$, $y^2(x) = e^{2\nu(r)}$ are introduced. With these transformations the Einstein–Maxwell field equations (2.32) to (2.36) may be expressed

in the following equivalent form

$$\frac{1-Z}{x}-2\dot{Z} = \frac{\rho}{C}+\frac{E^2}{2C} \tag{2.38}$$

$$\frac{Z-1}{x}+\frac{4Z\dot{y}}{y} = \frac{p}{C}-\frac{E^2}{2C} \tag{2.39}$$

$$4x^2Z\ddot{y}+2x^2\dot{Z}\dot{y}+\left(\dot{Z}x-Z+1-\frac{E^2x}{C}\right)y = 0 \tag{2.40}$$

$$\frac{\sigma^2}{C} = \frac{4Z}{x}\left(x\dot{E}+E\right)^2 \tag{2.41}$$

where dots represent differentiation with respect to x. This version has the distinct advantage that the equation of pressure isotropy (2.40) is now linear in one of the potentials y. This is bound to greatly assist in the process of locating exact solutions.

The exterior gravitational field for a static, spherically symmetric charged distribution is governed by the Reissner–Nordstrom [5, 6] solution. The Reissner–Nordstrom exterior line element has the form

$$ds^2=-\left(1-\frac{2M}{r}+\frac{Q^2}{r^2}\right)dt^2+\left(1-\frac{2M}{r}+\frac{Q^2}{r^2}\right)^{-1}dr^2+r^2(d\theta^2+\sin^2\theta d\phi^2) \tag{2.42}$$

where M and Q are associated with the mass and charge of the sphere respectively as measured by an observer at spatial infinity. For the Reissner–Nordstrom solution (2.42) the radial electric field is described by

$$E=\frac{Q}{r^2} \tag{2.43}$$

and consequently the proper charge density is $\sigma=0$ by (2.32). Thus $\mathbf{J}=\mathbf{0}$ which is consistent with the exterior. Observe that upon setting $Q=0$ in (2.42) we regain

the exterior Schwarzschild [2] solution. When the gravitational field is generated by a massless electromagnetic field, then such an exterior metric is referred to as an electrovacuum solution.

2.5 Einstein–Gauss–Bonnet gravity

We briefly introduce the Einstein–Gauss–Bonnet (EGB) theory which we consider in chapter 5. The Gauss–Bonnet action in five dimensions is written as

$$S = \int \sqrt{-g} \left[\frac{1}{2} \left(R - 2\Lambda + \alpha L_{GB} \right) \right] d^5x + S_{\text{ matter}}, \tag{2.44}$$

where α is the dimensionfull Gauss–Bonnet coupling constant which goes as $\frac{1}{L^2}$, L being a length in the Planck scale. The strength of the action L_{GB} lies in the fact that despite the Lagrangian being quadratic in the Ricci tensor, Ricci scalar and the Riemann tensor, the equations of motion turn out to be second order quasilinear which is expected in a theory of gravity. The Gauss–Bonnet term does not contribute to the dynamics of stellar evolution for $n \leq 4$ but is dynamic for $n > 4$. Specifically, it has been shown that for the Gauss–Bonnet case only the dimensions 5 and 6 are necessary to consider. Because the 5-D case leads to some mathematical simplifications, it is not surprising that practically all investigations in the literature have avoided the 6–D case.

The EGB field equations may be written as

$$G_{ab} + \alpha H_{ab} = T_{ab} \tag{2.45}$$

where we have adopted the metric signature $(-++++)$ and where G_{ab} is the usual Einstein tensor. The Lanczos tensor is given by

$$H_{ab} = 2 \left(R R_{ab} - 2 R_{ac} R^c_b - 2 R^{cd} R_{acbd} + R^{cde}_a R_{bcde} \right) - \frac{1}{2} g_{ab} L_{GB} \tag{2.46}$$

where the Lovelock term has the form

$$L_{GB} = R^2 + R_{abcd}R^{abcd} - 4R_{cd}R^{cd}. \tag{2.47}$$

2.6 Conditions for physical admissibility

We now briefly consider the conditions that have to be satisfied for solutions of the Einstein system to be physically reasonable. In order to obtain models that are physically plausible, the following constraints are applied on solutions of the Einstein–Maxwell system:

(a) The metric functions $e^{2\nu}$ and $e^{2\lambda}$ should be positive and non–singular everywhere in the interior of the star.

(b) Positivity and finiteness of pressure and energy density everywhere in the interior of the star including the origin and boundary:

$$0 \leq p < \infty \qquad 0 < \rho < \infty$$

(c) The pressure and energy density should be monotonic decreasing functions of the coordinate r. The pressure vanishes at the boundary $r = R$:

$$\frac{dp}{dr} \leq 0 \qquad \frac{d\rho}{dr} \leq 0 \qquad p(R) = 0$$

(d) Continuity of gravitational potentials across the boundary of the star. The interior line element should be matched smoothly to the exterior Reissner–Nordstrom [6] line element at the boundary:

$$e^{2\nu(R)} = e^{-2\lambda(R)} = 1 - \frac{2M}{R} + \frac{Q^2}{R^2}$$

(e) The principle of causality must be satisfied, i.e., the speed of sound should remain subluminal everywhere in the interior:

$$0 \leq \frac{dp}{d\rho} \leq 1$$

(f) The following energy conditions should be satisfied:

- Weak energy condition: $\rho - p > 0$
- Strong energy condition: $\rho + p > 0$
- Dominant energy condition: $\rho + 3p > 0$

(g) The Chandrasekhar [16] condition for adiabatic stability

$$\left(\frac{\rho + p}{p}\right)\frac{dp}{d\rho} > \frac{4}{3}$$

should be satisfied.

(h) Mass–Radius Ratio: The Buchdahl maximum mass to radius ratio for a static fluid sphere with a monotonically decreasing density profile must satisfy the condition

$$\frac{2 \times \text{mass}}{\text{radius}} < \frac{8}{9}$$

to ensure the stability of the sphere [17].

(i) Böhmer and Harko [18] determined the constraint

$$\frac{Q^2}{R^2}\left(\frac{18R^2 + Q^2}{12R^2 + Q^2}\right) \leq \frac{2M}{R}$$

for a compact general relativistic object under certain conditions.

(j) Andréasson [19] established the inequality

$$\sqrt{M} \leq \frac{\sqrt{R}}{3} + \sqrt{\frac{R}{9} + \frac{Q^2}{3R}}$$

which gives the upper bound for the mass for a given radius and charge.

(k) The mass–charge ratio

$$\frac{M}{Q} > 1$$

follows from the condition for equilibrium $M^2 > Q^2$ for charged stars with nonzero pressure in general as shown by Cooperstock and de la Cruz [20].

Most solutions reported in literature violate some of the conditions (a) to (k) within the interior of the charged star. We are interested in solutions that are physically reasonable.

Chapter 3

Conformally Flat Isotropic Charged Spheres

3.1 Introduction

Here we investigate some physically important configurations of the isotropic charged sphere. Exact solutions of the Einstein–Maxwell field equations are crucial in modelling compact objects such as white dwarfs, neutron stars and quark stars. This arises from the actuality that observational data has been shown to be discordant with standard neutron star models [21]. By generating exact solutions using the Einstein–Maxwell field equations, the issue of gravitational collapse of a spherically symmetric distribution can be studied. In this context the collapse of matter to a point singularity can be avoided since gravitational attraction is neutralized by the repulsive Coulombic force as well as the pressure gradient. The works of Ivanov [22] and Sharma *et al* [23] show the effect of the electric field on the luminosity, redshift and masses of a star. In this chapter, we specifically impose pressure isotropy and conformal flatness in order to solve the Einstein–Maxwell equations and attempt to produce new exact solutions for charged spheres.

3.2 Conformally flat charged spheres

In order to solve the Einstein-Maxwell field equations, geometric restrictions based on physical considerations are customarily imposed. One reasonable idea is that at spatial infinity, spacetimes should degenerate to the flat Minkowski metric. Conformal flatness requires the vanishing of the Weyl tensor (2.23) and this constrains the metric potentials to obey the relation

$$4x^2Z\ddot{y} + 2x^2\dot{Z}\dot{y} - \left(\dot{Z}x - Z + 1\right)y = 0 \tag{3.1}$$

which must be used in conjunction with the field equations. Note that in the absence of charge, (3.1) and pressure isotropy suggests that $\dot{Z}x - Z + 1 = 0$ or $Z = 1 + kx$ which is exactly the Schwarzschild interior spacetime solution in the static case. It is also known that if expansion is permitted then the unique conformally flat metrics are the Stephani stars [24].

With the aid of (3.1), equations (2.38) to (2.41) reduce to the system

$$\frac{\rho}{C} = -3\dot{Z} \tag{3.2}$$

$$\frac{p}{C} = \frac{\dot{Z}y + 4Z\dot{y}}{y} \tag{3.3}$$

$$\frac{E^2}{C} = 2\left(\frac{\dot{Z}x - Z + 1}{x}\right) \tag{3.4}$$

$$\frac{\sigma^2}{C} = \frac{4Z}{x}\left(x\dot{E} + E\right)^2 \tag{3.5}$$

$$y = A\sqrt{x}\cosh\left(\frac{1}{2}\int\frac{dx}{x\sqrt{Z}} + B\right) \tag{3.6}$$

where (3.6) is the integrated version of (3.1) [25]. This system constitutes a set of five independent equations in six unknowns governing the behaviour of charged conformally flat perfect fluids. One of the components may be specified initially to yield the remaining five. Alternatively, some of the variables may be connected on physical grounds such as an equation of state ($p = \alpha\rho$) or $\sigma = \pm\rho$ as demanded for stable equilibrium by De and Raychaudhuri [26].

Although no systematic algorithmic treatment of isotropic conformally flat static charged stars has been undertaken, there does exist isolated conformally flat solutions to the Einstein–Maxwell equations reported in the literature using *ad hoc* prescriptions. We shall mention some later. Banerjee and Santos [9] worked on anisotropic models for a charged dust sphere and Shi–Chang [10] obtained some interior isotropic solutions for a charged stable static sphere. These solutions however, are not free from singularities and do not satisfy all the energy conditions.

3.3 Existence of physically reasonable solutions

Before embarking on a search for exact solutions for conformally flat charged spacetimes, it is prudent to analyse whether solutions satisfying the elementary physical conditions exist. At the outset, it is clear that $Z(x) = e^{-2\lambda(r)} > 0$ as well as $y(x) = e^{\nu(r)} > 0$. Note that without loss of generality we assume $C > 0$. Then the density equation (3.2) suggests that $\dot{Z} < 0$, which implies the metric potential Z is always a monotonically decreasing function. It is also important to note that the conclusion $\dot{Z}y < 0$ follows and will be useful later. Positivity of the pressure demands that

$$-4Z\dot{y} < \dot{Z}y \tag{3.7}$$

as a further restriction on the metric functions. By using the result $\dot{Z}y < 0$, we conclude

$$Z\dot{y} > 0 \tag{3.8}$$

and hence $\dot{y} > 0$ since $Z > 0$. Thus the temporal metric potentials y must be monotonically increasing functions. Additionally, since $\dot{Z} < 0$ and $\dot{y} > 0$ we also deduce $\dot{Z}\dot{y} < 0$, which will be a useful result in the work to follow. Now turning our attention to the weak energy condition

$$\frac{\rho - p}{C} = -3\dot{Z} - \frac{\dot{Z}y + 4Z\dot{y}}{y} > 0$$

the inequality

$$(\dot{Zy}) < 0$$

or

$$\dot{Z}y < -Z\dot{y} \tag{3.9}$$

results, which is consistent with the result (3.7). Similarly the strong energy condition

$$\frac{\rho + p}{C} = -3\dot{Z} + \frac{\dot{Z}y + 4Z\dot{y}}{y} > 0$$

yields

$$\dot{Z}y < 2Z\dot{y} \tag{3.10}$$

which also harmonises with (3.7). The dominant energy condition

$$\frac{\rho + 3p}{C} = -3\dot{Z} + 3\left(\frac{\dot{Z}y + 4Z\dot{y}}{y}\right) > 0$$

leads to

$$Z\dot{y} > 0 \tag{3.11}$$

which is not in violation of any of the restrictions above. At this stage it is clear that spacetimes satisfying the energy conditions certainly exist. Requiring a causal soundspeed $0 < \frac{dp}{d\rho} < 1$ generates the condition

$$-1 < \frac{Z\ddot{y}}{\ddot{Z}y} + \frac{\dot{Z}\dot{y}}{\ddot{Z}y} - \frac{Z\dot{y}^2}{\ddot{Z}y^2} < -\frac{1}{4} \tag{3.12}$$

on the metric potentials. Recall that thus far we have established that for a positive definite energy density and pressure satisfying the weak, strong and dominant energy conditions we have $\dot{Z} < 0$, $\dot{y} > 0$, $Z > 0$, $y > 0$. Presently, there are no means available to constrain the second derivatives $\ddot{Z}$ and $\ddot{y}$ required in (3.12). For this reason we consider in turn all four possible signatures for $\ddot{Z}$ and $\ddot{y}$. For convenience we introduce the naming

$$f(x) = \frac{Z\ddot{y}}{\ddot{Z}y} + \frac{\dot{Z}\dot{y}}{\ddot{Z}y} - \frac{Z\dot{y}^2}{\ddot{Z}y^2} \tag{3.13}$$

and we note from (3.12) that $f(x) < 0$.

Case 1: $\ddot{Z} > 0, \ddot{y} > 0$

In this case $\frac{Z\ddot{y}}{\ddot{Z}y} > 0$, $\frac{\dot{Z}\dot{y}}{\ddot{Z}y} < 0$ and $\frac{Z\dot{y}^2}{\ddot{Z}y^2} > 0$ so it follows from the negativity of $f(x)$ that

$$Z\ddot{y} < Z\dot{y}^2 - \dot{Z}\dot{y} \tag{3.14}$$

Since both the left hand side and right hand side of (3.14) are positive, we have the constraint

$$0 < \ddot{y} < \dot{y}^2 - \frac{\dot{Z}\dot{y}}{Z} \tag{3.15}$$

for a causal solution. Hence a realistic solution exists provided (3.14) is satisfied.

Case 2: $\ddot{Z} < 0, \ddot{y} > 0$

Now $f(x) < 0$ requires

$$\frac{Z\ddot{y}}{\ddot{Z}y} + \frac{\dot{Z}\dot{y}}{\ddot{Z}y} < \frac{Z\dot{y}^2}{\ddot{Z}y^2} \tag{3.16}$$

But under the present hypothesis $\frac{Z\ddot{y}}{\ddot{Z}y} < 0$, $\frac{\dot{Z}\dot{y}}{\ddot{Z}y} > 0$ and $\frac{Z\dot{y}^2}{\ddot{Z}y^2} < 0$. Multiplying (3.16) by $\ddot{Z} < 0$ reverses the inequality

$$\frac{Z\ddot{y}}{y} + \frac{\dot{Z}\dot{y}}{y} > \frac{Z\dot{y}^2}{y^2} \tag{3.17}$$

and since the right hand side > 0, it follows that

$$Z\ddot{y} + \dot{Z}\dot{y} > 0 \tag{3.18}$$

that is

$$\frac{d}{dx}(Z\dot{y}) > 0 \tag{3.19}$$

This suggests that a solution satisfying (3.19), $\ddot{Z} < 0$, $\ddot{y} > 0$ will be physically reasonable.

Case 3: $\ddot{Z} < 0, \ddot{y} < 0$

In this case $\frac{Z\ddot{y}}{\ddot{Z}y} > 0$, $\frac{\dot{Z}\dot{y}}{\ddot{Z}y} > 0$ and $\frac{Z\dot{y}^2}{\ddot{Z}y^2} < 0$ so that $f(x)$ is the sum of three positive quantities and is thus positive which is a contradiction since $f(x) < 0$. Therefore, solutions satisfying $\ddot{Z} < 0$ and $\ddot{y} < 0$ are acausal and consequently not physically feasible.

Case 4: $\ddot{Z} > 0, \ddot{y} < 0$

Under these conditions we have $\frac{Z\ddot{y}}{\ddot{Z}y} > 0$, $\frac{\dot{Z}\dot{y}}{\ddot{Z}y} < 0$ and $\frac{Z\dot{y}^2}{\ddot{Z}y^2} > 0$. This indicates

that $f(x) < 0$ for all functions $\ddot{Z} > 0$ and $\ddot{y} < 0$. So a physically realistic model may be generated under these circumstances.

Finally, from the electric field intensity we get

$$\dot{Z}x - Z + 1 > 0 \tag{3.20}$$

then by Gronwall's Theorem [27],

$$Z > 1 + kx \tag{3.21}$$

and by (3.2) we see that $k < 0$. These impose boundaries on our choice for Z. To summarise, this analysis has demonstrated that an exact solution that satisfied the energy conditions and the causality requirements does indeed exist. In what is to follow, we pursue such solutions mindful of the constraints we have established here.

3.4 Known conformally flat isotropic solutions with charge

Wang Xingxiang [11] presented a set of ostensibly physically reasonable solutions of the Einstein–Maxwell field equations. Wang prescribed the form of the density as

$$\frac{\rho}{C} = \frac{6n(1-x)}{(1+(n-1)x)^3} \tag{3.22}$$

for an arbitrary parameter n. Note that this is analogous to prescribing $\dot{Z}$ by virtue of equation (3.2) and we obtain

$$\dot{Z} = \frac{-3n(1-x)}{(1+(n-1)x)^3} \tag{3.23}$$

which in turn can be integrated to give

$$Z = \frac{3n(-2nx + n + 2x - 2)}{2(n-1)^2((n-1)x + 1)^2}. \tag{3.24}$$

as the spatial metric potential. The solutions were considered for $n = 1$ and $n = 2$. Observe that $n = 1$ is prohibited in (3.24) but not in (3.23). His selections of n also admit particular solutions for y and p but these were not physically analysed.

Melfo and Rago [28] tested the conformal flatness case on an anisotropic but non-static charged fluid sphere. It was noted that the solutions favour static configurations. When imposing isotropic pressure, non-static solutions were generated and inconsistent models resulted. Herrera *et al* [25] attempted to find conformally flat, interior solutions to the Einstein equations for anisotropic fluids. The focus was to compare these with similar models that did not include the vanishing of the Weyl tensor in order to observe its effect on stellar models. Ivanov [22] treated conformal flatness and prescribed the potential λ which led to prescribing ρ effectively. The solutions were examined analytically and then compared to a real pulsar.

3.5 New conformally flat charged isotropic models

From (3.1) – (3.5) it is clear that we have a system of five equations in six unknowns. To close the system we could prescribe any one of the six variables and then solve the system for the remaining five. Since the pressure and charge density equations contain two variables on the right hand side, it is not feasible to prescribe one of these. It therefore remains to prescribe the density ρ, electric field intensity E, the metric potentials Z or y. This outlines the strategy we intend to follow. We consider some historically important cases for Z and also prescribe our own metric potentials in order to generate models.

3.5.1 Isothermal conformally flat sphere $Z =$ a constant

This prescription is a necessary and sufficient condition for isothermal behaviour of static neutral spheres both in Einstein gravity [29] and its generalisation Lovelock theory [30]. Isothermal behaviour is characterised by an inverse square law fall–off of the density and pressure in Einstein 4–dimensional gravity, as is the case in Newtonian physics.

Substituting $Z = k$ in equation (3.6), generates the equation

$$4kx^2\ddot{y} + (k-1)y = 0 \tag{3.25}$$

which has general solution

$$y = x^{\frac{1}{2}-\frac{1}{2\sqrt{k}}}\left(C_2 x^{\frac{1}{\sqrt{k}}} + C_1\right) \tag{3.26}$$

where C_1 and C_2 are constants of integration. However, this case is forbidden as inserting $Z = k$ into (3.2) results in $\rho = 0$. A zero density implies absence of matter. Therefore, we abandon this case and it is noteworthy that isothermal behaviour is not evident for conformally flat charged isotropic spheres. This raises the question of what metric (if it exists) will give the isothermal property if conformal flatness is also required.

As mentioned previously isothermal fluids display an inverse square law fall off of the energy density as well as a linear equation of state, $\rho \propto \frac{1}{r^2}$ and $p \propto \frac{1}{r^2}$. In the present context for the isothermal property let $\rho = \frac{A}{x}$ and $p = \frac{B}{x}$. Substituting these into (3.2) and (3.3) yields

$$Z = C_1 - \frac{1}{3}A\log x \tag{3.27}$$

$$y = C_2\left(1 - \frac{B}{A}\right)\log x. \tag{3.28}$$

where C_1 and C_2 are constants of integration. Since the system of equations is now over determined, it remains to be checked that the condition for pressure isotropy is satisfied for suitable A and B. Substituting these expressions into (3.1) generates the relationship

$$\log x(A\log x - 5A + 3) - 3C_1(\log x - 4) = 0 \tag{3.29}$$

which is an algebraic equation quadratic in $\log(x)$. Setting the coefficients of the powers of $\log(x)$ to zero gives $A = 0$ and also $2A - 3C_1 = 0$ which implies that $C_1 = 0$. Finally, $-5A + 3 + 12C_1 = 0$ which is a false statement. Accordingly, we conclude that no conformally flat charged isothermal isotropic fluid spheres exist.

3.5.2 The Schwarzschild interior potential

Substituting $Z = 1 + x$ in equation (3.2) gives

$$\frac{\rho}{C} = -3 \tag{3.30}$$

for the density. However, we also obtain $E = 0$ and $\sigma = 0$. This case is defective as it is known that no neutral solution of Einstein's equations can generate a charged model [24]. The metric potentials must be modified accordingly to acccomodate charge. Note that the most general conformally flat static neutral perfect fluid metric is the Schwarzschild interior metric but it is unsuitable in modelling a charged star let alone imposing the additional constraint of conformal flatness.

Naturally this raises the question whether a constant density sphere that is conformally flat exists. If we set ρ to some constant K which represents an incompressible fluid sphere, then from integrating (3.2) we get $Z = -\frac{k}{3C}x + C_1$, where C_1 is a constant of integration. This case boils down to the Schwarzschild interior solution which we have already discussed in the previous chapter. Briefly, no conformally flat incompressible isotropic fluid sphere exists.

3.5.3 The Vaidya–Tikekar superdense star ansatz

Vaidya and Tikekar [31] constructed models of superdense static stars with the metric ansatz equivalent to $Z = \frac{1+ax}{1+bx}$, for a and b being real constants. With this form, equation (3.1) simplifies to

$$4(ax+1)(bx+1)\ddot{y} + (a-b) + 2\,(a-b)\,\dot{y} + b\,(a-b)\,y = 0 \tag{3.31}$$

with general solution

$$\begin{aligned} y &= C_2\,(a(a-b)(bx+1))^{3/2}\ {}_2F_1\left(1 - \frac{\sqrt{b}}{2\sqrt{a}}, \frac{\sqrt{b}}{2\sqrt{a}} + 1; \frac{5}{2}; \frac{a(bx+1)}{a-b}\right) \\ &\quad + C_1\ {}_2F_1\left(-\frac{\sqrt{b}}{2\sqrt{a}} - \frac{1}{2}, \frac{1}{2}\left(\frac{\sqrt{b}}{\sqrt{a}} - 1\right); -\frac{1}{2}; \frac{a(bx+1)}{a-b}\right) \end{aligned} \tag{3.32}$$

where ${}_2F_1$ is the hypergeometric function and C_1 and C_2 are constants of integration. The solution (3.32) is not suitable for modelling astrophysical objects in its current form. We are interested in special cases of (3.32) that reduce to elementary functions. Interestingly when b is an integral multiple of a, solutions in terms of elementary functions result. Consider the case where $b = 9a$. The solution for this case has the form

$$y = C_1\left(27a^2x^2 + 18ax - 1\right) + C_2\sqrt{ax+1}(9ax+1)^{3/2} \tag{3.33}$$

which is a smooth singularity free curve. The dynamical quantities accordingly have the form

$$\frac{\rho}{C} = \frac{24a}{(9ax+1)^2} \tag{3.34}$$

$$\frac{p}{C} = \frac{8aC_1\left(243a^3x^3+324a^2x^2+99ax+10\right)\sqrt{ax+1}}{C_1\left(27a^2x^2+18ax-1\right)\sqrt{ax+1}(9ax+1)^2+C_2(ax+1)(9ax+1)^{7/2}}$$

$$+\frac{24C_2\left(27a^3x^3+48a^2x^2+23ax+2\right)\sqrt{9ax+1}}{C_1\left(27a^2x^2+18ax-1\right)\sqrt{ax+1}(9ax+1)^2+C_2(ax+1)(9ax+1)^{7/2}} \tag{3.35}$$

$$\frac{E^2}{C} = \frac{144a^2x}{(9ax+1)^2} \tag{3.36}$$

$$\frac{\sigma^2}{C} = \frac{1296a^2(ax+1)(3ax+1)^2}{(9ax+1)^5}. \tag{3.37}$$

Observe that the model above is completely free of singularities at the centre of the stellar distribution.

3.5.4 The Finch–Skea potential

The special case of Vaidya–Tikekar where $a = 0$, $b = 1$ corresponds to the Finch–Skea [15] metric which is known to have pleasing physical properties. Equation (3.31) yields a solution in elementary functions. The complete solution for this case has the form

$$
\begin{aligned}
y &= c_1\left(\sqrt{x+1}\cosh\left(\sqrt{x+1}\right)-\sinh\left(\sqrt{x+1}\right)\right)\\
&\quad +c_2\left(\cosh\left(\sqrt{x+1}\right)-\sqrt{x+1}\sinh\left(\sqrt{x+1}\right)\right)
\end{aligned}
\tag{3.38}
$$

and bears a strong resemblance to the Finch–Skea static neutral star metric with trigonometric functions exchanged for hyperbolic functions. Putting $u=\cosh\sqrt{x+1}$ and $v=\sinh\sqrt{x+1}$, the dynamical quantities have the form

$$
\frac{\rho}{C} = \frac{3}{(x+1)^2} \tag{3.39}
$$

$$
\frac{p}{C} = \frac{\sqrt{x+1}\,(v-\beta u)+(2x+3)\,(\beta v-u)}{(x+1)^2\left(\sqrt{x+1}\,(\beta u-v)+(u-\beta v)\right)} \tag{3.40}
$$

$$
\frac{E^2}{C} = \frac{2x}{(x+1)^2} \tag{3.41}
$$

$$
\frac{\sigma^2}{C} = \frac{2(x+3)^2}{(x+1)^5} \tag{3.42}
$$

for a conformally flat star with Finch–Skea potential. Note we have introduced $\beta=\frac{C_1}{C_2}$ following Finch and Skea. The solution also admits an equation of state

$$
p=\frac{\rho\left[\left(2\beta\sqrt{\frac{3}{\rho}}+\beta+\sqrt[4]{\frac{3}{\rho}}\right)\sinh\left(\sqrt[4]{\frac{3}{\rho}}\right)-\left(\beta\sqrt[4]{\frac{3}{\rho}}+2\sqrt{\frac{3}{\rho}}+1\right)\cosh\left(\sqrt[4]{\frac{3}{\rho}}\right)\right]}{3\left(\beta\sqrt[4]{\frac{3}{\rho}}+1\right)\cosh\left(\sqrt[4]{\frac{3}{\rho}}\right)-3(\beta+1)\sinh\left(\sqrt[4]{\frac{3}{\rho}}\right)} \tag{3.43}
$$

expressing the pressure as a function of the density. The expressions for the energy conditions are given by

$$\rho - p = \frac{2\left(\sqrt{x+1}\,(2u-2\beta v)+(x+1)\,(\beta u-v)\right)}{(x+1)^{5/2}\left(\sqrt{x+1}\,(\beta u-v)+(u-\beta v)\right)} \tag{3.44}$$

$$\rho + p = \frac{4\left(\sqrt{x+1}\left(\frac{1}{2}u-\frac{1}{2}\beta v\right)+(x+1)\,(\beta u-v)\right)}{(x+1)^{5/2}\left(\sqrt{x+1}\,(\beta u-v)+(u-\beta v)\right)} \tag{3.45}$$

$$\rho + 3p = \frac{6\,(\beta u-v)}{(x+1)^{3/2}\left(\beta\left(u\sqrt{x+1}-v\right)+\left(u-v\sqrt{x+1}\right)\right)} \tag{3.46}$$

and these are all expected to be positive. The speed of sound squared index is given by

$$\begin{aligned}\frac{dp}{d\rho} = {} & \frac{\beta^2\left(2u^2(x+1)^{3/2}+uv(x+1)-2v^2\sqrt{x+1}\right)}{6\sqrt{x+1}\left(\beta\left(v-u\sqrt{x+1}\right)+\left(v\sqrt{x+1}-u\right)\right)^2} \\ & -\frac{\beta\left(u^2(x+1)+4uvx\sqrt{x+1}+v^2(x+1)\right)}{6\sqrt{x+1}\left(\beta\left(v-u\sqrt{x+1}\right)+\left(v\sqrt{x+1}-u\right)\right)^2} \\ & +\frac{\left(-2u^2\sqrt{x+1}+uv(x+1)+2v^2(x+1)^{3/2}\right)}{6\sqrt{x+1}\left(\beta\left(v-u\sqrt{x+1}\right)+\left(v\sqrt{x+1}-u\right)\right)^2}\end{aligned} \tag{3.47}$$

and finally the adiabatic stability index of Chandrasekhar may be expressed as

$$\begin{aligned}\left(\frac{\rho+p}{p}\right)\frac{dp}{d\rho} = {} & \left(\sqrt{x+1}\,(u-\beta v)+2(x+1)\,(\beta u-v)\right)(x+1)\,(u-\beta v)\,(v-u\beta)\times \\ & \left(\sqrt{x+1}\left(\beta^2\left(u^2(x+1)-v^2\right)-\left(u^2-v^2(x+1)\right)-2\beta uvx\right)\right)/ \\ & \left(3\sqrt{x+1}\left(\sqrt{x+1}\,(\beta u-v)+u-\beta v\right)^2\right)\times \\ & \left(\sqrt{x+1}\,(\beta v-u)+(x+1)\,(\beta u-v)\right).\end{aligned} \tag{3.48}$$

In the Finch–Skea case, from (3.39) it may be observed that the density is positive everywhere. The electric field intensity and charge density are well behaved functions, decreasing outwardly from the centre. The electric field intensity vanishes when x is zero.

We now analyse graphical plots of the dynamical quantities. These plots have been constructed using parameter values $C_1 = 12$, $C_2 = 4$ and $\beta = 3$.

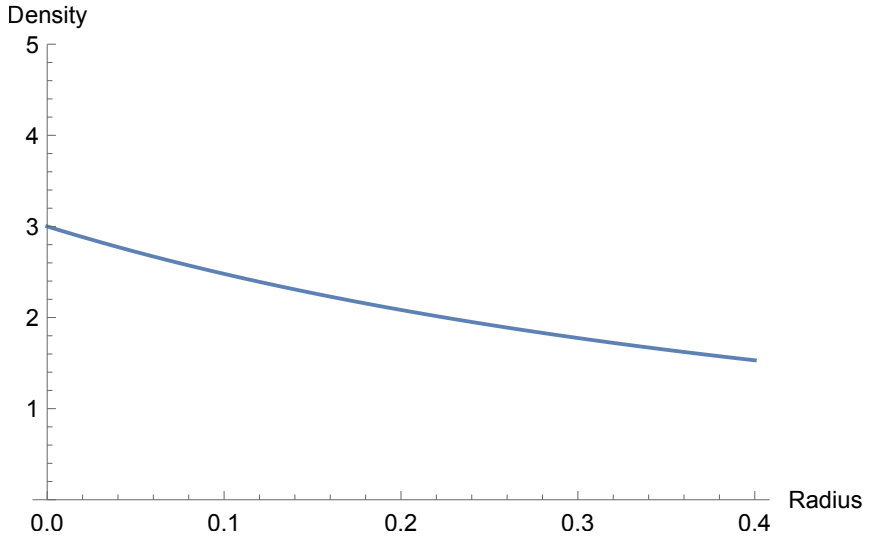

Figure 3.1: Density ρ versus the radial variable x.

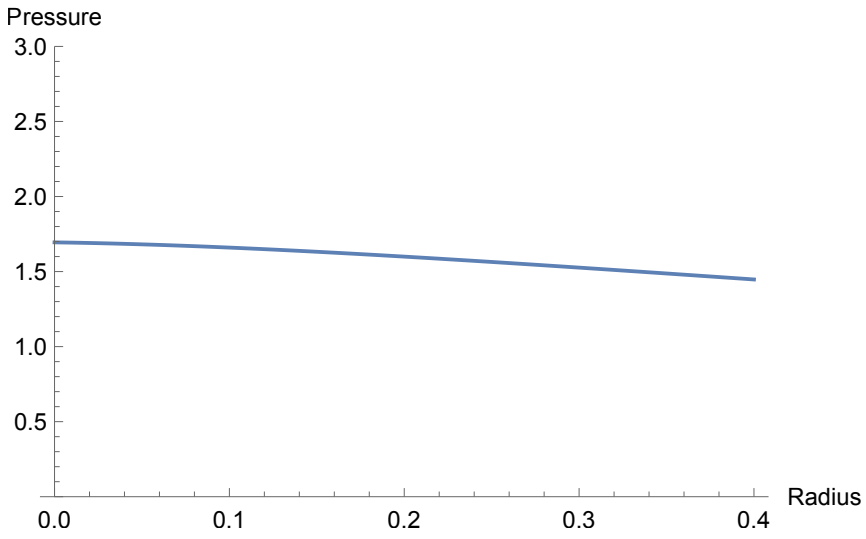

Figure 3.2: Pressure p versus the radial variable x.

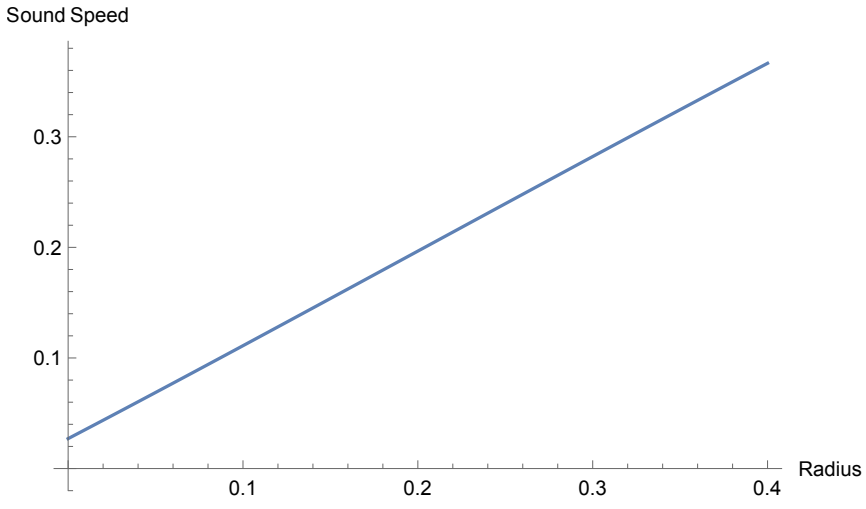

Figure 3.3: Sound speed index $\frac{dp}{d\rho}$ versus the radial variable x.

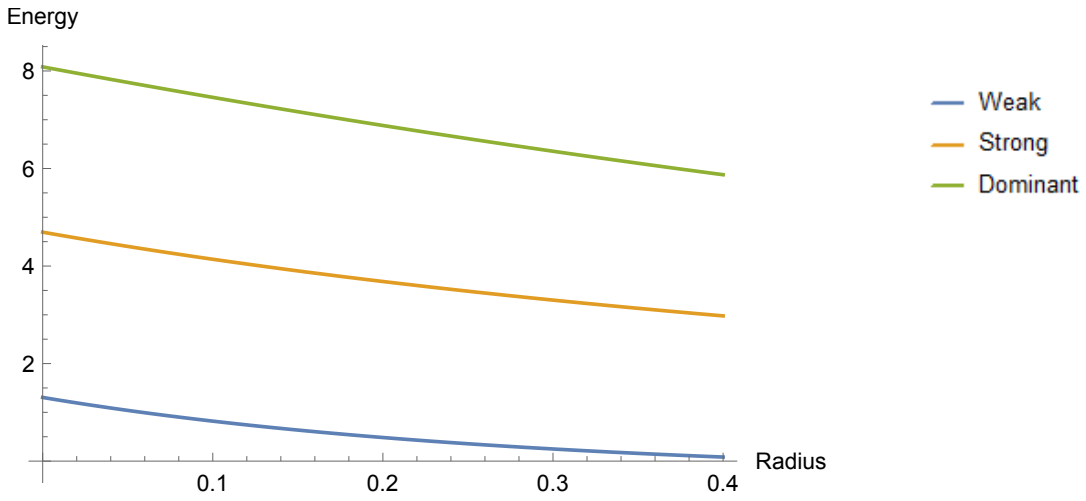

Figure 3.4: Energy conditions versus the radial variable x.

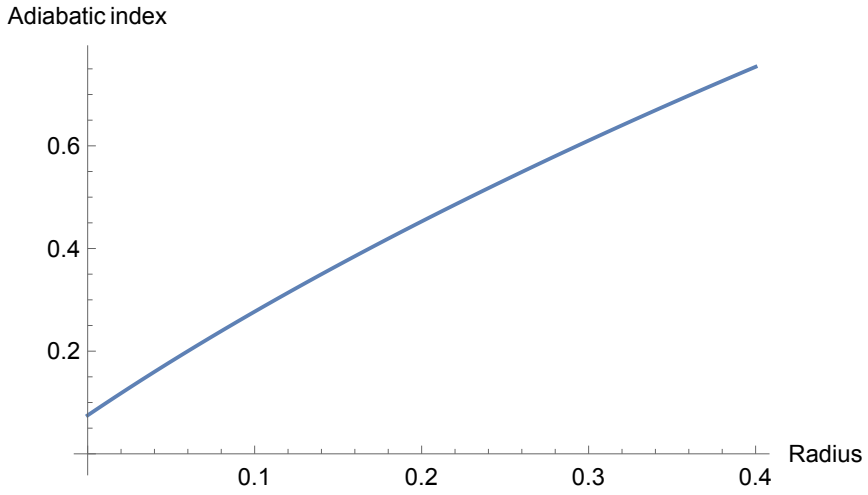

Figure 3.5: Chandrasekhar adiabatic stability index versus the radial variable x.

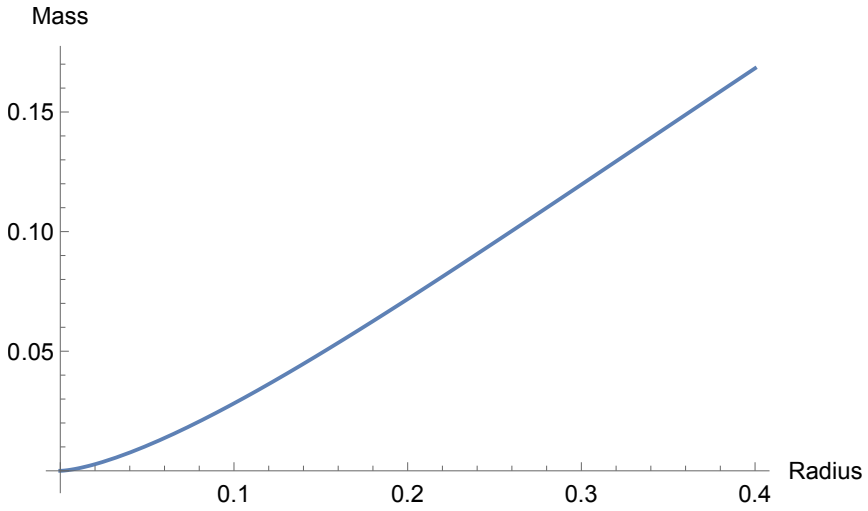

Figure 3.6: Mass profile versus the radial variable x.

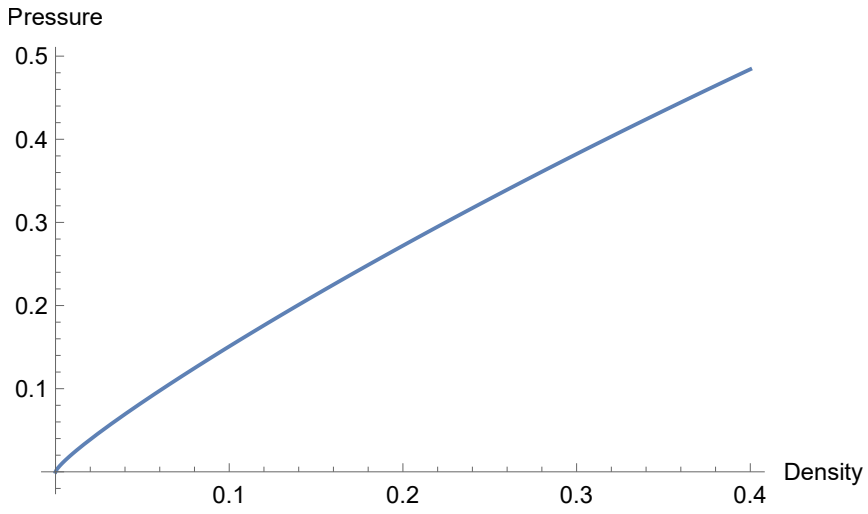

Figure 3.7: Pressure p versus the density ρ

From the plots, in Figure 3.1 and Figure 3.2 we see that the pressure and density are both monotonically decreasing, which is expected. The pressure fails to vanish for a finite radius because of the presence of inverse hyperbolic functions. This means there is no finite boundary. The fluid at hand has cosmological significance and is not suitable to model astrophysical closed compact objects. In contrast, the original Finch–Skea model without the restriction of conformal flatness generated a fixed boundary as trigonometric functions appeared whereas, in the present case hyperbolic functions are evident. Figure 3.3 shows that the sound speed index is less than 1 which confirms the model as causal for a range of radial values. From Figure 3.4 it can be observed that all the energy conditions are positive and hence satisfied. The adiabatic index shown in Figure 3.5 is positive however, it falls short of the accepted range of being more than $\frac{4}{3}$. This motivates us to find such a model where the adiabatic criterion is satisfied. This suggests that the Chandrasekhar limit may need to be adjusted in the presence of an electric field. The mass profile displayed in Figure 3.6 appears well behaved as an increasing function of the radius. Importantly from Figure 3.7, a barotropic equation of state is explicitly realisable. This model therefore satisfies most requirements for physical viability of cosmological fluids.

3.5.5 The metric potential - $Z = \frac{1}{x^n}$

We seek a spacetime that satisfies the Chandrasekhar stability condition. The choice of metric potential we made immediately has a defect in being singular at the centre. However it is interesting to study the consequences since the centre may contain a different fluid core. With the stipulation $Z = \frac{1}{x^n}$, equation (3.1) becomes

$$2x\left(2x\ddot{y} - n\dot{y}\right) + \left(-x^n + n + 1\right)y = 0 \tag{3.49}$$

and the general solution has the form

$$y = C_1\sqrt{x}\exp\left(\frac{(-1)^{n+1}x^{n/2}}{n}\right) + C_2\sqrt{x}\exp\left(\frac{(-1)^{n}x^{n/2}}{n}\right) \tag{3.50}$$

for constants of integration C_1 and C_2. The choice $Z = \frac{1}{x}$ $(n = 1)$ is appropriate since Z is a decreasing function. The general solution (3.50) simplifies to

$$y = \sqrt{x}\left(C_1 e^{\sqrt{x}} - C_2 e^{-\sqrt{x}}\right). \tag{3.51}$$

for the temporal metric potential. The dynamical quantities have the form

$$\frac{\rho}{C} = \frac{3}{x^2} \tag{3.52}$$

$$\frac{p}{C} = \frac{C_1\left(2\sqrt{x}+1\right)e^{2\sqrt{x}} + C_2\left(2\sqrt{x}-1\right)}{x^2\left(C_1 e^{2\sqrt{x}} - C_2\right)} \tag{3.53}$$

$$\frac{E^2}{C} = \frac{2(x-2)}{x^2} \tag{3.54}$$

$$\frac{\sigma^2}{C} = \frac{2}{(x-2)x^2}. \tag{3.55}$$

This solution also admits an equation of state

$$p = \frac{2\sqrt[4]{3}}{3}\rho^{3/4}\left(C_2\left(C_3\exp(\rho^{-1/4}) - C_2\right)^{-1} + 1\right) + \frac{\rho}{3} \tag{3.56}$$

where C_3 is a constant. Clearly a major drawback of this model is the irremovable singularity at the centre. However, this case may still be useful if the centre was filled with a different non-singular fluid and enveloped by the fluid described above with metric components $Z = \frac{1}{x}$ and satisfying equation (3.51).

The expressions for the energy conditions are given by

$$\rho - p = \frac{2\left(C_1\left(\sqrt{x}-1\right)e^{2\sqrt{x}} + C_2\left(\sqrt{x}+1\right)\right)}{x^2\left(C_1 e^{2\sqrt{x}} - C_2\right)} \tag{3.57}$$

$$\rho + p = \frac{2\left(C_1\left(\sqrt{x}+2\right)e^{2\sqrt{x}} + C_2\left(\sqrt{x}-2\right)\right)}{x^2\left(C_1 e^{2\sqrt{x}} - C_2\right)} \tag{3.58}$$

$$\rho + 3p = \frac{6\left(C_1\left(\sqrt{x}+1\right)e^{2\sqrt{x}} + C_2\left(\sqrt{x}-1\right)\right)}{x^2\left(C_1 e^{2\sqrt{x}} - C_2\right)} \tag{3.59}$$

and these are all expected to be positive. The speed of sound squared index is given by

$$\frac{dp}{d\rho} = \frac{C_1^2\left(3\sqrt{x}+2\right)e^{4\sqrt{x}} + 4C_1C_2e^{2\sqrt{x}}(x-1) + C_2^2\left(2-3\sqrt{x}\right)}{6\left(C_2 - C_1e^{2\sqrt{x}}\right)^2}. \tag{3.60}$$

Finally the adiabatic stability index is given by

$$\begin{aligned}\left(\frac{\rho+p}{p}\right)\frac{dp}{d\rho} = {} & \left(C_1\left(\sqrt{x}+2\right)e^{2\sqrt{x}} + C_2\left(\sqrt{x}-2\right)\right)\times \\ & \left(C_1^2\left(3\sqrt{x}+2\right)e^{4\sqrt{x}} + 4C_1C_2e^{2\sqrt{x}}(x-1) + C_2^2\left(2-3\sqrt{x}\right)\right)/ \\ & 3\left(C_2 - C_1e^{2\sqrt{x}}\right)^2\left(C_1\left(2\sqrt{x}+1\right)e^{2\sqrt{x}} + C_2\left(2\sqrt{x}-1\right)\right).\end{aligned} \tag{3.61}$$

In view of the simplicity of this solution, graphical analysis is warranted despite the singularities at the origin. These plots have been constructed using parameter values $C_1 = 1$ and $C_2 = 0$ for illustrative purposes. In general none of the constants of integration can vanish as they must be expressed in terms of the mass, radius and charge of the sphere via the process of matching with the exterior spacetime.

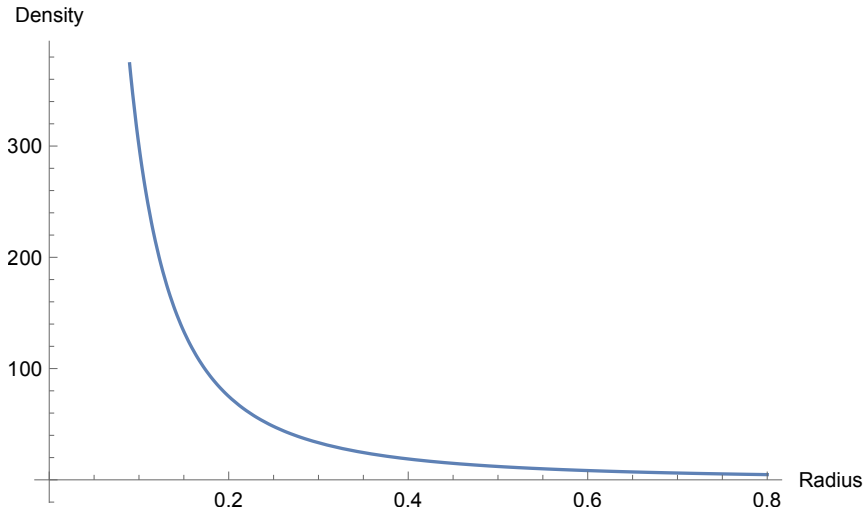

Figure 3.8: Density ρ versus the radial variable x.

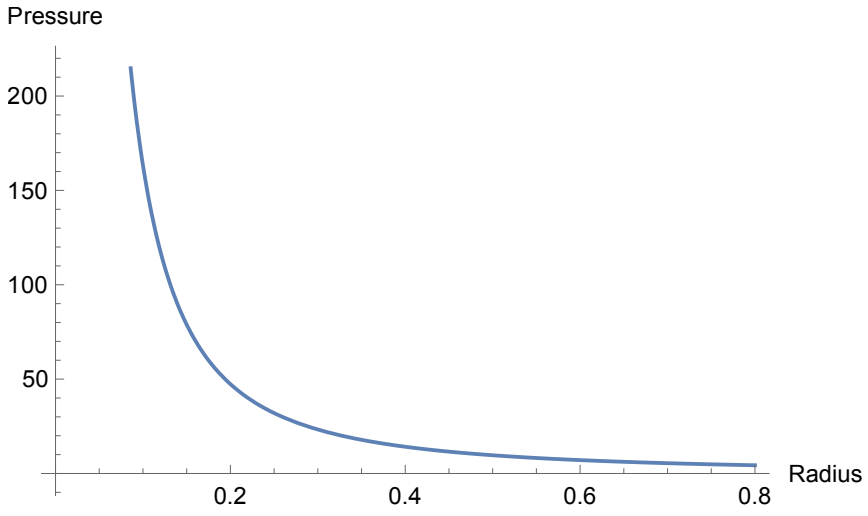

Figure 3.9: Pressure p versus the radial variable x.

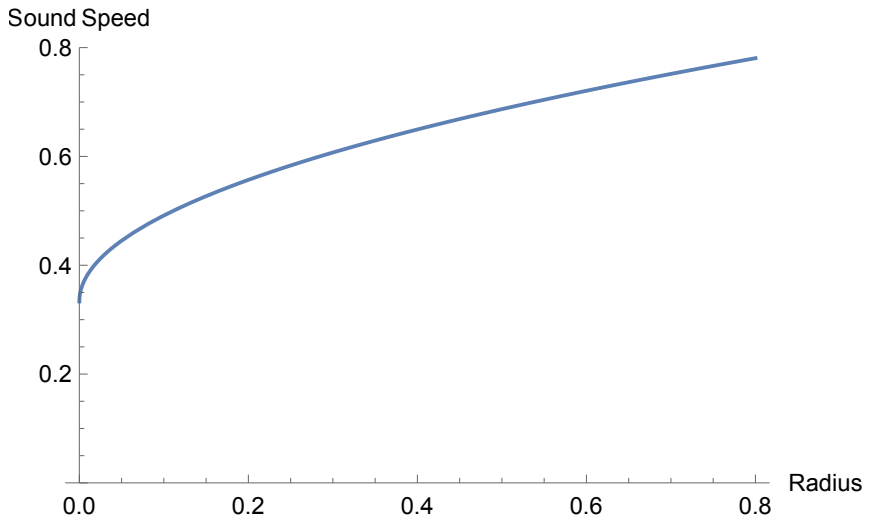

Figure 3.10: Sound speed index $\frac{dp}{d\rho}$ versus the radial variable x.

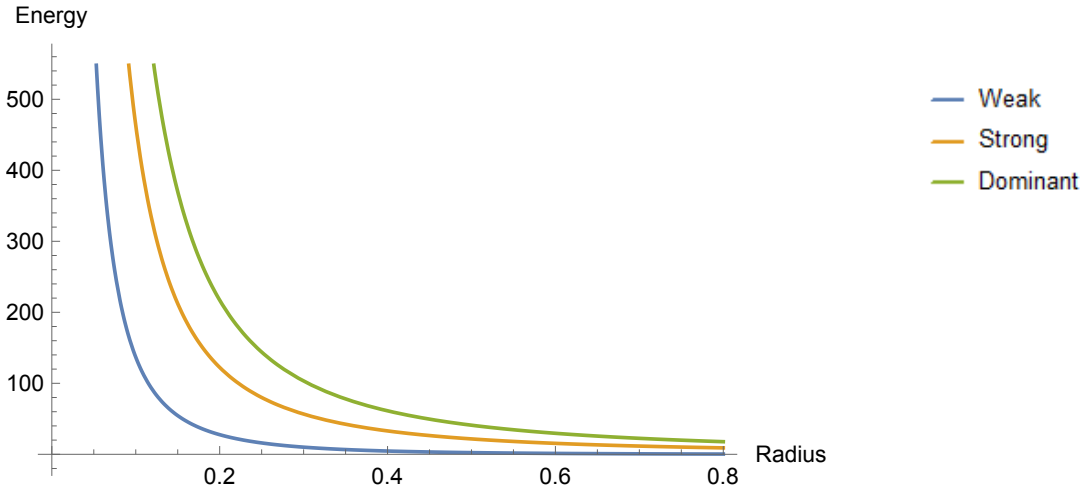

Figure 3.11: Energy conditions versus the radial variable x.

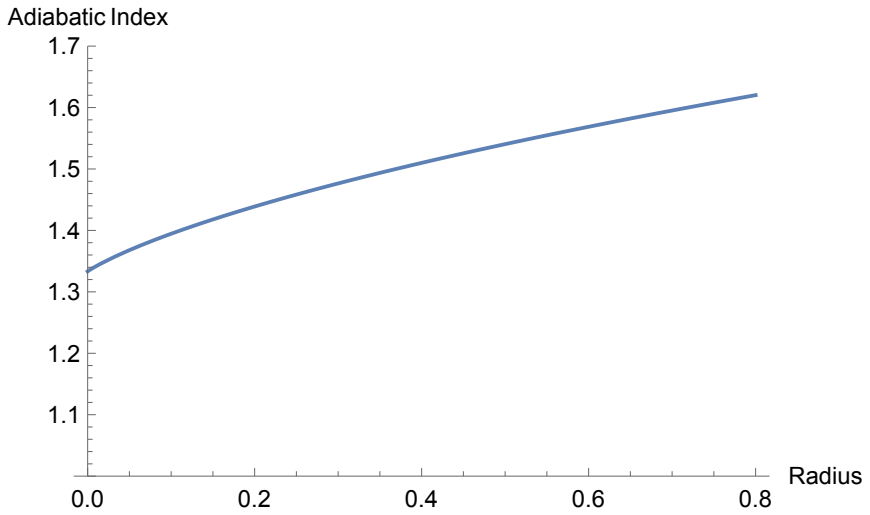

Figure 3.12: Chandrasekhar adiabatic stability index versus the radial variable x.

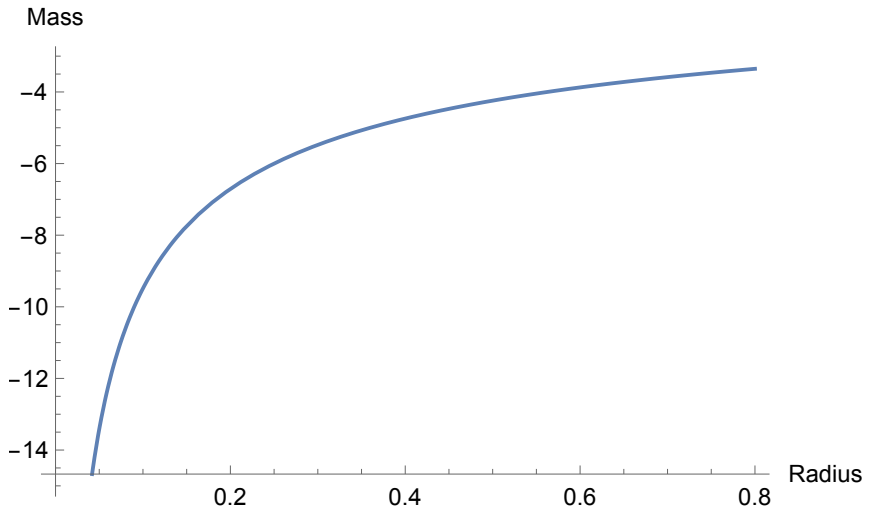

Figure 3.13: Mass profile versus the radial variable x.

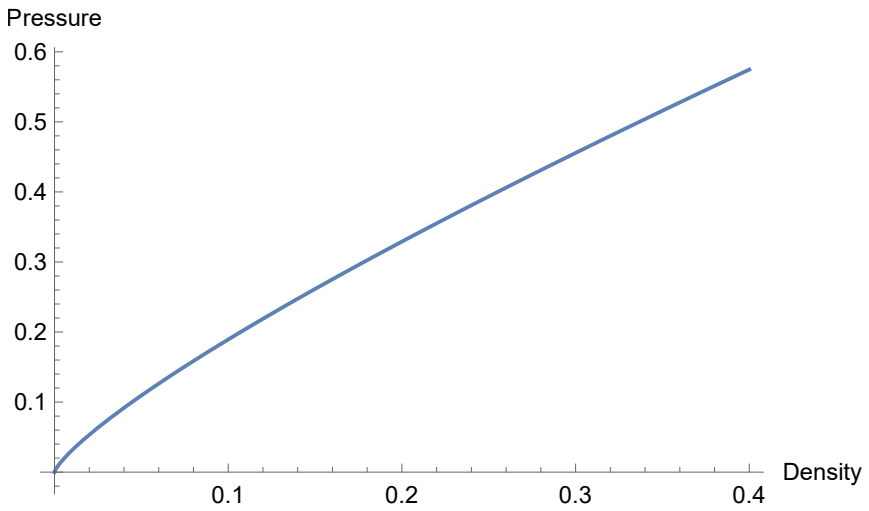

Figure 3.14: Pressure p versus the density ρ.

From the plots, in Figure 3.8 we observe an inverse square law decrease for the density, also noting that the x-axis is a horizontal asymptote. The pressure shown in Figure 3.9 is also decreasing but does not touch the x-axis to indicate the radius of our star. The sound speed displayed in Figure 3.10 is within an acceptable range. From Figure 3.11 it may be observed that all the energy conditions are satisfied. The adiabatic index exhibited in Figure 3.12 falls perfectly within the range of $\frac{4}{3}$ and 2, with 2 being the upperbound applicable to neutron stars. The mass profile presented in Figure 3.13 starts off negative but this is increasing, which could be a result of the constant of integration. This is a further drawback of the model rendering it unrealistic. This indicates the complexity of finding solutions compatible with all the physical requirements. Lastly, the pressure has an almost linear relationship against the density, which is shown in Figure 3.14 and suggests a barotropic equation of state.

3.5.6 Charged dust $p = 0$

Charged dust is the simplest matter field to consider. Here, Coulombic repulsion opposes the gravitational field to prevent collapse to a point singularity. This case was analysed by Hansraj *et al* [24]. Substituting $p = 0$ in (3.3) we obtain,

$$y = C_1 Z^{-\frac{1}{4}} \tag{3.62}$$

for the temporal potential, where C_1 is a constant of integration. Inserting (3.62) into (3.1), the differential equation

$$3x^2\dot{Z}^2 - 4Z\left(x\left(\dot{Z} + x\ddot{Z}\right) + 1\right) + 4Z^2 = 0 \tag{3.63}$$

results. The general solution of (3.63) is given by

$$Z = \frac{C_2}{256x^2}\left(\left(C_3 - C_1 x\right)^2 - 64x^2\right)^2 \tag{3.64}$$

where C_2 and C_3 are constants of integration. This is the unique solution for all conformally flat charged dust spheres. We also list the other physical quantities, with $(C_1)^2 = K_1$ and $(C_2)^2 = K_2$,

$$\frac{\rho}{C} = -\frac{3C_3\left(\left(C_1 - 8\right)x - C_2\right)\left(\left(C_1 + 8\right)x - C_2\right)\left(\left(K_1 - 64\right)x^2 - K_2\right)}{128x^3} \tag{3.65}$$

$$\frac{E^2}{C} = \frac{C_3\left(C_1^4x^4 + 128K_2x^2 - 2K_1\left(3K_2x^2 + 64x^4\right) + 8C_1C_2^3x - 3C_2^4 + 4096x^4\right)}{128x^3} + \frac{2}{x} \tag{3.66}$$

$$\begin{aligned}\frac{\sigma^2}{C} = {} & C_3\left(\left(C_2 - C_1x\right)2 - 64x^2\right)^2\left(32768x^6\right)^{-1} \\ & \times\left(C_3\left(3\left(K_1 - 64\right)^2x^4 + \left(128 - 6K_1\right)K_2x^2 + 3C_2^4\right) + 256x^2\right)^2 \\ & \times\left[C_3\left(C_1x - 8x - C_2\right)\left(C_1x + 8x - C_2\right)\right]^{-1} \\ & \times\left[\left(\left(K_1 - 64\right)x^2 + 2C_1C_2x - 3K_2\right) + 256x^2\right]^{-1}\end{aligned} \tag{3.67}$$

The model above has a singularity at the origin as expected. In the case of dust, it is customary to locate the boundary of the distribution from $\rho(R) = 0$ since $p = 0$ for all r.

3.5.7 De and Raychaudhuri equilibrium $\sigma = \pm\rho$

De and Raychaudhuri [26] established that for a charged star to attain equilibrium the condition $\sigma^2 = \rho^2$ must be satisfied. This occurs when Coulombic repulsion equals the gravitational attraction. So we are therefore able to equate (3.2) and (3.5) to get

$$9\dot{Z}^2 = \frac{4Z}{x}\left(x\dot{E} + E\right)^2. \tag{3.68}$$

We now attempt to separate the variables:

$$x\dot{E} + E = \frac{3}{2}\dot{Z}\sqrt{\frac{x}{Z}} \tag{3.69}$$

$$\Rightarrow \frac{d}{dx}(xE) = \frac{3}{2}\dot{Z}\sqrt{\frac{x}{Z}} \tag{3.70}$$

$$\Rightarrow E = \frac{3}{2x}\int\left(\dot{Z}\sqrt{\frac{x}{Z}}\right)dx + C_1 \tag{3.71}$$

where C_1 is a constant of integration. With the help of (3.4) we obtain the integro–differential relationship

$$\frac{9}{4x^2}\left[\int\left(\dot{Z}\sqrt{\frac{x}{Z}}\right)dx\right]^2 = \frac{2}{x}\left(\dot{Z}x - Z + 1\right)$$

which may be recast as

$$\int \dot{Z}\sqrt{\frac{x}{Z}}dx = \frac{2\sqrt{2x}}{3}\sqrt{\dot{Z}x - Z + 1}. \tag{3.72}$$

Taking the derivative on both sides yields

$$\dot{Z}\sqrt{\frac{x}{Z}} = \frac{2}{3}\frac{d}{dx}\left(2\dot{Z}x^2 - 2Zx + 2x\right)^{\frac{1}{2}}. \tag{3.73}$$

After some simplification, we obtain the differential equation

$$9\dot{Z}^2x^2\left(\dot{Z}x - Z + 1\right) - Z\left(-Z + x\dot{Z} + x^2\ddot{Z} + 1\right)^2 = 0 \tag{3.74}$$

where the particular solution $Z = 1 + x$ may be inferred. However, we are unable to resolve the complete exact solution. The particular form $Z = 1 + x$ is precisely the Schwarzschild potential and has been shown to lead to a neutral sphere. However, we cannot rule out a more general solution to equation (3.74). A non–trivial general solution to (3.74) will be the unique solution for conformally flat charged spheres in equilibrium. If the Schwarzschild metric is the only such solution it will mean that conformally flat charged spheres cannot attain equilibrium.

3.5.8 Embedding class one

In order to embed a lower dimensional Riemannian spacetime into a higher dimensional Euclidean one, Karmarkar [32] established the necessary condition between the metric potentials. These spacetimes are referred to as being of embedding class 1 and the Riemann tensor components must obey [32]

$$R_{0303} = \frac{R_{0101}R_{2323} + R_{0113} + R_{0223}}{R_{1212}} \tag{3.75}$$

with $R_{1212} \neq 0$ [33]. The Karmarkar condition constrains the metric potentials according to the relationship

$$y = A + B\int\sqrt{\frac{1-Z}{Zx}}dx \tag{3.76}$$

where A and B are arbitrary constants. Observe that the Schwarzschild interior potential $Z = 1 + x$ is not admissible in equation (3.76) since this will require the function Z being negative, which is false, hence the Schwarzschild metric cannot be embedded into a higher dimensional spacetime. Combining with (3.6) we obtain

$$H\sqrt{x}\cosh\left(\frac{1}{2}\int\frac{dx}{x\sqrt{Z}}+J\right)=A+B\int\sqrt{\frac{1-Z}{Zx}}dx \tag{3.77}$$

where H and J are arbitrary constants for conformal flatness. An exact solution of (3.77) will be the unique solution for conformally flat charged spacetimes of embedding class 1. Clearly (3.77) appears to be an intractable equation to solve and so this remains an open problem. Again it is easy to see from the right hand side that the Schwarzschild potential $Z = 1 + x$ is inadmissible.

3.5.9 Conformal Killing vector

It is known from the work of Rahaman *et al* [34] and Ray *et al* [35] that for a spacetime to admit a one–parameter group of conformal motions, the temporal metric potential must be proportional to the square of the radius. In our scheme we put $y = ax$ for this purpose. Using this condition in equation (3.1) we get the metric potential,

$$Z = 1 + \frac{C_1}{x} \tag{3.78}$$

where C_1 is a constant of integration. Following this, we then obtain the other dynamical quantities from the field equations (2.38) to (2.41),

$$\frac{\rho}{C} = \frac{3C_1}{x^2} \tag{3.79}$$

$$\frac{p}{C} = \frac{3C_1 + 4x}{x^2} \tag{3.80}$$

$$\frac{E^2}{C} = -\frac{4C_1}{x^2} \tag{3.81}$$

$$\frac{\sigma^2}{C} = 0. \tag{3.82}$$

We do not proceed to plot these graphically as there are numerous contradictions in this case, such as a null charge density with the presence of an electric field. This is unacceptable. It has also been shown by [24] that no conformally flat charged spheres exist admitting a one–parameter group of conformal motions. We therefore see that this case is not physically viable.

3.5.10 Equation of state

The most physically important case is that of an equation of state $p = p(\rho)$ relating the pressure and energy density functionally. There are two important types which we consider below:

Barotropic: $p = \alpha\rho$

Applying this condition to (3.2) and (3.3) we have

$$\frac{\dot{Z}y + 4Z\dot{y}}{y} = -3\alpha\dot{Z} \tag{3.83}$$

and re-arranging results in

$$\frac{\dot{y}}{y} = -\frac{1+3\alpha}{4}\frac{\dot{Z}}{Z} \tag{3.84}$$

which has a first integral

$$y = C_1 Z^{-\frac{1+3\alpha}{4}} \tag{3.85}$$

where C_1 is a constant of integration. Substituting (3.85) in (3.1) gives a differential equation in terms of Z only

$$4(3\alpha+1)x^2 Z\ddot{Z} - 3(\alpha+1)(3\alpha+1)x^2\dot{Z}^2 + 4xZ\dot{Z} - 4Z^2 + 4Z = 0. \tag{3.86}$$

It is a difficult task solving (3.86) in general. For this reason different values of α within the range $[0, 1]$ could be considered to solve this differential equation.
Some relevant physical cases and the assosciated equation (3.86) are examined below.

(a) $\alpha = 0$ (Charged dust):

$$4x^2 Z\ddot{Z} + 4xZ\dot{Z} - 3x^2\dot{Z}^2 - 4Z^2 + 4Z = 0 \tag{3.87}$$

and the solution to this equation is given by

$$Z = \frac{C_2}{256x^2}\left((C_3 - C_1 x)^2 - 64x^2\right)^2 \tag{3.88}$$

as previously established.

(b) $\alpha = -1$ (Dark matter): This corresponds to a state of cosmic inflation for cosmological models. We then have

$$2x^2\ddot{Z} - x\dot{Z} + Z - 1 = 0 \tag{3.89}$$

and the non-trivial solution is given by

$$Z = C_2 x + C_1\sqrt{x} + 1 \tag{3.90}$$

with

$$p = -\rho = 3\left(\frac{C_1}{2\sqrt{x}} + C_2\right). \tag{3.91}$$

(c) $\alpha = \frac{1}{3}$ (Incoherent radiation): Here we consider a make up of relativistic massless particles. Equation (3.86) may be cast as

$$8x^2Z\ddot{Z} + 4xZ\dot{Z} - 8x^2\dot{Z}^2 - 4Z^2 + 4Z = 0. \tag{3.92}$$

In this case we were unable to find the general solution for Z, although $Z = 1$ is a known particular solution.

(d) $\alpha = 1$ (Stiff Fluid): Stiff fluids are the extreme cases where the sound speed equals the light speed. The master equation (3.86) assumes the form

$$4x^2Z\ddot{Z} + xZ\dot{Z} - 6x^2\dot{Z}^2 - Z^2 + Z = 0. \tag{3.93}$$

Once again we are unable to generate a general solution for this case as well but it may be noted that (3.93) admits the particular solution $Z = 1$.

Polytropic $p = \rho^n$

Using this prescription in (3.2) and (3.3) we obtain the equation

$$4Z\dot{y} + \left(\dot{Z} - \left(-3\dot{Z}\right)^n\right) y = 0 \tag{3.94}$$

which is complicated to manipulate. Therefore consider the special case for $n = 2$. Equation (3.94) reduces to

$$\dot{Z} + \frac{4Z\dot{y}}{y} = 9\dot{Z}^2 \tag{3.95}$$

which can be re-arranged as

$$\frac{\dot{y}}{y} = \frac{\dot{Z}(9\dot{Z} - 1)}{4Z}. \tag{3.96}$$

We now compute the derivative on both sides to get an expression for $\ddot{y}$ which becomes

$$\frac{\ddot{y}}{y} = \frac{\left(9\dot{Z} - 5\right)\left(9\dot{Z} - 1\right)\dot{Z}^2 + 4Z\left(18\dot{Z} - 1\right)\ddot{Z}}{16Z^2}. \tag{3.97}$$

If we divide (3.1) by y we obtain

$$4x^2Z\frac{\ddot{y}}{y} + 2x^2\dot{Z}\frac{\dot{y}}{y} - (\dot{Z}x - Z + 1) = 0. \tag{3.98}$$

And finally by inserting (3.97), the formidable differential equation

$$4x^2\left(18\dot{Z} - 1\right)\ddot{Z}Z - 4x\dot{Z}Z + x\dot{Z}^2\left(9\dot{Z} - 1\right)\left(9x\dot{Z} - 5x + 2\right) + 4Z^2 - 4Z = 0 \tag{3.99}$$

results. This illustrates the major challenge in modelling realistic relativistic stars. The analysis often reduces to solving an apparently intractible differential equation. It is hoped that more sophisticated mathematical techniques such as Lie group analysis may aid in unlocking the solutions. For now we were not able to isolate any exact soluton for conformally flat polytropes for the charged isotropic Einstein–Maxwell field equations.

3.6 Conclusion

In this chapter we have considered some prescriptions for the metric potential λ which generate exact solutions in terms of elementary functions. We first conducted an analysis of the equations in order to check for existence of solutions. Our analysis showed that spacetimes satisfying all the physical requirements were shown to exist subject to certain restriction. Graphical studies reveal that physically acceptable models are possible although each of our models suffered at least one major drawback. We have also investigated some cases of historical importance. These include incompressible fluid spheres, charged dust, isothermal fluids, conformal killing vector, De and Raychaudhuri equilibrium, embedding class 1 and various equations of state. In some cases it was possible to determine an exact solution however, in most situations the governing differential equations proved extremely complicated and did

not yield to known integration techniques. Such models could provide some insight if they were subjected to the approximation techniques of numerical analysis.

Chapter 4

Charged Stars of Embedding Class One

4.1 Introduction

In this chapter we abandon the geometric condition of conformal flatness but impose a new assumption of physical significance. We consider metrics of embedding class 1. The technique of embedding has been used to generate exact models in relativistic astrophysics. The Karmarkar condition gives a differential equation which relates the two gravitational potentials for static spherical spacetimes. This method has been used by Bhar *et al* [36], Maurya *et al* [37, 38, 39, 40] and Singh *et al* [41, 42] to generate anisotropic solutions of Embedding class 1. Two well known isotropic solutions are the Schwarzschild interior solution [4] and the Kohler-Chao solution [43], however these are not valid for charged stars. For our work, we set out to find new isotropic solutions using the Karmarkar condition incorporating the electromagnetic field.

4.2 New exact solutions of embedding class 1

As stated previously, the condition for a pseudo–Riemannian spacetime to be embedded into a higher dimensional pseudo–Euclidean one amounts to the restriction on the metric potentials

$$y = A + B\int \sqrt{\frac{1-Z}{Zx}}dx \tag{4.1}$$

where A and B are arbitrary constants. By specifying a metric potential Z, we are theoretically able to find a solution for y. The condition for pressure isotropy remains unchanged and can be rearranged in the following form

$$\frac{E^2}{C} = \frac{4x^2Z\ddot{y} + x\left(2x\dot{y} + y\right)\dot{Z} + y\left(1-Z\right)}{xy} \tag{4.2}$$

from which we can obtain the electric field intensity E once Z and y are known. We now can revisit (2.38), (2.39) and (2.41) to obtain the other dynamical quantities ρ, p and σ which we list below:

$$\frac{\rho}{C} = \frac{2y\left(1-Z\right) - 4xy\dot{Z} - 4x^2Z\ddot{y} - x\left(2x\dot{y} + y\right)\dot{Z} - y(Z-1)}{2xy} \tag{4.3}$$

$$\frac{p}{C} = \frac{2y\left(Z-1\right) + 8xZ\dot{y} + 4x^2Z\ddot{y} + x\left(2x\dot{y} + y\right)\dot{Z} + y(Z-1)}{2xy} \tag{4.4}$$

$$\frac{\sigma^2}{C} = \frac{4Z}{x}\left(x\dot{E} + E\right)^2. \tag{4.5}$$

The exercise of finding suitable metrics for charged perfect fluids of embedding class 1 reduces to finding Z, y functions satisfying (4.1). Theoretically this is a very straight forward exercise however, the challenge lies in locating solutions that satisfy the elementary physical requirements.

4.2.1 $Z = k$ – a constant

We begin with the simple prescription of Z being a constant. The importance of this selection in relation to the isothermal behaviour of static neutral spheres has already been discussed in the previous chapter. Using $Z = k$ in (4.1) we get

$$y = A + 2B\sqrt{\frac{x\,(1-k)}{k}} \tag{4.6}$$

where A and B are arbitrary constants. We immediately see a restriction. To obtain real valued functions, k must lie between 0 and 1. We can then obtain the dynamical quantities in the form

$$\frac{\rho}{C} = \frac{(k-1)\,(Ak\alpha\sqrt{x} + 2Bx)}{2x\,(2B(k-1)x - Ak\alpha\sqrt{x})} \tag{4.7}$$

$$\frac{p}{C} = \frac{A^2(k-1)k + 6ABk^2\alpha\sqrt{x} + 4B^2(k-1)(4k-1)x}{2x\,(A^2k + 4B^2(k-1)x)} \tag{4.8}$$

$$\frac{E^2}{C} = \frac{(k-1)\,(2B(2k-1)x - Ak\alpha\sqrt{x})}{x\,(Ak\alpha\sqrt{x} - 2B(k-1)x)} \tag{4.9}$$

$$\begin{aligned}\frac{\sigma^2}{C} = {} & (k-1)^2k^2x\left(A^3(k-1)k + 3A^2Bk(3k-2)\alpha\sqrt{x}\right. \\ & \left.-2AB^2(k-1)(11k-6)x - 8B^3(k-1)(2k-1)x\alpha\sqrt{x}\right)^2 \Big/ \\ & \left(2B(k-1)x - Ak\alpha\sqrt{x}\right)^5\left(2B(2k-1)x - Ak\alpha\sqrt{x}\right)\end{aligned} \tag{4.10}$$

where we have set $\alpha = \sqrt{\left(\frac{1}{k} - 1\right)}$ for simplicty. We do not plot the graphs here, in favour of more pleasing physical models to follow. What may be observed is that the solution is not isothermal except when $A = 0$, in which case ρ and p vary as $\frac{1}{r^2}$. However, $A = 0$ leads to a constant potential y which is not physically viable.

4.2.2 $Z = 1 + x$ - the Schwarzschild interior ansatz

Another popular case worth examining is the Schwarzschild interior metric [4]. Introducing the prescription $Z = 1 + x$ in (4.1) we get

$$y = A + 2B\sqrt{1 + x} \tag{4.11}$$

where A and B are arbitrary constants. But it is known that the Schwarzschild interior metric cannot be valid for charged stars as shown by Hansraj *et al* [24] since the electric field vanishes. We merely include this case for completeness.

4.2.3 $Z = \frac{1}{1+x}$ – The Finch–Skea metric ansatz

Using the Finch-Skea [15] metric $Z = \frac{1}{1+x}$, the general solution to equation (4.1) has the form

$$y = A + Bx \tag{4.12}$$

where A and B are arbitrary constants. It is convenient to let $\beta = \frac{A}{B}$, and so the dynamical quantities may be expressed as

$$\frac{\rho}{C} = \frac{\beta(x + 6) + x(x + 8)}{2(x + 1)^2(\beta + x)} \tag{4.13}$$

and at the centre

$$\left(\frac{\rho}{C}\right)_0 = 3 \tag{4.14}$$

where the subscript 0 is used to denote quantity values at the stellar centre $x = 0$. For the pressure

$$\frac{p}{C} = \frac{(-x^2 + 4x + 8) - \beta(x + 2)}{2(x + 1)^2(\beta + x)} \tag{4.15}$$

and at the centre

$$\left(\frac{p}{C}\right)_0 = \frac{8-2\beta}{2\beta} \tag{4.16}$$

for $x = 0$. Positivity of the central pressure demands

$$0 < \beta < 4 \tag{4.17}$$

as a constraint on β. The electric field intensity is given by

$$\frac{E^2}{C} = \frac{x[\beta + (x-2)]}{(x+1)^2(\beta+x)} \tag{4.18}$$

and this quantity vanishes at the centre, as expected. The charge density has the form

$$\left(\frac{\sigma^2}{C}\right) = \frac{\left[\beta^2(x+3) + 2\beta(x-1)(x+3) + (x-1)x(x+4)\right]^2}{(x+1)^5(\beta+x-2)(\beta+x)^3} \tag{4.19}$$

and at the centre

$$\left(\frac{\sigma^2}{C}\right)_0 = \frac{3}{\beta^2} \tag{4.20}$$

which is positive for all β values. The expressions for the energy conditions are given by

$$\rho - p = \frac{\beta(x+4) + (x^2+2x-4)}{(x+1)^2(\beta+x)} \tag{4.21}$$

$$\rho + p = \frac{2(\beta + (3x+2))}{(x+1)^2(\beta+x)} \tag{4.22}$$

$$\rho + 3p = \frac{(-x^2+10x+12) - \beta x}{(x+1)^2(\beta+x)} \tag{4.23}$$

and these are all expected to be positive. The square of the speed of sound index is given by

$$\left(\frac{dp}{d\rho}\right) = \frac{-\beta^2(x+3) - 2\beta\,(x^2-5) + (-x^3+9x^2+24x+8)}{\beta^2(x+11) + 2\beta\,(x^2+12x-1) + x^2(x+15)} \tag{4.24}$$

and at the centre ($x = 0$):

$$\left(\frac{dp}{d\rho}\right)_0 = \frac{-3\beta^2+10\beta+8}{11\beta^2-2\beta} \tag{4.25}$$

which places a further restriction on β, namely

$$1.3 < \beta < 4. \tag{4.26}$$

The adiabatic stability index has the form

$$\left(\frac{\rho+p}{p}\right)\frac{dp}{d\rho} = \frac{4(\beta+3x+2)\,(\beta^2(x+3)+2\beta\,(x^2-5)+(x(x^2-9x-24)-8))}{(\beta x+2\beta+x^2-4x-8)\,(\beta^2(x+11)+2\beta(x^2+12x-1)+x^3+15x)} \tag{4.27}$$

and at the centre ($x = 0$):

$$\left[\left(\frac{\rho+p}{p}\right)\frac{dp}{d\rho}\right]_0 = \frac{4(\beta+2)(3\beta^2-10\beta-8)}{(2\beta-8)(11\beta^2-2\beta)} > \frac{4}{3} \tag{4.28}$$

giving

$$0.18 < \beta < 2.52 \tag{4.29}$$

as a restriction on β. Finally harmonising all the restrictions we have established, we obtain the window

$$1.3 < \beta < 2.52 \tag{4.30}$$

on β which we will use when choosing suitable constants to model stars. The mass profile is given by

$$\begin{aligned} M &= \{(x+1)\left(4A^{3/2}\sqrt{B}\tan^{-1}\left(\sqrt{\frac{Bx}{A}}\right)+\left(3A^2-12AB+5B^2\right)\tan^{-1}\left(\sqrt{x}\right)\right) \\ &\quad +\sqrt{x}(A-B)(A(2x-3)+B(5-2x))\} \\ &\quad \div\left[4(x+1)(A-B)^2\right] \end{aligned} \tag{4.31}$$

and the compactification expression $\frac{m}{r}$ reduces to

$$\begin{aligned} \frac{M}{\sqrt{x}} &= \{(x+1)\left(4A^{3/2}\sqrt{B}\tan^{-1}\left(\sqrt{\frac{Bx}{A}}\right)+\left(3A^2-12AB+5B^2\right)\tan^{-1}\left(\sqrt{x}\right)\right) \\ &\quad +\sqrt{x}(A-B)(A(2x-3)+B(5-2x))\} \\ &\quad \div\left[4\sqrt{x}(x+1)(A-B)^2\right]. \end{aligned} \tag{4.32}$$

Finally, the equation of state expression $\frac{p}{\rho}$ has the form

$$\frac{p}{\rho}=\frac{4(\beta+3x+2)}{\beta(x+6)+x(x+8)}-1 \tag{4.33}$$

In the Finch-Skea case, from (4.13) we see that the density is always positive. From equation (4.15) it is possible to infer the existence of a finite boundary $p(R)=0$ on account of the existence of a zero of the numerator. The electric field intensity and charge density are well behaved functions, decreasing outwardly from the centre.
We now analyse graphical plots of the dynamical quantities. These plots have been constructed using parameter values $A=1$ and $B=0.5$, so $\beta=2$ which fall within the accepted range shown in (4.30).

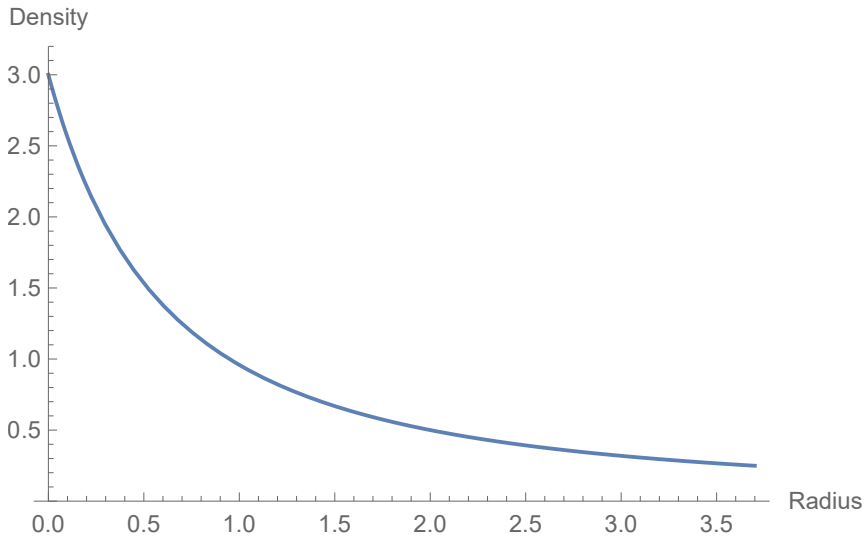

Figure 4.1: Density ρ versus the radial variable x.

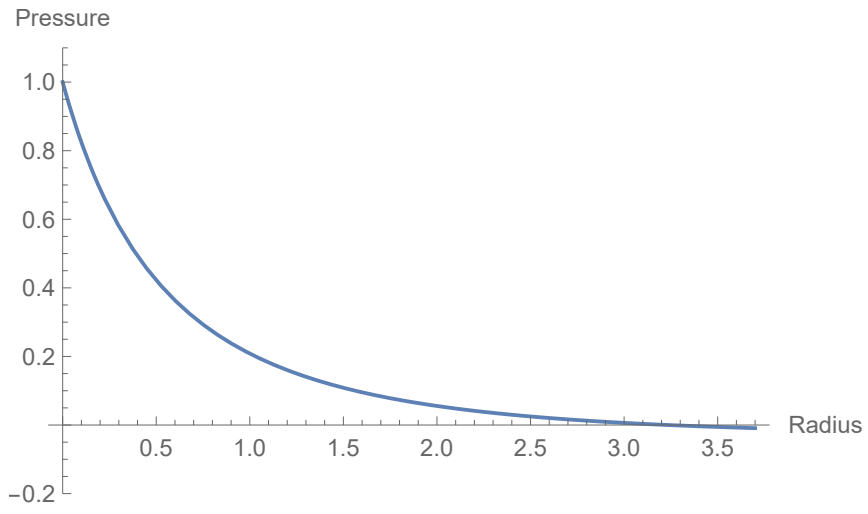

Figure 4.2: Pressure p versus the radial variable x.

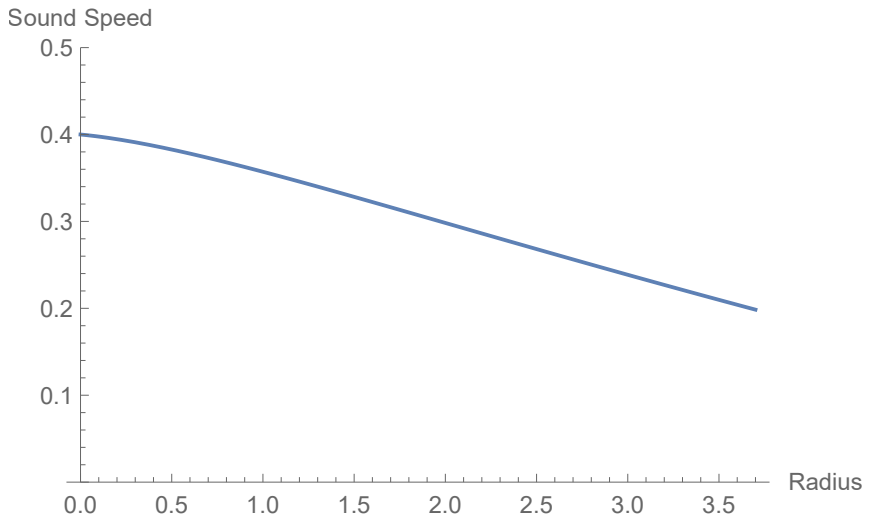

Figure 4.3: Sound speed index $\frac{dp}{d\rho}$ versus the radial variable x.

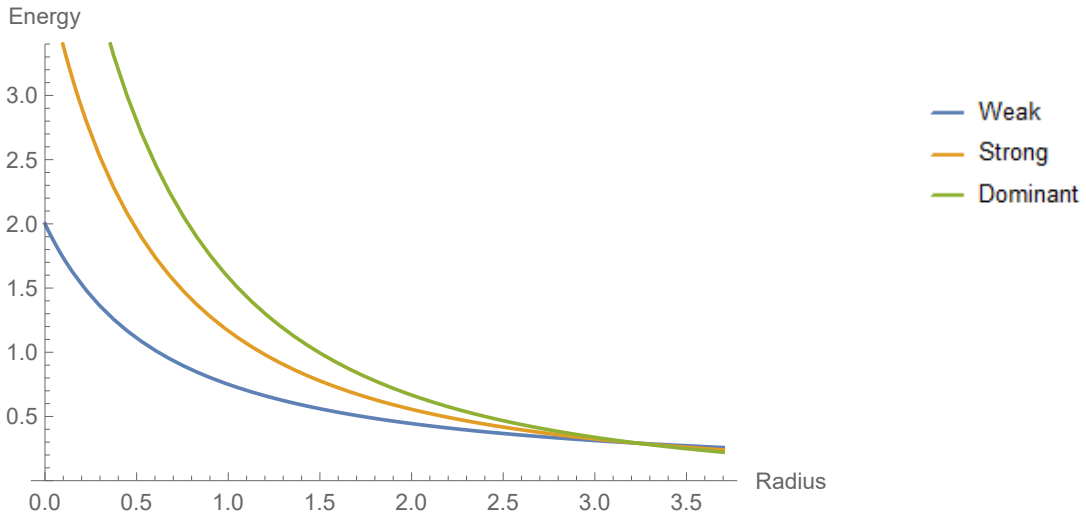

Figure 4.4: Energy conditions versus the radial variable x.

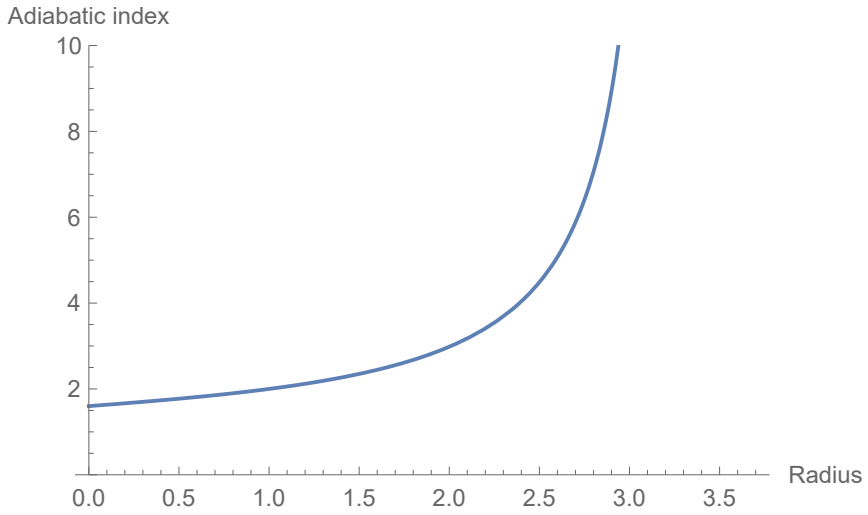

Figure 4.5: Chandrasekhar adiabatic stability index versus the radial variable x.

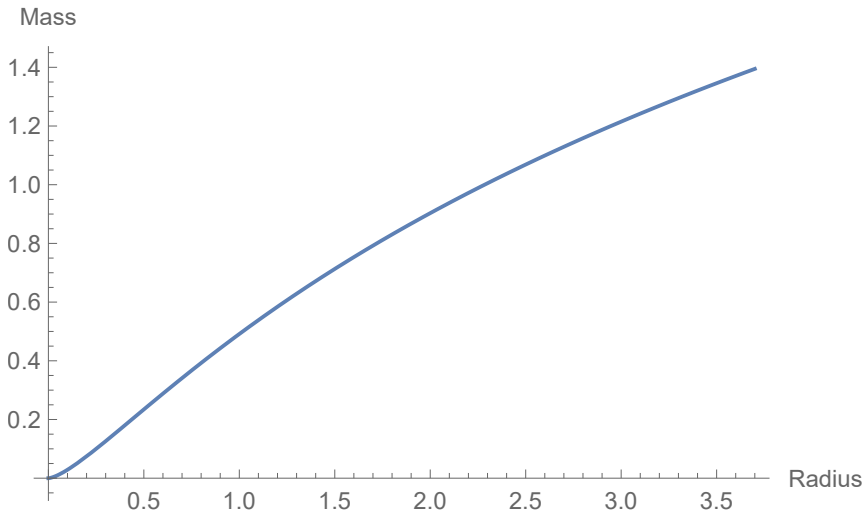

Figure 4.6: Mass profile versus the radial variable x.

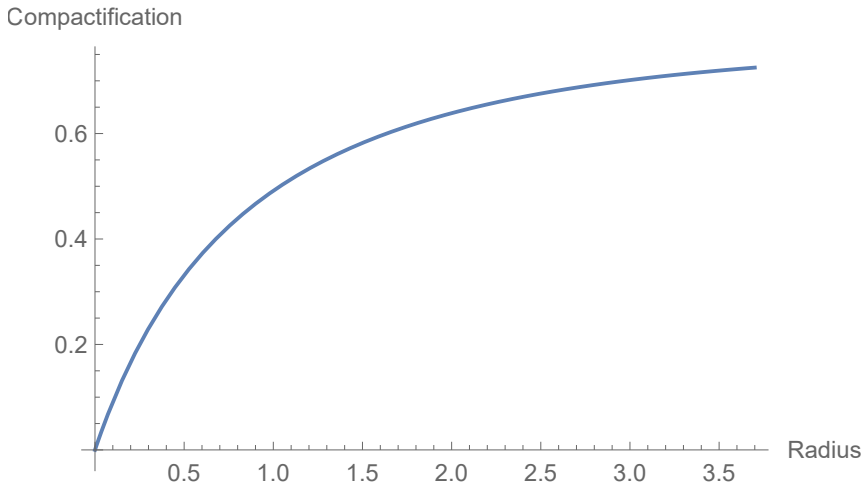

Figure 4.7: Compactification versus the radial variable x.

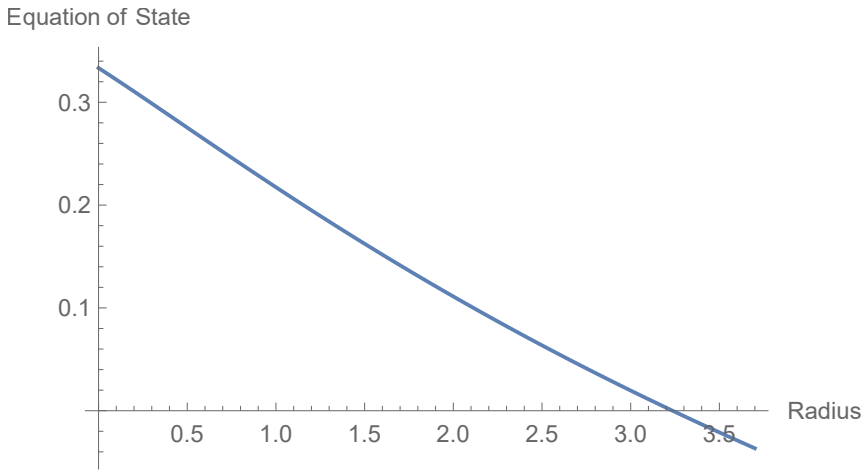

Figure 4.8: Equation of state $\frac{p}{\rho}$ versus the radial variable x.

From Figure 4.1 and Figure 4.2 we see that the pressure and density are both monotonically decreasing, which is expected. We also note that the pressure cuts the x-axis at $x = 3.23$, which determines the radius of the star. The sound speed index shown in Figure 4.3 is less than 1 which confirms the model as causal. It can be observed from Figure 4.4 that all the energy conditions are positive and hence satisfied. The adiabatic index demonstrated in Figure 4.5 is positive and is in the accepted range of being more than $\frac{4}{3}$ for the radius of the star. In Figure 4.6 we see that the mass profile appears well behaved as an increasing function of the radius with a value of $M = 1.27$ at the radius. The compactification curve displayed in Figure 4.7 is a smooth, increasing function. The equation of state profile against the radial variable in Figure 4.8 is almost linear and decreasing.

The line element for the star at the boundary ($r = R$) has the form

$$ds^2 = -\left(A + BCR^2\right)^2 dt^2 + \left(1 + CR^2\right) dr^2 + r^2(d\theta^2 + \sin^2\theta d\phi^2) \tag{4.34}$$

which can be matched with the Reissner-Nordstrom exterior line element [5, 6] shown in (2.42). This gives

$$\frac{1}{1 + CR^2} = \left(A + BCR^2\right)^2 = 1 - \frac{2M}{R} + \frac{Q^2}{R^2}. \tag{4.35}$$

The pressure vanishing at the boundary results in the following condition

$$\left(-C^2R^4 + 4CR^2 + 8\right) - \frac{A}{B}\left(CR^2 + 2\right) = 0 \tag{4.36}$$

from which we can get a relation on the integration constants as

$$A = \frac{B\left(-C^2R^4 + 4CR^2 + 8\right)}{CR^2 + 2} \tag{4.37}$$

and using the condition from (4.35) we are able to write B as

$$B = \left(1 - \frac{2M}{R} + \frac{Q^2}{R^2}\right)^{\frac{1}{2}} \left[6 - \frac{4}{CR^2 + 2}\right]^{-1} \tag{4.38}$$

which settles the integration constants A and B. We are now able to proceed to use numerical values to settle the other constants and find the relevant ratios. From (4.36) using our careful selection of $A = 1$ and $B = 0.5$ which yielded a radius at the boundary of $R = 3.23$, we obtain $C = 0.31$. Taking into consideration the radial electric field (2.43) we get the following expression

$$\frac{CR^2\left(\frac{A}{B} + CR^2 - 2\right)}{\left(CR^2+1\right)^2\left(\frac{A}{B} + CR^2\right)} = \frac{Q}{R^2} \tag{4.39}$$

where the numerical values are again used to obtain $Q = 1.16$. A maximum mass–radius ratio of 0.79 was determined and this is less than $\frac{8}{9}$ as required by Buchdahl [17]. The Böhmer and Harko [18] upper bound is also satisfied with a left hand side of 0.19 which is less than the limit 0.79. The Andréasson [19] limit has also been satisfied, with the left hand side value of 1.13 being less than the limit of 1.30. Finally, we obtain a mass–charge ratio of 1.09 which is greater than 1 as demanded by Cooperstock and de la Cruz [20]. We can now state that this model satisfies all requirements for physical viability.

4.2.4 $Z = \frac{1+x}{1+2x}$ – A special case of Vaidya–Tikekar

Another interesting case is that of a superdense star. Such a model was developed by Vaidya and Tikekar [31]. Using the metric ansatz $Z = \frac{1+x}{1+2x}$, the general solution has the form

$$y = A + 2B\sqrt{x+1} \tag{4.40}$$

which turns out to be the Schwarzschild interior temporal potential. For simplicity, we now set $\sqrt{1+x} = u$ and we let $\beta = \frac{A}{B}$. The dynamical quantities have the form

$$\left(\frac{\rho}{C}\right) = \frac{\beta(x+3)u + (4x+6)}{(2x+1)^2(\beta u + 2)} \tag{4.41}$$

and at the centre ($x = 0$):

$$\left(\frac{\rho}{C}\right)_0 = 3 \tag{4.42}$$

For the pressure

$$\left(\frac{p}{C}\right) = \frac{u(4x+2)-\beta}{(2x+1)^2\,(\beta u+2)} \tag{4.43}$$

which should vanish at the radius, giving us the roots

$$\begin{aligned} x_0 &= \frac{1}{12}\left(\sqrt[3]{54\beta^2+6\sqrt{3}\sqrt{\beta^2\,(27\beta^2-8)}-8}\right. \\ &\left. +\frac{2^{5/3}}{\sqrt[3]{27\beta^2+3\sqrt{3}\sqrt{\beta^2\,(27\beta^2-8)}-4}}-8\right) \end{aligned} \tag{4.44}$$

$$\begin{aligned} x_{1,2} &= \frac{1}{24}\left[\left(\pm i\sqrt{3}-1\right)\sqrt[3]{54\beta^2+6\sqrt{3}\sqrt{\beta^2\,(27\beta^2-8)}-8}\right. \\ &\left. \mp\frac{2\;2^{2/3}\left(\pm 1+i\sqrt{3}\right)}{\sqrt[3]{27\beta^2+3\sqrt{3}\sqrt{\beta^2\,(27\beta^2-8)}-4}}-16\right] \end{aligned} \tag{4.45}$$

consequently, for the real root (4.44) to be positive it requires

$$\beta < -2 \vee \beta > 2 \tag{4.46}$$

and at the centre ($x = 0$):

$$\left(\frac{p}{C}\right)_0 = \frac{2-\beta}{2+\beta} \tag{4.47}$$

and since the pressure must be positive it demands

$$-2 < \beta < 2 \tag{4.48}$$

which contradicts (4.46). The electric field intensity is given by

$$\frac{E^2}{C} = \frac{2\beta ux}{(2x+1)^2(\beta u+2)} \tag{4.49}$$

and this has a 0 value at the centre. The charge density has the form

$$\left(\frac{\sigma^2}{C}\right) = \frac{2\beta u^3\left(\beta^2(2x+3)+\beta(6x^2+19x+12)u+2(2x^2+9x+6)\right)^2}{(2x+1)^5(\beta u+2)^5} \tag{4.50}$$

which simplifies to

$$\left(\frac{\sigma^2}{C}\right)_0 = \frac{2\beta\left(3\beta^2+12\beta+12\right)^2}{(\beta+2)^5} \tag{4.51}$$

at the centre of a charged star. The expressions for the energy conditions are given by

$$\rho - p = \frac{2\beta(x+2)u+4}{(2x+1)^2(\beta u+2)} \tag{4.52}$$

$$\rho + p = \frac{2\beta u+8(x+1)}{(2x+1)^2(\beta u+2)} \tag{4.53}$$

$$\rho + 3p = \frac{2\left(8x+6-\beta ux\right)}{(2x+1)^2(\beta u+2)} \tag{4.54}$$

and these are all expected to be positive.

The speed of sound squared index is given by

$$\left(\frac{dp}{d\rho}\right) = \frac{\beta^2(2x+3)+\beta\left(2x^2+5x+4\right)u-8\left(2x^2+3x+1\right)}{\beta^2(2x+11)+\beta\left(10x^2+53x+42\right)u+8\left(2x^2+7x+5\right)} \tag{4.55}$$

and is reduced to

$$\left(\frac{dp}{d\rho}\right)_0 = \frac{3\beta^2+4\beta-8}{11\beta^2+42\beta+40} \tag{4.56}$$

at the centre, which places a further restriction on β

$$\beta < -2.43 \vee \beta > 1.09 \tag{4.57}$$

to ensure a subluminal sound speed $0 < \frac{dp}{d\rho} < 1$ at $x = 0$. The adiabatic stability index given by

$$\left(\frac{\rho+p}{p}\right)\frac{dp}{d\rho} = \frac{-u\left(2\beta u + 8(x+1)\right)\left(\beta^2(2x+3) + u\beta(2x^2+5x+4) - 8(2x^2+3x+1)\right)}{\left(u(4x+2)-\beta\right)\left(\beta^2(2x+11) + u\beta(10x^2+53x+42) + 8(2x^2+7x+5)\right)} \tag{4.58}$$

evaluates to

$$\left[\left(\frac{\rho+p}{p}\right)\frac{dp}{d\rho}\right]_0 = \frac{(-2\beta-8)\left(3\beta^2+4\beta-8\right)}{(2-\beta)\left(11\beta^2+42\beta+40\right)} > \frac{4}{3} \tag{4.59}$$

at the centre. This inequality is satisfied provided

$$-2.25 < \beta < -2 \vee -1.81 < \beta < -0.62 \vee 2 < \beta < 3.49 \tag{4.60}$$

From our restrictions on β, it is evident that there is no interval that would give a valid selection for our constants. The mass profile is given by

$$\begin{aligned}
M \;=\; & \left[\frac{2\sqrt{x}}{2x+1}\left(A^2-2B^2\right)\left(A^2(8x-1)+\frac{2AB}{u}-16B^2x\right)\right. \\
& +\frac{A}{B}\left[-2\left(A^2-2B^2\right)^2\log\left(u\sqrt{x}+x+u\right)\right. \\
& +2A\left(4B^2-A^2\right)^{3/2}\tan^{-1}\left(\frac{2B\sqrt{x}}{\sqrt{4B^2-A^2}}\right) \\
& -8AB^2\sqrt{4B^2-A^2}\tan^{-1}\left(\frac{Au\sqrt{x}}{\sqrt{4B^2-A^2}}\right) \\
& -4B^2\left(A^2-4B^2\right)\tan^{-1}\left(u\sqrt{x}\right)+\sqrt{2}AB\left(3A^2-10B^2\right)\tan^{-1}\left(\sqrt{2}\sqrt{x}\right) \\
& \left.\left.+2A^3\sqrt{4B^2-A^2}\tan^{-1}\left(\frac{Au\sqrt{x}}{\sqrt{4B^2-A^2}}\right)\right]\right] \\
& \div 16\left(A^2-2B^2\right)^2
\end{aligned} \tag{4.61}$$

and the compactification expression takes the form

$$\begin{aligned}\frac{M}{\sqrt{x}} &= \left[\frac{2\sqrt{x}}{2x+1}\left(A^2-2B^2\right)\left(A^2(8x-1)+\frac{2AB}{u}-16B^2x\right)\right.\\
&+\frac{A}{B}\left[-2\left(A^2-2B^2\right)^2\log\left(u\sqrt{x}+x+u\right)\right.\\
&+2A\left(4B^2-A^2\right)^{3/2}\tan^{-1}\left(\frac{2B\sqrt{x}}{\sqrt{4B^2-A^2}}\right)\\
&-8AB^2\sqrt{4B^2-A^2}\tan^{-1}\left(\frac{Au\sqrt{x}}{\sqrt{4B^2-A^2}}\right)\\
&-4B^2\left(A^2-4B^2\right)\tan^{-1}\left(u\sqrt{x}\right)+\sqrt{2}AB\left(3A^2-10B^2\right)\tan^{-1}\left(\sqrt{2}\sqrt{x}\right)\\
&\left.\left.+2A^3\sqrt{4B^2-A^2}\tan^{-1}\left(\frac{Au\sqrt{x}}{\sqrt{4B^2-A^2}}\right)\right]\right]\\
&\div 16\sqrt{x}\left(A^2-2B^2\right)^2. \qquad (4.62)\end{aligned}$$

Finally, the equation of state indicator $\frac{p}{\rho}$ is given by

$$\frac{p}{\rho}=\frac{u(4x+2)-\beta}{u\left[u\beta(x+3)+(4x+6)\right]}. \qquad (4.63)$$

In this case, from (4.41) we see that the density is positive. The electric field intensity and charge density are well behaved functions, decreasing outwardly from the centre.

We now analyse graphical plots of the dynamical quantities. These plots have been constructed using parameter values $A=-7$ and $B=10$ for illustrative purposes. Note that $\beta=-0.7$, which violates the requirement for the existence of a boundary $\beta<-2$ or $\beta>2$. In other words we sacrifice the boundedness property and consequently the fluid must have a cosmological application.

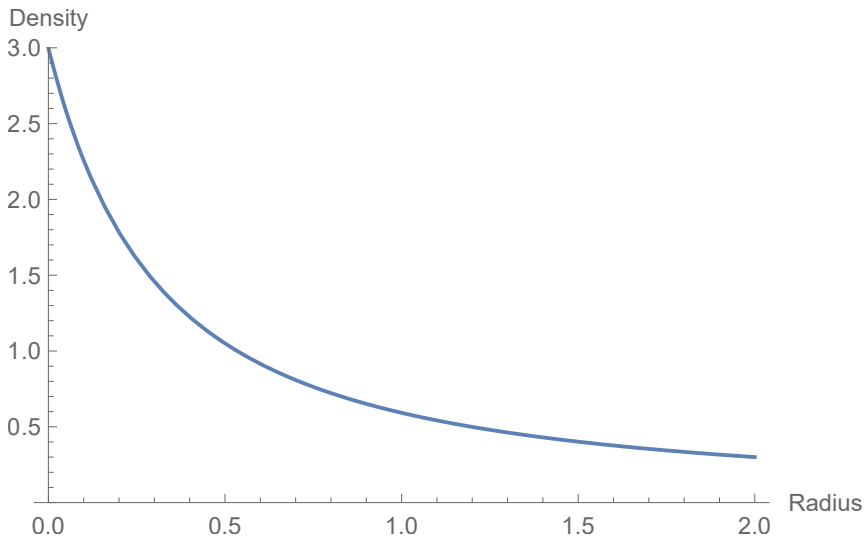

Figure 4.9: Density ρ versus the radial variable x.

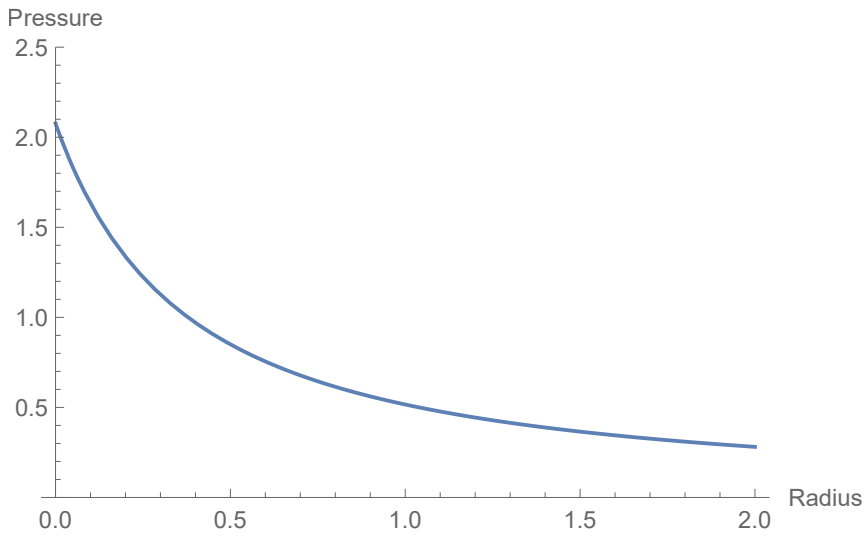

Figure 4.10: Pressure p versus the radial variable x.

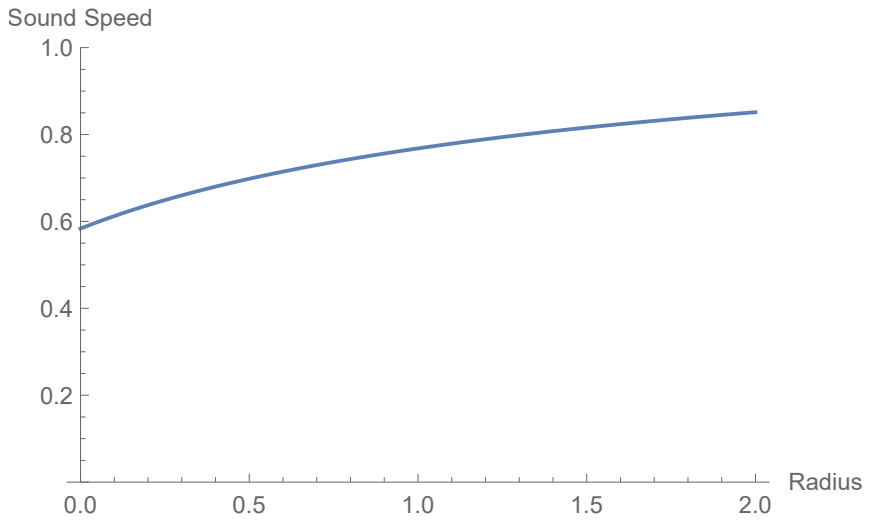

Figure 4.11: Sound speed index $\frac{dp}{d\rho}$ versus the radial variable x.

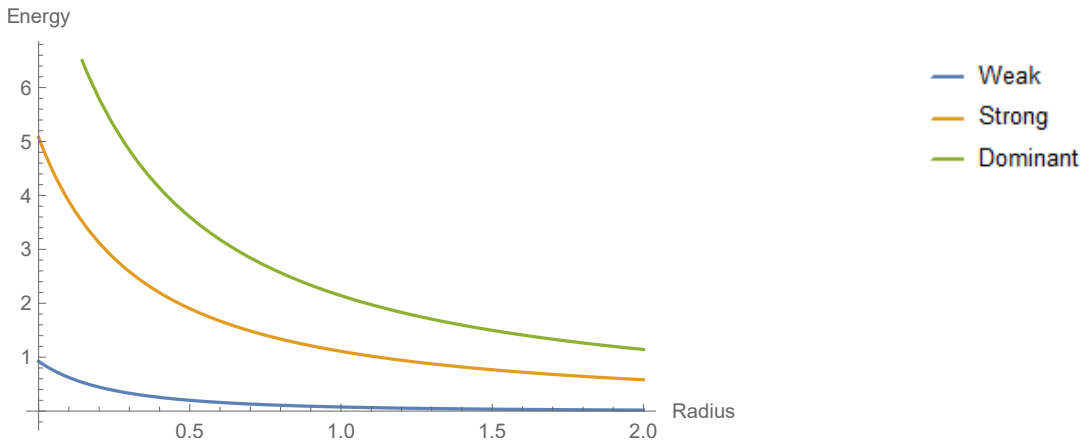

Figure 4.12: Energy conditions versus the radial variable x.

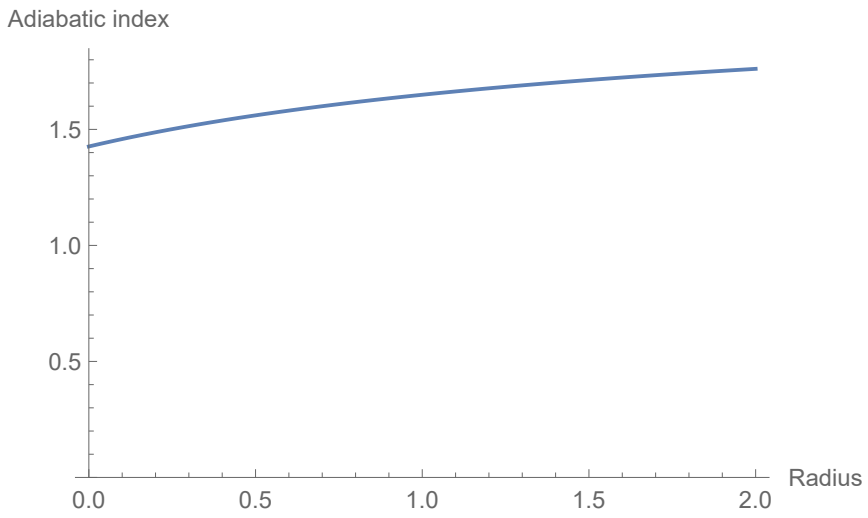

Figure 4.13: Chandrasekhar adiabatic stability index versus the radial variable x.

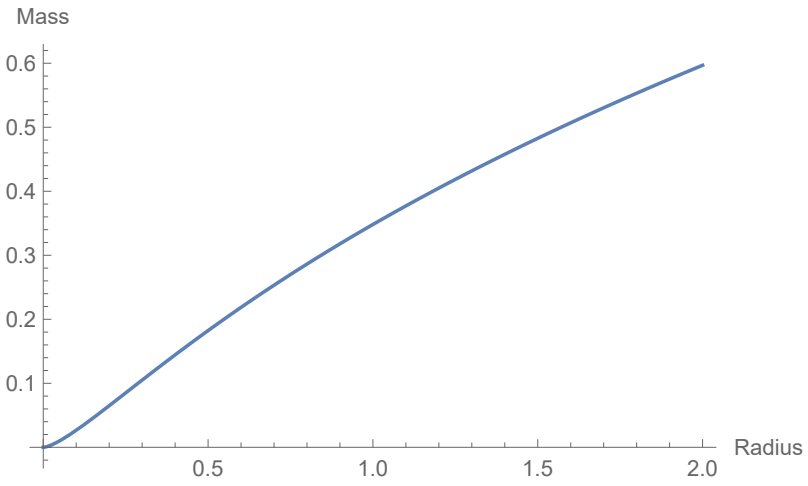

Figure 4.14: Mass profile versus the radial variable x.

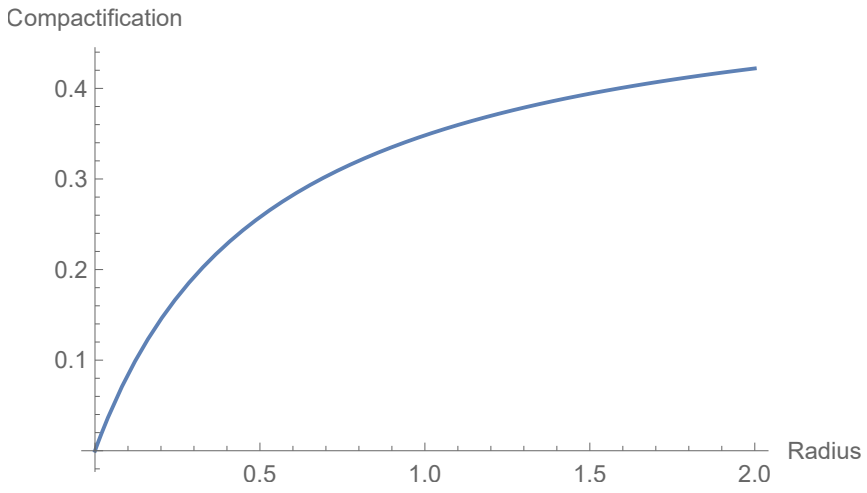

Figure 4.15: Compactification versus the radial variable x.

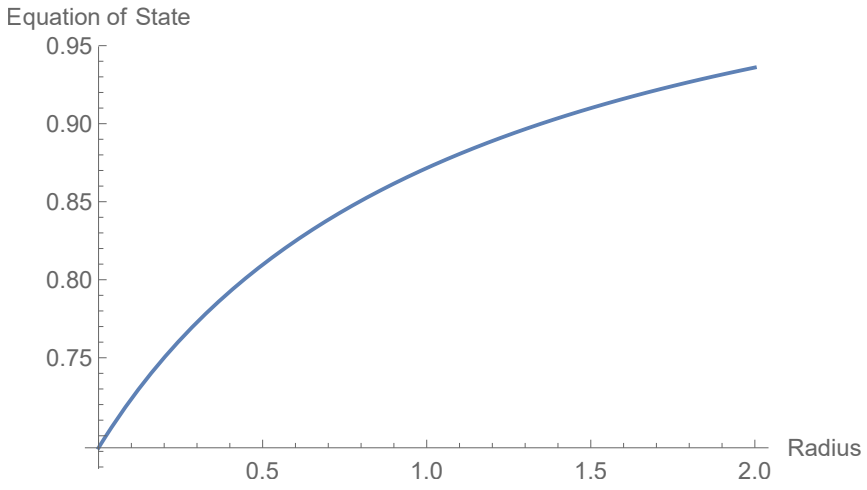

Figure 4.16: Equation of state $\frac{p}{\rho}$ versus the radial variable x.

Figure 4.9 and Figure 4.10 depict the pressure and density are both monotonically decreasing, which is expected. We also note that the pressure is asymptotic hence the model may be interpreted as a cosmological fluid. The sound speed index in Figure 4.11 is less than 1 which confirms the model as causal. It can be observed from Figure 4.12 that all the energy conditions are positive and hence satisfied. The adiabatic index shown in Figure 4.13 is positive and is in the accepted range of being more than $\frac{4}{3}$ for the radius of the star. The mass profile and compactification displayed in Figure 4.14 and Figure 4.15 appears well behaved as increasing functions of the radius. The equation of state profile demonstrated in Figure 4.16 is a smooth and increasing function. This model therefore satisfies most requirements for physical viability as a cosmological fluid in view of the absence of a vanishing pressure surface.

4.3 Other solvable cases

There exists a large number of exact models for charged isotropic fluid spheres of embedding class 1. We tabulate a few solutions in Table 4.1 but do not engage in a study of any, as we have exhibited two simple models that satisfy all or most physical requirements.

Table 4.1: Viable metric potentials for embedding class 1 spacetimes

Z	y
$\frac{1}{x}$	$A+B\left(\sqrt{x\left(x+1\right)}+\cos^{-1}\sqrt{x}\right)$
$\frac{1}{1+x^2}$	$A+\frac{2}{3}Bx^{3/2}$
$\frac{1}{1+x^3}$	$A+\frac{1}{2}Bx^2$

The table contains a small sample of exact solutions. A much wider class exists for charged spheres of embedding class 1.

4.4 Conclusion

In this chapter, we used the Karmarkar condition for metrics of embedding class 1 in order to generate new exact models. We first looked at some simple cases and then analysed the Finch-Skea solution in detail, where we have found new results for charged stars that satisfy all the physical conditions. In addition, the Vaidya–Tikekar solution was also analysed and models were produced. Finally, we listed some other metric potentials that may also produce viable solutions.

Chapter 5

Einstein–Gauss–Bonnet Theory

5.1 Introduction

The general theory of relativity faces challenges in explaining the strange behaviour of some gravitational phenomena such as the late time accelerated expansion of the universe [44, 45]. This has piqued interest in alternate or extended theories of gravity in order to better explain these observations. One approach to solving this is conjecturing the existence of exotic matter fields such as dark matter, dark energy, phantom fields and quintessence fields. Alternatively one can re-examine the geometrical side of the field equations. It is also important to consider the effects of higher curvature contributions. Particularly, Einstein–Gauss–Bonnet (EGB) theory which is extensively studied, as it has proved quite promising in this regard. Note that EGB belongs to a more general class of theories called the Lovelock polynomial Lagrangians which constitute the most general tensor theory generating at most second order equations of motion. If the Lagrangian is allowed to involve both tensor and scalar fields then the most general such theory is due to Horndeski [46]. Another powerful motivation for EGB theory is the natural appearance of the Gauss–Bonnet Lagrangian in the effective action of heterotic string theory in the low energy

limit [47]. The singularities which have a causal structure is different from general relativity for inhomogeneous distributions of dust and null dust [48].

Historically black hole models in EGB theory have been thoroughly studied. Boulware and Deser [49] generalized the higher dimensional solutions in Einstein theory due to Tangherlini [50], and by Myers and Perry [51] to include the contribution of the EGB theory with quadratic curvature terms. Wheeler [52], Torii and Maeda [53] and Myers and Simons [54] have also considered black hole solutions in EGB theory. Pressure–free fluid with non–interacting particles, known as the inhomogenous collapse of dust was studied by Maeda [55]. Explicit exact solutions were obtained by Jhingan and Ghosh [56]. An important proof by Dadhich *et al* [57] was that the constant density Schwarzschild interior solution is universal in the sense that it is valid in both higher dimensional Einstein theory as well as in EGB gravity and its generalisation Lovelock theory. Analytical models were produced by matching of these exterior metrics to an interior for brane world stars also requiring dimensions higher than 4 and was investigated by Casadio and Ovalle [58]. Clifton *et al* [59] analysed the matching of isolated masses to a Schwarzschild exterior.

The first nontrivial compact star object in 5–dimensional EGB theory was the constant density configuration of Dadhich *et al* [57] but it suffers a major drawback, like its 4–dimensional counterpart, of having an infinite sound speed thus making it non-physical. The static spherically symmetric star of Kang *et al* [60] needs to satisfy the junction conditions of EGB gravity so that matching is possible at the stellar hypersurface. Davis [61] derived the junction conditions for EGB which are nontrivial and very different from general relativity. Note that the variable density model of Kang *et al* [60] requires a further integration to produce an exact solution. Variable density spherically symmetric exact solutions to the EGB field equations were first obtained by Hansraj *et al*, Maharaj *et al*, Chilambwe *et al* [62, 63, 64] and shown to

be consistent with the usual elementary expectations of astrophysical models. When one of the field equations are replaced by the equation of hydrodynamic equilibrium, namely the vanishing divergence of the energy momentum tensor, then it is advisable to invoke an equation of state relating the pressure and energy density. This approach has been used by [60] in their attempt to find an exact model. Interestingly the interior model presented in [60] generates the well known vacuum metric [49] of EGB in the limit of vanishing pressure and density.

Local anisotropy in self-gravitating systems within the framework of classical general relativity has been extensively studied [65, 66, 67, 68]. In the study of compact objects such as pulsars, neutrons stars and quark stars in 4–D gravity the inclusion of pressure anisotropy has led to physically viable stellar models. Analyses of the physical attributes of these models such as density profiles, pressure profiles, compactness and surface redshift agree with observed data within experimental error. The anisotropy parameter $\Delta = p_T - p_R$ can either be positive or negative at each interior point of the matter configuration. When $p_T > p_R$ it is indicative of a repulsive force due to local anisotropy which can lead to more massive and stable configurations. A worthwhile approach to generating physically realizable models of compact objects is considering the idea of embedding a 4–dimensional spherically symmetric spacetime into a 5–dimensional Euclidean space. This is known as embedding class 1 by Karmarkar [69] which we have discussed in detail in the previous chapter. It has been demonstrated by Bowers and Liang [70] that the surface redshift can be arbitrarily large in the presence of pressure anisotropy. They were able to show that if the fractional anisotropy, $\frac{p_T - p_R}{p} > 0$, then the associated surface redshift is greater than its isotropic counterpart. The enhancement of the surface redshift is comparable to the magnitude of the anisotropy incorporated into the model. The role of anisotropy during dissipative collapse has yielded many interesting results [71]. Herrera and co-workers have shown that the effects of anisotropy on the dy-

namical instability of the star undergoing collapse [72, 73, 74, 75]. The stability factor Γ in both the Newtonian and post-Newtonian approximations deviate from the well-known result ($\Gamma > \frac{4}{3}$) first derived by Chandrasekhar [16]. The sign of the anisotropic factor leads to a further deviation from the classical case. The formation of the horizon can either be advanced or delayed by the presense of anisotropic stresses within the collapsing core. From a thermodynamical point of view, it has been shown that pressure anisotropy leads to higher core temperatures. During the late stages of collapse, this effect is enhanced when the differences in the anisotropic stresses are much larger [76].

Our intention in this chapter is to solve the nonlinear EGB equations for a static spherically symmetric matter distribution with anisotropic stresses and with a strange star equation of state. We briefly outline the basic equations in EGB gravity. The field equations in 5–dimensional EGB gravity are presented for a spherically symmetric metric, and they are then transformed to an equivalent form through a coordinate redefinition. Then the generalized Vaidya–Tikekar [31] superdense star ansatz is examined and a number of well known special cases are considered. Thereafter the physical features of the Finch–Skea model are investigated with the help of graphical plots and a comparison with the 5–dimensional Einstein counterpart is made. We make use of data associated with the X–ray pulsar LMC X–4 in order to determine the values of constants in the problem and from the plots we deduce that the model displays the necessary qualititative features expected of such astrophysical objects.

5.2 New exact solutions in 5–D Einstein-Gauss-Bonnet theory

The generic 5–dimensional line element for static spherically symmetric spacetimes is taken as

$$ds^2 = -e^{2\nu}dt^2 + e^{2\lambda}dr^2 + r^2\left(d\theta^2 + \sin^2\theta d\phi^2 + \sin^2\theta\sin^2\phi d\psi^2\right) \tag{5.1}$$

where $\nu(r)$ and $\lambda(r)$ are the gravitational potentials. We utilise a comoving fluid velocity of the form $u^a = e^{-\nu}\delta^a_0$ and the matter field is that of a perfect fluid with energy momentum tensor $T_{ab} = (\rho + p)u_a u_b + pg_{ab}$. Accordingly the EGB field equations (2.45) reduce to

$$\rho = \frac{3}{e^{4\lambda}r^3}\left(4\alpha\lambda' + re^{2\lambda} - re^{4\lambda} - r^2e^{2\lambda}\lambda' - 4\alpha e^{2\lambda}\lambda'\right) \tag{5.2}$$

$$p_R = \frac{3}{e^{4\lambda}r^3}\left(-re^{4\lambda} + \left(r^2\nu' + r + 4\alpha\nu'\right)e^{2\lambda} - 3\alpha\nu'\right) \tag{5.3}$$

$$\begin{aligned} p_T = {} & \frac{1}{e^{4\lambda}r^2}\left(-e^{4\lambda} - 4\alpha\nu'' + 12\alpha\nu'\lambda' - 4\alpha\left(\nu'\right)^2\right) \\ & + \frac{1}{e^{2\lambda}r^2}\left(1 - r^2\nu'\lambda' + 2r\nu' - 2r\lambda' + r^2\left(\nu'\right)^2\right) \\ & + \frac{1}{e^{2\lambda}r^2}\left(r^2\nu'' - 4\alpha\nu'\lambda' + 4\alpha\left(\nu'\right)^2 + 4\alpha\nu''\right). \end{aligned} \tag{5.4}$$

where the subscripts R and T refer to the radial and transverse components respectively. The system (5.2)–(5.4) comprises three field equations in five unknowns and is trivially solved by choosing any arbitrary metric. This approach is however unlikely to yield exact models that conform to the elementary tests for physical viability. Accordingly inserting some constraints of physical importance will likely give solutions that may be used to model compact stars. In this work, we prescribe a strange

star equation of state and this immediately increases the mathematical complexity. However, there remains one more prescription to make to close the system. We shall employ a metric ansatz of a superdense star in order to determine a unique solution. Observe that the vacuum metric describing the gravitational field exterior to the 5–dimensional static perfect fluid may be described by the Boulware–Deser [49] spacetime as

$$ds^2 = -F(r)dt^2 + \frac{dr^2}{F(r)} + r^2\left(d\theta^2 + \sin^2\theta d\phi + \sin^2\theta\sin^2\phi d\psi\right) \tag{5.5}$$

where

$$F(r) = 1 + \frac{r^2}{4\alpha}\left(1 - \sqrt{1 + \frac{8M\alpha}{r^4}}\right).$$

In the above M is associated with the gravitational mass of the hypersphere. The exterior solution is unique up to branch cuts, however, there appears to be no equivalent of the Birkhoff theorem of the 4–dimensional Einstein gravity case. Bogdanos *et al* [77] have investigated the 6–dimensional case in EGB and demonstrated that Birkhoff's theorem holds for particular assumptions. At this point we also note that the Buchdahl [17] compactness limit for a perfect fluid sphere $\frac{M}{R} = \frac{4}{9}$ was recently improved to the case of 5–dimensional EGB [78] but the results depend on the sign of the coupling constant α.

To enhance our chances of locating exact solutions, we make the following change of variables $e^{2\nu} = y^2(x)$, $e^{-2\lambda} = Z(x)$ and $x = Cr^2$ (C being an arbitrary constant). This set of transformations has proved particularly useful in the case of isotropic fluids since the isotropy equation may be written as linear differential equations in either variable y or Z in Einstein gravity. In EGB, the same equation is linear in y but nonlinear in Z. For applications of this approach to charged anisotropic relativistic matter see the recent works of Mafa Takisa and Maharaj [79] and Maharaj *et al*

[80] in 4–dimensional Einstein theory. The field equations (5.2)–(5.4) may now be expressed as

$$-3\dot{Z} - \frac{3(Z-1)(1-4\beta\dot{Z})}{x} = \frac{\rho}{C}, \tag{5.6}$$

$$\frac{3(Z-1)}{x} + \frac{6Z\dot{y}}{y} - \frac{6\beta(Z-1)Z\dot{y}}{xy} = \frac{p_R}{C}, \tag{5.7}$$

$$\begin{aligned} & 4Z\left[\beta(1-Z)+x\right]\frac{\ddot{y}}{y} \\ & + \left[\frac{2\beta Z(1-Z)}{x} + 2(x+\beta)\dot{Z} + 6Z(1-\beta\dot{Z}\right]\frac{\dot{y}}{y} \\ & + \left[\frac{Z-1}{x} + 2\dot{Z}\right] = \frac{p_T}{C}, \end{aligned} \tag{5.8}$$

where we have introduced the constant $\beta = 4\alpha C$ containing the EGB coupling constant.

We now utilise a physically important equation of state relating the density and pressure. The prescription $p_R = \gamma\rho - \xi$ is understood to be valid for strange star material or quark stars which have a higher density and larger rotation than neutron stars. The special case $\gamma = \frac{1}{3}$ corresponds to the well studied MIT Bag model where quarks are considered as free particles and their thermodynamic properties are generated by treating them as a Fermi (ideal) gas. With this equation of state (5.6) and (5.7) together yield

$$\frac{\dot{y}}{y} = \left[6Z - \frac{6\beta(Z-1)Z}{x}\right]^{-1}\left[3\gamma\dot{Z} + \frac{3(Z-1)(\gamma-1-\beta\gamma Z)}{x} - \xi\right] \tag{5.9}$$

where γ and $\beta \geq 0$ are constants. Equation (5.9) integrates as

$$y = C_1 \exp\left(\int \frac{3\gamma x\dot{Z} + 3(Z-1)(\gamma-1-\beta\gamma Z) - \xi x}{6xZ - 6\beta(Z-1)Z}dx\right) \tag{5.10}$$

where C_1 is an integration constant. It now remains to detect forms for Z that will permit the complete integration of (5.10).

Equation (5.10) admits a large number of potentials Z for which an exact solution exists. Therefore, it is prudent to make a selection from well studied models which are known to be physically reliable. Expressed in terms of our coordinates the generalised Vaidya–Tikekar potential prescription, known to generate super-dense stellar models [31], is given by

$$Z = \frac{1+ax}{1+bx} \tag{5.11}$$

where a and b are arbitrary real numbers related to the spheroidal parameter. Note that specifying the spatial metric potential is tantamount to determining the law of variation of the density profile. The special case $b = 0$ corresponds to the constant density Schwarzschild interior solution whilst the case $a = 0$ is the Finch–Skea [15] ansatz first proposed by Duorah and Ray [81]. An exact solution for spheroidally distributed matter was examined in the case $a = -1$ and $b = 2$ by Vaidya and Tikekar [31] and shown to admit models with surface densities $2 \times 10^{14}\ g/cm^3$ with masses of about 4 times the solar mass. The choice $b = 1$ was studied by Buchdahl [17, 82] and recently Molina *et al* used this ansatz to find models of stars in pure Gauss–Bonnet gravity [83]. The general integral of (5.10) has the form

$$\begin{aligned} y \;=\; \exp\Bigg[\frac{1}{6}\Big(a^2\Big(\Big(-3a^2\beta^2\gamma + a\beta(b(3(\beta+1)\gamma - \beta\xi - 3) + 3\gamma) \\ +b(b\beta(\beta\xi - 3\gamma + 3) - 3(\beta-1)\gamma))\log(-a\beta + b(\beta + x) + 1)) \\ -b\Big(\log(ax+1)\Big(a^2(6\gamma-3) - a(3b(\gamma-1)+\xi) + b\xi\Big)\Big) - ab^2\xi x\Big)/(ab(a\beta-1))\Bigg] \end{aligned} \tag{5.12}$$

for the potential (5.11).

5.2.1 Schwarzschild incompressible star

The choice $Z = 1+x$ is known to generate a constant density fluid sphere by equation (5.6). For this case (5.12) reduces to

$$y = \exp\left(\frac{3a\beta\gamma(ax+1) + (-6a\gamma + 3a + \xi)\log(ax+1)}{6a(a\beta-1)}\right) \tag{5.13}$$

which is not the same temporal potential as for the isotropic Schwarzschild sphere. In respect of the proposed strange star equation of state we are considering the energy density, radial and tangential pressures evaluate to

$$\rho = 3a\left(-\beta a + 2\right) \tag{5.14}$$

$$p_R = \frac{\xi\left(1-a\beta\right) - 3a\gamma\left(a\beta-1\right)\left(a\beta x+\beta-2\right)}{a\beta-1} \tag{5.15}$$

$$\begin{aligned} p_T = {} & \frac{-9a}{(a\beta-1)^2(ax+1)} \\ & - \frac{3\left(\beta x(a(ax^2+5x-2)+4) - \beta - x(2ax+3)\right)\left(3a(\gamma(a\beta x+\beta-2)+1)+\xi\right)}{x\left(a\beta-1\right)^3\left(ax+1\right)^2} \\ & + \frac{x(1-a\beta)\left(6a(1-a\beta)(a(3-6\gamma)+\xi) + (3a(\gamma(a\beta x+\beta-2)+1)+\xi)^2\right)}{\left(a\beta-1\right)^2\left(ax+1\right)} \end{aligned} \tag{5.16}$$

where we have set $C = 1$. We neglect conducting a more comprehensive analysis of this particular solution in light of the fact that the sound speed being infinite is not physically viable. Instead, we concentrate on a solution that has the potential to model realistic stars below.

5.2.2 Finch–Skea spatial potential

The Finch–Skea potential $Z = \frac{1}{1+x} = \frac{1}{1+Cr^2}$ was used to model four dimensional static stars with behaviors consistent with the astrophysical theory of Walecka [84]. It is also well known that for regular stars, that is models that are singularity–free, it is necessary that the spatial potential has the form $1 + O(r^2)$ [85]. This proves to be useful in this higher curvature analysis as well and it will be observed that all physical quantities are free of the defect of being singular somewhere within the distribution. For the Finch–Skea prescription the potential (5.12) assumes the simplified form

$$y = A\left(\beta+v\right)^{a_1}\exp\left(-\frac{1}{12}\left(a_2+\xi x\right)\left(\beta+v\right)\right) \tag{5.17}$$

where we make the substitutions $a_1 = \frac{1}{6}(3\beta\gamma - \beta(\beta\xi - 3\gamma + 3) - 3\gamma)$, $a_2 = 6\xi\gamma - 3\xi\beta + \xi - 6$, $w_1 = 1 + x$, $w_2 = 1 + x + \beta$ and $w_3 = 1 + 2x + \beta$ to shorten the lengthy expressions to follow. The associated dynamical quantities have the form

$$\frac{\rho}{C} = \frac{3(\beta + x(w_1 + 2) + 2)}{{w_1}^3} \tag{5.18}$$

$$\frac{p_R}{C} = \frac{12a_1 - a_2w_2 - \xi w_2w_3 - 6w_1}{2{w_1}^2} \tag{5.19}$$

$$\begin{aligned}\frac{p_T}{C} = {} & \left[-6\xi\left(3(\beta+1)^2 + 8x^3 + (6\beta+20)x^2 + 15(\beta+1)x\right) - 36w_1(x+3)\right. \\ & +2\xi x w_1 w_2 w_3 + \frac{144{a_1}^2 x w_1}{w_2}\xi^2 + x w_1 w_2 {w_3}^2 \\ & \left.+a_2\left(a_2 x w_1 w_2 - 6\left(3\beta + 2x^2 + 5x + 3\right)\right)\right] / 36{w_1}^3\end{aligned} \tag{5.20}$$

while the measure of the pressure anisotropy $\Delta = p_T - p_R$ is given by the expression

$$\begin{aligned}\frac{\Delta}{C} &= \left[72w_1 - 6\xi\left(-3\beta^2 - 3\beta x + x(2x+5) + 3\right) + \xi^2 w_1 w_2 {w_3}^2\right. \\ &\quad + \frac{144{a_1}^2 w_1}{w_2} - 24a_1\left(a_2 w_1 + \xi w_1 w_3 + 9\right) \\ &\quad \left. + a_2\left(a_2 w_1 w_2 + 2\xi w_1 w_2 w_3 + 6(3\beta + x + 1)\right)\right] / 36{w_1}^2. \end{aligned} \tag{5.21}$$

Observe that a hypersurface of vanishing pressure exists when $p_R = 0$ demarcating the boundary of the 5–dimensional hypersphere at

$$x = \frac{1 - 2a_1\beta - 2a_1 - 2a_2}{2a_1 - 1} \tag{5.22}$$

in terms of the constants associated with the strange star equation of state and Gauss–Bonnet coupling constant. The ratio of the pressure to the energy density $\frac{p}{\rho}$ is understood to give an indication of the equation of state of the model. In this case we obtain

$$\left(\frac{p}{\rho}\right)_R = \frac{w_1\left(12a_1 - a_2 w_2 - \xi w_2 w_3 - 6w_1\right)}{6(\beta + x(x+3) + 2)} \tag{5.23}$$

$$\begin{aligned}\left(\frac{p}{\rho}\right)_T &= \left[-36w_1(x+3) - 6\xi\left(3(\beta+1)^2 + 8x^3 + (6\beta+20)x^2 + 15(\beta+1)x\right)\right. \\ &\quad + \frac{144{a_1}^2 x w_1}{\beta + x + 1} + \xi^2 + x w_1 w_2 {w_3}^2 - 24a_1\left(a_2 x w_1 + \xi x w_1 w_3 - 9\right) \\ &\quad \left. + a_2\left(a_2 x w_1 w_2 - 6\left(3\beta + 2x^2 + 5x + 3\right) + 2\xi x w_1 w_2 w_3\right)\right] \\ &\quad \times \left[108(\beta + x(x+3) + 2)\right]^{-1} \end{aligned} \tag{5.24}$$

for the radial and transverse components. The causal behavior of stars is studied by examining the square of the sound speed given by the formula $v^2 = \frac{dp}{d\rho}$. This

evaluates to

$$v_R^2 = -\frac{w_1\left(a_2(2\beta+x+1)-24a_1+\xi\left(2\beta^2+\beta+3\beta x-x-1\right)+6w_1\right)}{6\left(3\beta+x^2+4x+3\right)} \tag{5.25}$$

$$\begin{aligned} v_T^2 = & -\{\,36w_1(x+5)+6\xi\left(9\beta^2+3\beta+6\beta x(x+3)-2w_1(2x+3)\right) \\ & +\xi^2 w_1 w_3\left((\beta+1)^2+4x^3+2(\beta+5)x^2-(\beta-7)(\beta+1)x\right) \\ & -\frac{144{a_1}^2 w_1\left(2x^2+\beta(x-1)+x-1\right)}{{w_2}^2}+6a_2\left(9\beta+2x(x+3)+4\right) \\ & +24a_1\left(a_2\left(x^2-1\right)+\xi w_1(\beta(x-1)-3x-1)-27\right) \\ & +2a_2\xi w_1\left((\beta+1)^2+2x^3+6x^2-(\beta-5)(\beta+1)x\right) \\ & +{a_2}^2(\beta+x(-\beta x+x+2)+1)\}\,/\,108\left(3\beta+x^2+4x+3\right) \end{aligned} \tag{5.26}$$

and the expectation is that both these quantities should be constrained in the interval $(0,1)$ to guarantee that the sound speed remains subluminal. The possibility of superluminal behavior in ultrabaric matter in special relativity was discussed by Caporaso and Bescher [86] and ruled out. The difference between the squares of the radial and transverse sound speeds given by

$$
\begin{aligned}
v_R^2 - v_T^2 &= \{324{w_1}^2\left[a_2(2\beta+x+1)-24a_1+\xi\left(2\beta^2+\beta+3\beta x-x-1\right)+6w_1\right]^2 \\
&\quad -\left[6\xi\left(9\beta^2+3\beta+6\beta x(x+3)-2w_1(2x+3)\right)+36w_1(x+5)\right. \\
&\quad +\xi^2 w_1 w_3\left((\beta+1)^2+4x^3+2(\beta+5)x^2-(\beta-7)(\beta+1)x\right) \\
&\quad -\frac{144{a_1}^2 w_1\left(2x^2+\beta(x-1)+x-1\right)}{{w_2}^2}+6a_2(9\beta+2x(x+3)+4) \\
&\quad +24a_1\left(a_2\left(x^2-1\right)+\xi w_1(\beta(x-1)-3x-1)-27\right) \\
&\quad +2a_2\xi w_1\left((\beta+1)^2+2x^3+6x^2-(\beta-5)(\beta+1)x\right) \\
&\quad \left.+{a_2}^2(\beta+x(-\beta x+x+2)+1)\right]^2\} \,/\, 11664\left(3\beta+x^2+4x+3\right)^2
\end{aligned}
\tag{5.27}
$$

provides an indication of the stability of the model. Graphical plots will be used to analyse these features. The active gravitational mass is computed via the formula $\frac{1}{3}\int \rho r^{d-2}dr$ where d is the spacetime dimension. In the five dimensional case we obtain

$$
M(r) = \frac{k}{3}+\frac{1}{2C^2}\left(x-\frac{\beta+2(\beta-1)x-2}{2{w_1}^2}\right) \tag{5.28}
$$

and correspondingly the compactification parameter

$$
\frac{M(r)}{r} = \left[\frac{k}{3}+\frac{1}{2C^2}\left(x-\frac{\beta+2(\beta-1)x-2}{2{w_1}^2}\right)\right]\times\sqrt{\frac{c}{x}} \tag{5.29}
$$

will be useful in determining whether the Buchdahl limit for the mass-radius ratio applicable to Einstein stars is still valid when higher curvature effects are included. Another indicator of stability devised by Chandrasekhar [16] is the adiabatic stability

parameter $\Gamma = \left(\frac{\rho+p}{p}\right)\frac{dp}{d\rho}$ which assume the forms

$$\begin{aligned}\Gamma_R &= \frac{(a_2(2\beta+x+1)-24a_1+\xi\left(2\beta^2+\beta+3\beta x-x-1\right)+6w_1)}{6\left(3\beta+x^2+4x+3\right)\left(a_2w_2-12a_1+\xi w_2w_3+6w_1\right)}\\ &\times\frac{\left(w_2\left(a_2w_1+\xi w_1w_3-6\right)-12a_1w_1\right)}{6\left(3\beta+x^2+4x+3\right)\left(a_2w_2-12a_1+\xi w_2w_3+6w_1\right)}\end{aligned} \tag{5.30}$$

$$\begin{aligned}\Gamma_T &= -\{36\left(3\beta+2x^2+5x+3\right)-24a_1\left(a_2xw_1+\xi xw_1w_3-9\right)\\ &-6\xi\left(3(\beta+1)^2+8x^3+(6\beta+20)x^2+15(\beta+1)x\right)+\xi^2+x{w_1}{w_2}{w_3}^2\\ &+a_2\left(a_2xw_1w_2-6\left(3\beta+2x^2+5x+3\right)+2\xi xw_1w_2w_3\right)\}\\ &\times\{6\xi\left(9\beta^2+3\beta+6\beta x(x+3)-2w_1(2x+3)\right)+36w_1(x+5)\\ &+\xi^2w_1w_3\left((\beta+1)^2+4x^3+2(\beta+5)x^2-(\beta-7)(\beta+1)x\right)\\ &+24a_1\left(a_2\left(x^2-1\right)+\xi w_1(\beta(x-1)-3x-1)-27\right)+\frac{144{a_1}^2xw_1}{\beta+x+1}\\ &-\frac{144{a_1}^2w_1\left(2x^2+\beta(x-1)+x-1\right)}{{w_2}^2}+6a_2(9\beta+2x(x+3)+4)\\ &+2a_2\xi w_1\left((\beta+1)^2+2x^3+6x^2-(\beta-5)(\beta+1)x\right)\\ &+{a_2}^2(\beta+x(-\beta x+x+2)+1)\}\,/\,\{108(3\beta+x^2+4x+3)\\ &\times\left[-6\xi\left(3(\beta+1)^2+8x^3+(6\beta+20)x^2+15(\beta+1)x\right)-36w_1(x+3)\right.\\ &+\frac{144{a_1}^2xw_1}{\beta+x+1}+\xi^2+x{w_1}{w_2}{w_3}^2-24a_1\left(a_2xw_1+\xi xw_1w_3-9\right)\\ &\left.+a_2\left(2\xi xw_1w_2w_3-6\left(3\beta+2x^2+5x+3\right)\right)+{a_2}^2xw_1w_2\right]\}\end{aligned} \tag{5.31}$$

for the anisotropic model under consideration. Adiabatic stability occurs provided that Γ exceeds the critical value $\frac{4}{3}$. For a recent study of this property in the context of neutron stars see the work of Koliogiannis and Moustakidis [87]. The gravitational

surface redshift z obtained from the formula $z = e^{-\nu} - 1$ is given by

$$z = \frac{1}{A} w_2^{-a_1} \exp\left(\frac{1}{12} w_2 \left(a_2 + \xi x\right)\right) - 1 \tag{5.32}$$

for our model. The energy conditions for anisotropic matter may be investigated with the help of the expressions $\rho - p$ (weak energy condition), $\rho + p$ (strong energy condition) and $\rho + 3p$ (dominant energy condition). For the radial and transverse directions we obtain

$$\frac{(\rho - p)_R}{C} = \left[w_1 \left(a_2 w_2 - 12a_1 + \xi w_2 w_3 + 6w_1\right) + 6(\beta + x(x+3) + 2)\right] / 2{w_1}^3 \tag{5.33}$$

$$\begin{aligned}\frac{(\rho - p)_T}{C} = {} & \{36\left(3\beta + 4x^2 + 13x + 9\right) - \xi^2 x w_1 w_2 {w_3}^2 + 24a_1 \left(a_2 x w_1 + \xi x w_1 w_3 - 9\right) \\ & - \frac{144{a_1}^2 x w_1}{\beta + x + 1} + 6\xi\left[3(\beta+1)^2 + 8x^3 + (6\beta + 20)x^2 + 15(\beta+1)x\right] \\ & + a_2\left[18(\beta+1) - a_2 x w_1 w_2 - 2\xi x w_1 w_2 w_3 + 6x(2x+5)\right]\} / 36{w_1}^3\end{aligned} \tag{5.34}$$

$$\frac{(\rho + p)_R}{C} = \frac{12a_1 w_1 - w_2\left(a_2 w_1 + \xi w_1 w_3 - 6\right)}{2{w_1}^3} \tag{5.35}$$

$$\begin{aligned}\frac{(\rho + p)_T}{C} = {} & \{36\left(3\beta + 2x^2 + 5x + 3\right) + \xi^2 + x w_1 w_2 {w_3}^2 - 24a_1\left(a_2 x w_1 + \xi x w_1 w_3 - 9\right) \\ & + \frac{144{a_1}^2 x w_1}{\beta + x + 1} - 6\xi\left[3(\beta+1)^2 + 8x^3 + (6\beta + 20)x^2 + 15(\beta+1)x\right] \\ & + a_2\left[a_2 x w_1 w_2 - 6\left(3\beta + 2x^2 + 5x + 3\right) + 2\xi x w_1 w_2 w_3\right]\} / 36{w_1}^3\end{aligned} \tag{5.36}$$

$$\begin{aligned}\frac{\rho + 3p}{C} = {} & \{3\xi\left[9(\beta+1)^2 + 22x^3 + (21\beta + 55)x^2 + 3(\beta+1)(\beta+14)x\right] + 18\left[3(\beta+5)\right. \\ & \left. + x(8x+23)\right] - \xi^2 x w_1 w_2 {w_3}^2 - \frac{144{a_1}^2 x w_1}{\beta + x + 1} + 12a_1\left(2a_2 x w_1 + 2\xi x w_1 w_3 - 9(x+3)\right) \\ & + a_2\left[-a_2 w_1 x w_2 + 21x^2 - 2\xi w_1 x w_2 w_3 + 9\beta(x+3) + 48x + 27\right]\} / 18{w_1}^3.\end{aligned} \tag{5.37}$$

We now discuss the physical plausibility of our compact star model. In order to generate the plots we have utilized mass and radius data associated with the pulsar LMC X–4 which qualifies as a superdense star to determine integration constants while other constants were assigned special values through fine–tuning.

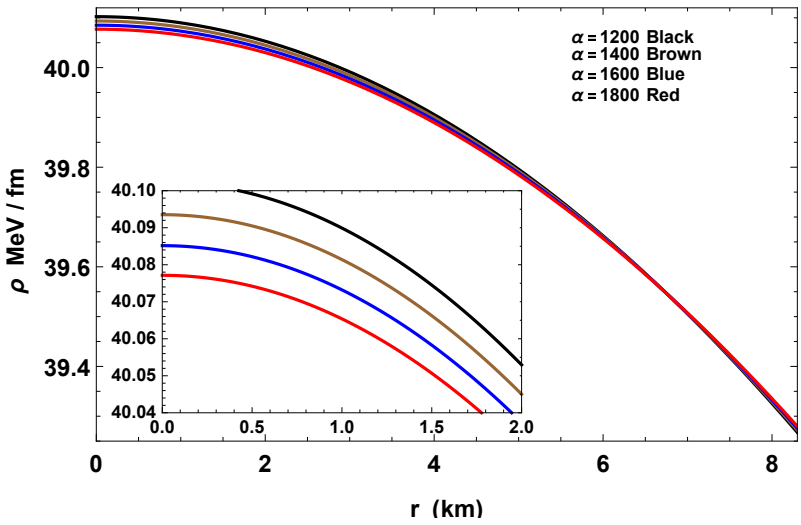

Figure 5.1: Variation of density ρ with radial coordinate for LMC X–4 with $M = 1.04M_{\odot}$, $R = 8.3km$ and $\gamma = 1/3$ in EGB.

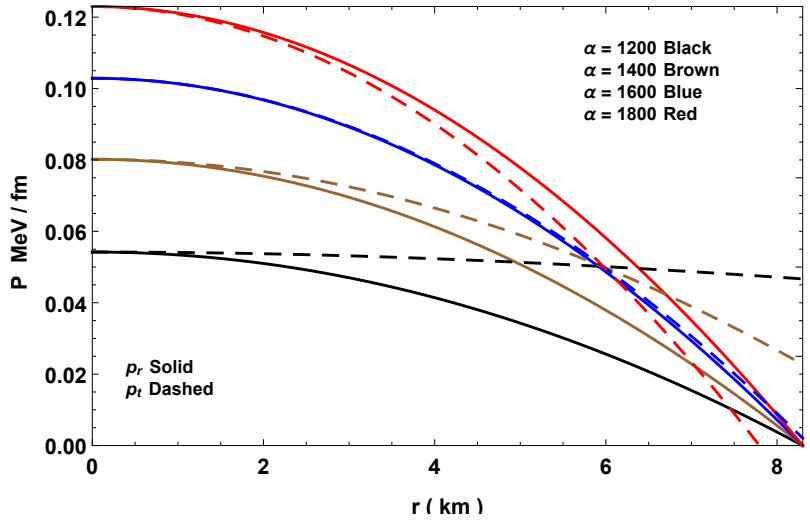

Figure 5.2: Variation of pressures p with radial coordinate for LMC X–4 with $M = 1.04M_{\odot}$, $R = 8.3km$ and $\gamma = 1/3$ in EGB.

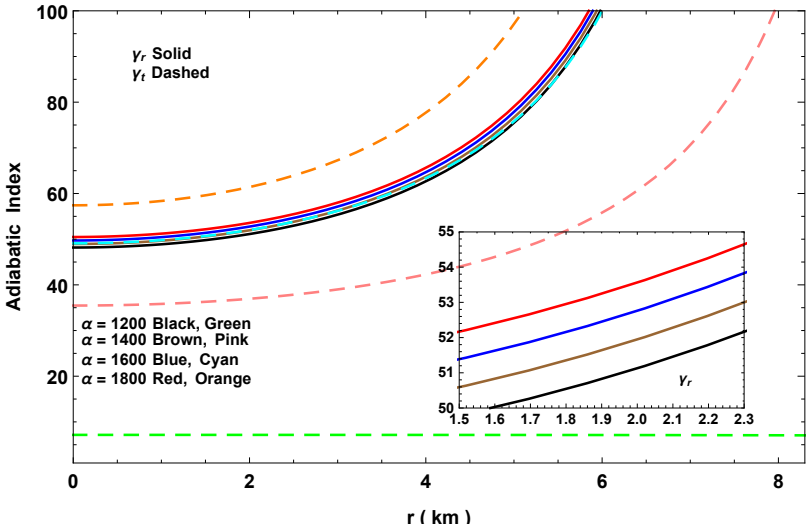

Figure 5.3: Variation of adiabatic index Γ with radial coordinate for LMC X-4 with $M = 1.04M_{\odot}$, $R = 8.3km$ and $\gamma = 1/3$ in EGB.

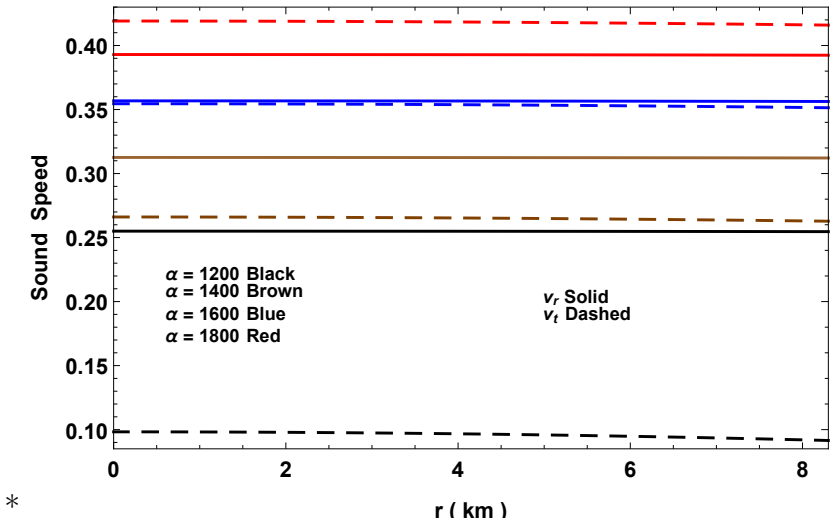

*

Figure 5.4: Variation of sound speed with radial coordinate for LMC X–4 with $M = 1.04M_{\odot},\ R = 8.3km$ and $\gamma = 1/3$ in EGB.

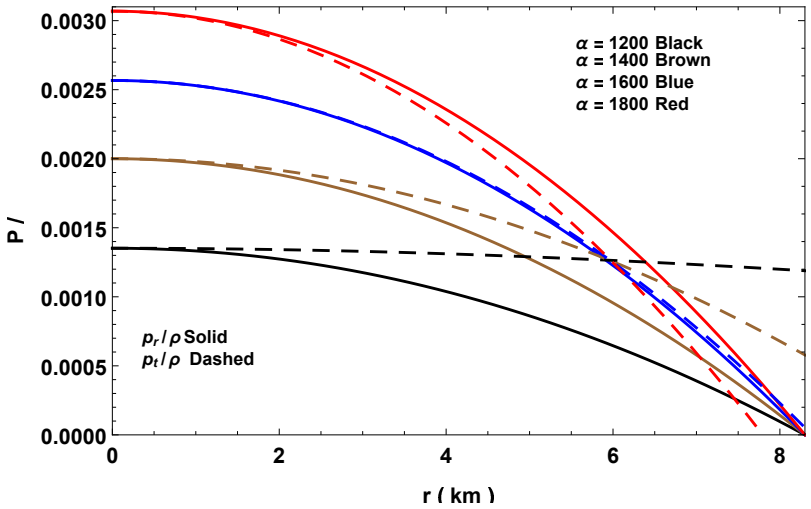

Figure 5.5: Variation of equation of state parameters with radial coordinate for LMC X–4 with $M = 1.04M_{\odot},\ R = 8.3km$ and $\gamma = 1/3$ in EGB.

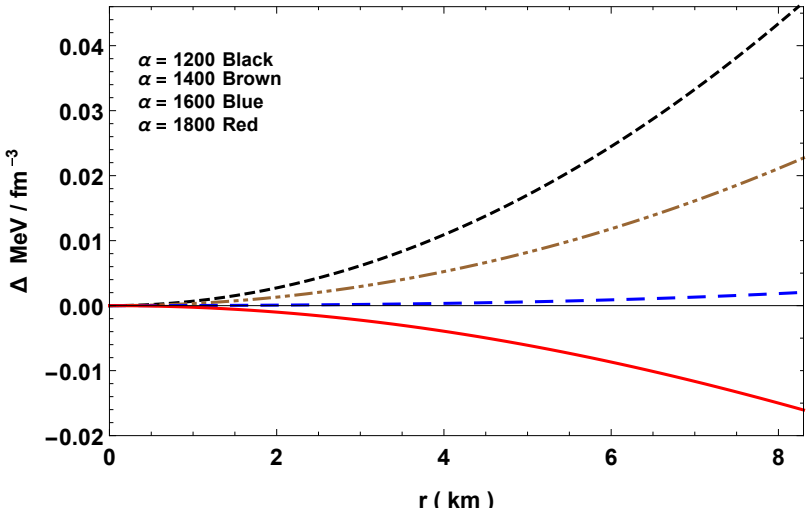

Figure 5.6: Variation of anisotropy with radial coordinate for LMC X–4 with $M = 1.04M_{\odot}$, $R = 8.3km$ and $\gamma = 1/3$ in EGB.

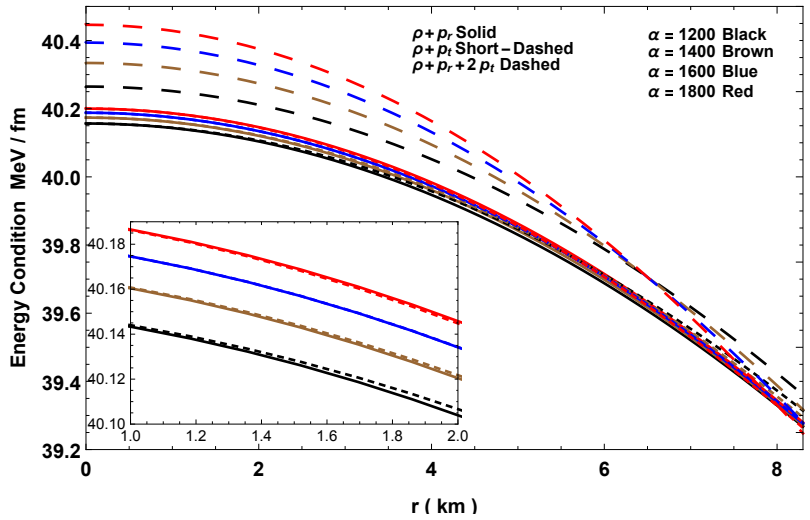

Figure 5.7: Variation of energy conditions with radial coordinate for LMC X–4 with $M = 1.04M_{\odot}$, $R = 8.3km$ and $\gamma = 1/3$ in EGB.

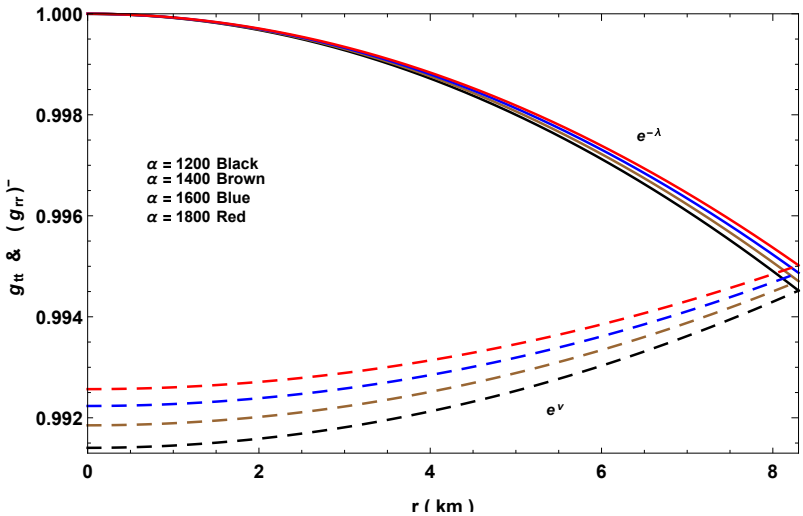

Figure 5.8: Variation of metric potentials with radial coordinate for LMC X-4 with $M = 1.04M_{\odot},\ R = 8.3km$ and $\gamma = 1/3$ in EGB.

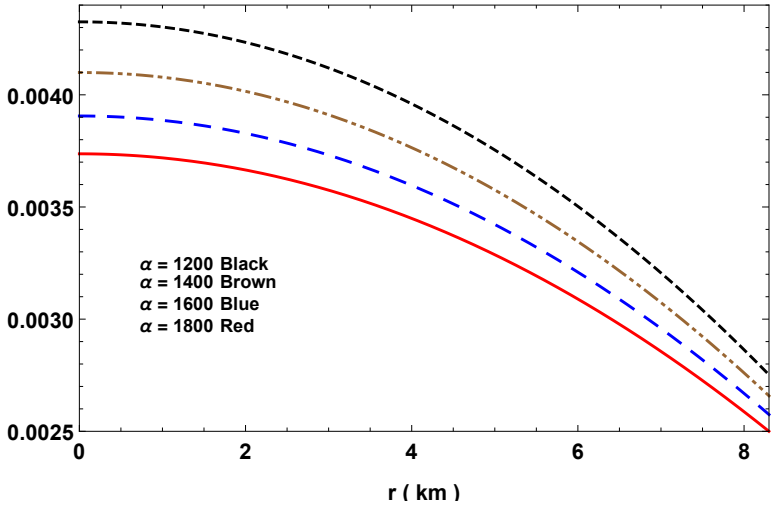

Figure 5.9: Variation of red-shift with radial coordinate for LMC X-4 with $M = 1.04M_{\odot},\ R = 8.3km$ and $\gamma = 1/3$ in EGB.

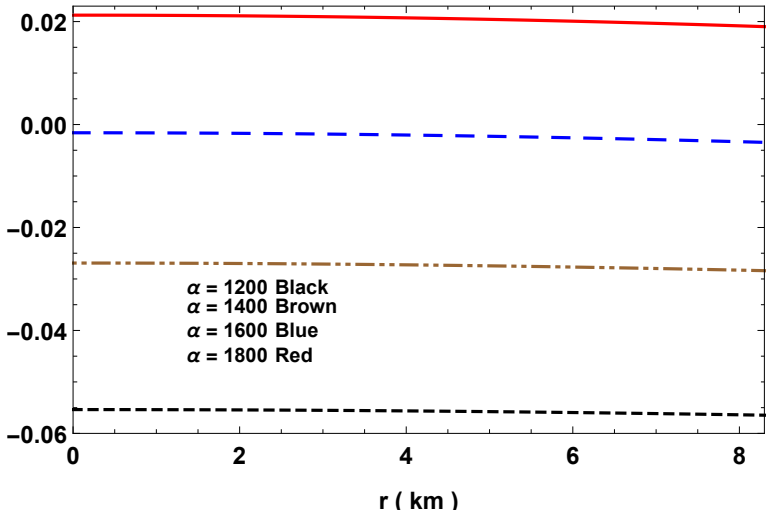

Figure 5.10: Variation of stability factor with radial coordinate for LMC X–4 with $M = 1.04M_{\odot},\ R = 8.3km$ and $\gamma = 1/3$ in EGB.

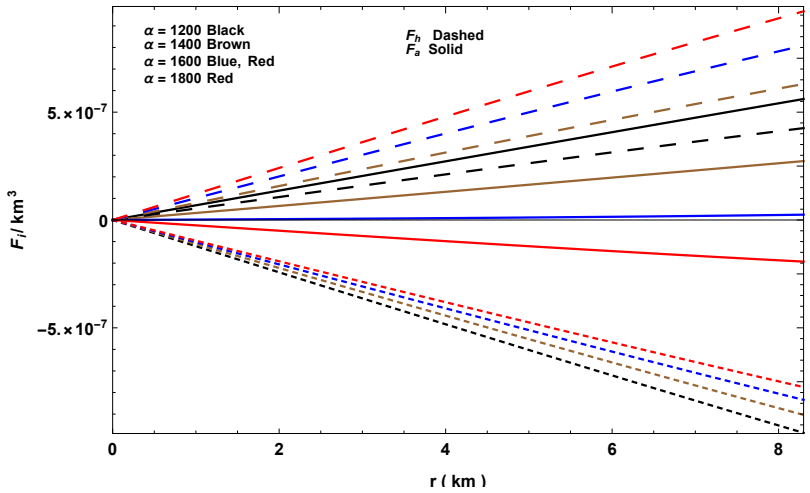

Figure 5.11: Variation of forces in TOV-equation with radial coordinate for LMC X–4 with $M = 1.04M_{\odot},\ R = 8.3km$ and $\gamma = 1/3$ in EGB.

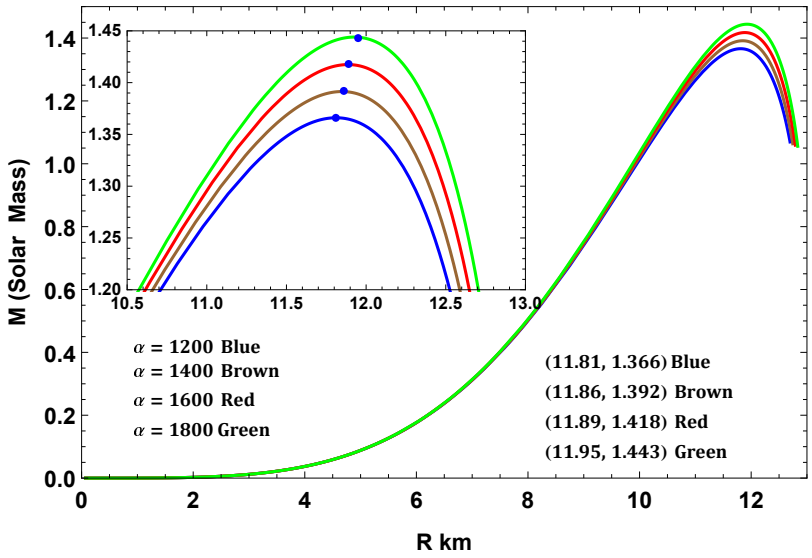

Figure 5.12: $M - R$ graph assuming $M = 1.04M_{\odot},\ R = 8.3km$ in EGB.

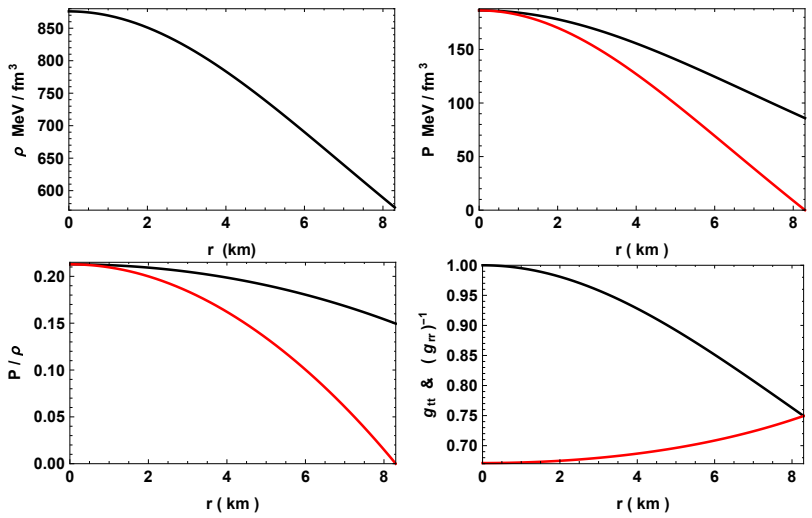

Figure 5.13: Graphs of metric potentials, density, pressure and P/ρ for LMC X–4 with $M = 1.04M_{\odot},\ R = 8.3km$ and $\gamma = 1/3$ in GR limit.

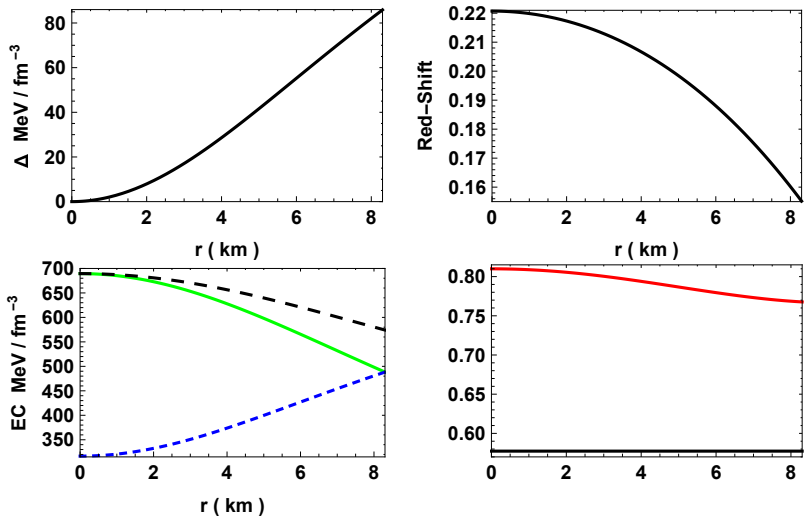

Figure 5.14: Graphs of anisotropy, red–shift, energy conditions and sound speeds for LMC X–4 with $M = 1.04M_{\odot},\ R = 8.3km$ and $\gamma = 1/3$ in GR limit.

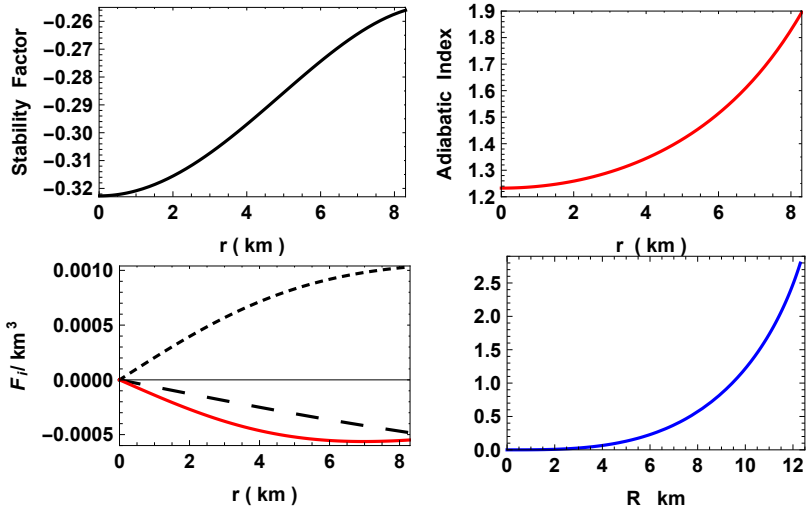

Figure 5.15: Graphs of stability factor, adiabatic index, TOV–equation and $M - R$ curve with $M = 1.04M_{\odot},\ R = 8.3km$ and $\gamma = 1/3$ in GR limit.

In Figure 5.1 the density is shown to be a smooth singularity–free monotonically decreasing function of the radial coordinate. We observe that the density decreases with an increase in magnitude of the coupling constant. Figure 5.2 shows that the radial and tangential pressures decrease monotonically outwards towards the stellar surface. This is expected as the density in the central regions of the star is much higher than the surface density. It is interesting to note that the radial pressure is greater than the tangential pressure for large values of the coupling constant. This suggests that the force due to the pressure anisotropy is attractive in this regime. As the coupling constant decreases the tangential pressure dominates the radial pressure leading to a repulsive contribution from the anisotropy. Most importantly a hypersurface of vanishing radial pressure is clearly visible for a radial value of approximately 8.3 km. The behavior of all physical quantities should be studied within this radius. The central pressure is well behaved displaying no singularities for any value of the coupling constant α. Observations of the adiabatic stability index Γ in Figure 5.3 shows that the fluid is more stable for increasing α. This implies that higher order corrections tend to make the compact object more stable against perturbations. The critical lower bound of $\frac{4}{3}$ established by Chandrasekhar for Einstein gravity is always exceeded for both tangential and transverse directions. Causality is obeyed throughout the fluid configuration as exhibited in Figure 5.4. Both the radial and tangential speed of sound lie within the bounds $(0, 1)$. The equation of state parameter is an important indicator of the relationship between the pressure and density at each interior point of the star. From Figure 5.5 we observe that the ratio of the pressure to density increases with an increase in the coupling constant. This implies that stronger contributions from higher corrections lead to more compact objects. In Figure 5.6 we observe that the anisotropy changes sign which implies that force associated with anisotropy can be repulsive ($p_T > p_R$) or attractive ($p_T < p_R$). Lower order contributions (smaller values of α) lead to repulsive effects due to anisotropy. All the energy conditions being positive as displayed in Figure

5.7 are satisfied. The metric potentials are continuous and well-behaved throughout the star as evidenced in Figure 5.8. The surface redshift is illustrated in Figure 5.9. We observe that the surface redshift is higher for smaller values of α which supports our observation of the density increasing with smaller values of the coupling constant (Figure 5.1). The forces required for equilibrium are illustrated in Figure 5.11. In order to achieve equilibrium we require that $F_g + F_h + F_a = 0$ where F_g, F_h and F_a are the gravitational, hydrostatic and anisotropic forces respectively. Figure 5.12 displays the variation of the mass with respect to the radius. Clearly within the stellar radius 8.3 km there appears to be little difference in the mass profile for various α values. If the gravitational field admitted a higher radial value, then the plot displays that a maximum mass is achieved and some discrimination in values occur near this maximum.

The frames in Figure 5.13 to Figure 5.15 display the various physical quantities of our compact model in the 5–D classical Einstein limit (i.e., $\alpha = 0$). Radial quantities are in red while transverse items are in black. We observe that the respective quantities such as density, pressures, redshift and anisotropy are all substantially higher than their EGB counterparts hence the need for separate plots. Xian–Feng & Huan–Yu [88] established that through relativistic mean field theory that the surface gravitational redshift of the star PSR J0348+0432 is in the region of about 0.3473 to 0.4064 which was higher than the canonical mass neutron star with a redshift of 0.226. Our 5–D stellar model (Figure 5.14) displays a redshift in the range 0.15 to 0.22 within the distribution. This is therefore comparable with a neutron star. Note that when higher curvature terms are present as depicted in Figure 5.9, the surface redshift drops dramatically to the range of order 0.0025 to 0.0050. Figure 5.14 also demonstrates that the measure of anisotropy, the energy conditions and the speed of sound are all within the expected levels. The stability measures shown in Figure 5.15 confirm that the 5–D Einstein model is stable with a well behaved mass profile.

These stability features are not disturbed by the introduction of higher curvature effects due to the Gauss–Bonnet action.

In Table 5.1 we exhibit a few stellar models which fall in the range of the mass and radius comparable to LMC X–4. This shows that our qualitative results are consistent with a large number of known stars.

Table 5.1: Parameter of few well-known compact star candidates

Object	$\frac{M}{M_\odot}$	R	γ	$c \times 10^{-3}$	α	χ	$\rho_c \times 10^{13}$	$\rho_b \times 10^{13}$	$p_c \times 10^{33}$
		km					g/cc	g/cc	$dyne/cm^2$
LMC X-4	1.04	8.3	0.33	0.161	1200	0.06885	7.15	6.99	8.68
SMC X-4	1.29	8.831	0.33	0.155	1250	0.07931	6.93	6.77	9.50
EXO 1785-248	1.3	8.849	0.33	0.154	1300	0.12468	6.89	6.77	1.06
4U 1820-30	1.58	9.1	0.33	0.163	1350	0.27091	7.52	7.32	1.78
PSR J1614-2230	1.97	9.69	0.33	0.158	1400	0.2788	7.32	7.13	1.93

5.3 Conclusion

In this work we have generated the equations governing the dynamical evolution of astrophysical models in the Einstein–Gauss–Bonnet gravity paradigm with anisotropic stresses. After electing to use a strange star equation of state we employed the gravitational potential of Vaidya and Tikekar which was used to construct models of superdense stars in four dimensional gravity. The remaining gravitational potential was settled by solving differential equation emanating from the equation of state. It was then possible to calculate all the remaining dynamical variables and stability indicators. Graphical plots assisted us in investigating the behavior of the model with and without higher curvature effects. It was found that lower energy densities were realizable for increasing values of the coupling constant α. The pulsar LMC X–4 supplied mass and radius values to analyse other features of the star. It was also found that higher curvature terms resulted in a significant reduction in surface grav-

itational redshift values when compared to the 5–dimensional Einstein star. With regards to stability we concluded that the Gauss–Bonnet terms did not disturb the stability of the model in the Chandrasekhar adiabatic stability sense nor in the sense of the TOV equation components. Lower sound speeds were evident in the EGB models however neither model became acausal within the radial value. It was shown that the EGB model produced characteristics not out of sync with a range of known compact objects. This study demonstrates that the higher curvature Gauss–Bonnet terms should not be dismissed as corrections to the standard Einstein gravity theory.

Chapter 6

Conclusion

In our study, we commenced by imposing the physically significant conformal flatness condition in solving the Einstein-Maxwell field equations in a systematic way. Firstly, an extensive analysis of the equations was conducted to test for the existence of viable solutions. Then we investigated various conformally flat charged stars and calculated their dynamical quantities. For the special case of the Vaidya-Tikekar superdense star, we generated new exact solutions. A further class of solutions, which satisfied the Chandrasekhar adiabatic stability criterion, was demonstrated. We noted certain drawbacks in some of our models, which highlighted the challenge in finding exact solutions that satisfy all required conditions for physical admissibility. We further analysed a variety of linear and polytropic equations of state and in some cases obtained exact solutions. There remain some unsolved differential equations presented, thus further analysis and possibly new integrating techniques are required to find solutions for these. There are also further constraints that can be applied to our models, such as the Böhmer and Harko [18] upper bound and the Andréasson [19] limit in order to give physically acceptable solutions. In addition to solving the intractable differential equations, each complete model must be analysed and compared to known realistic candidates. This will be pursued more vigorously

in future studies.

The next aspect of our study involved using the Karmarkar condition [32] which is used to embed a lower dimensional spacetime into a higher dimensional one. We imposed the condition of pressure isotropy for charged stars with the aim of generating new exact solutions, as this was not successfully demonstrated in the literature. A complete model using the Finch–Skea [15] metric has been generated. The model has been subject to graphical analysis as well as physical plausibility checks by matching the solution to the Reissner–Nordstrom [5, 6] exterior line element. This model proved effective as it met all the necessary physical conditions required for a charged isotropic sphere. A different special case of the Vaidya–Tikekar [31] metric ansatz was also considered. Most physical requirements were satisfied here but due to the non-vanishing pressure condition, this model may be interpreted as a cosmological fluid and was not further analysed as our interest lies in exact solutions for charged stars. We concluded the chapter by listing a few other solutions that satisfy the Karmarkar condition in our case, which can be further studied.

In the final chapter of our study we adopted an anisotropic approach in pursuit of new exact solutions in 5–dimensional Einstein–Gauss–Bonnet gravity, for a static spherically symmetric matter distribution with a strange star equation of state. The electric field in this chapter plays no role. We employed the Vaidya–Tikekar superdense star ansatz and consider various special cases. The Finch–Skea model was analysed using graphical plots and compared to the 5–dimensional Einstein counterpart. We utilized the X–ray pulsar LMC X–4 to supply the mass and radius values in order to determine the constants for our solution and analyse the physical features. We also presented a table with a few stellar models which are comparable to LMC X–4 to enforce that our qualitative results are accordant with a large number of known stars. Furthermore it has been demonstrated in this study that the higher curvature Gauss–Bonnet terms should not be dismissed as corrections to the standard Einstein gravity theory as they influence the gravitational behaviour of fluids.

Several new directions of research emanate from this work. The role of Karmarkar's condition in the higher curvature gravity is worth pursuing with and without an electric field in attendance. Moreover, our Gauss–Bonnet model with strange star equation of state may be studied in conjunction with an electromagnetic field. These problems will be examined in forthcoming research.

Bibliography

[1] B. P. Abbott *et al.*, *Phys. Rev. D* **116**, 061102 (2016).

[2] K. Schwarzschild, *Sitzungsber Preuss. Akad. Wiss. Phys. Math.* **K1**, 424 (1916a).

[3] G. D. Birkhoff, *Relativity and Modern Physics.* Cambridge, MA: Harvard University Press. (1923).

[4] K. Schwarzschild, *Sitzungsber Preuss. Akad. Wiss. Phys. Math.* **K1**, 424 (1916b).

[5] G. Nordstrom, *Proc. Ned. Akad. Wet.* **26**, 1201-1208 (1918).

[6] H. Reissner, *Ann. Phys. Lpz.* **50**, 106 (1916).

[7] P. C. Vaidya, *Proc. Indiana Acad. Sci. A* **33**, 26458 (1951).

[8] R. P. Kerr, *Phys. Rev. Lett.* 11 **5**, 237-238 (1963).

[9] A. Banerjee and N. O. Santos, *J Math. Phys.* **22**, 824 (1981).

[10] Z. Shi-Chang, *Gen Rel. Grav.* **15**, 293 (1983).

[11] W. Xingxiang, *J Math. Phys.* **28**, 2697 (1987).

[12] L. Herrera and J. Ponce de Leon, *J. Math. Phys.* **26**, 2302 (1985).

[13] M. C. Durgapal and R. Bannerji, *Phys. Rev. D* **27**, 328 (1983).

[14] M. C. Durgapal and R. S. Fuloria, *Class. Quant. Grav.* **6**, 467 (1985).

[15] M. R. Finch and J. E. F. Skea, *Class. Quant. Grav.* **6**, 467 (1989).

[16] S. Chandrasekhar, *Astrophys. J.* **140**, 417 (1964).

[17] H. A. Buchdahl, *Phys. Rev. D* **116**, 1027 (1959).

[18] C. G. Böhmer and T. Harko, *Gen Rel. Grav.* **39**, 757-775 (2007).

[19] G. K. Andréasson, *J. Math. Phys.* **300**, A69 (2009).

[20] F. C. Cooperstock and V. de la Cruz, *Gen. Rel. Grav.* **9**, 835 (1978).

[21] V. Pandharipande, D. Pines and R. A. Smith, *Astrophys. J.* **208**, 550 (1976).

[22] B. V. Ivanov, *Phys. Rev. D* **65**, 10411 (2002).

[23] R. Sharma, S. Mukherjee, and S. D. Maharaj, *Gen. Rel. Grav.* **33**, 999 (2001).

[24] S. Hansraj, S. D. Maharaj, S. Mlaba and N. Qwabe, *J. Math. Phys.* **58**, 052501 (2017).

[25] L. Herrera, *J. Math. Phys.* **42**, 2129 (2001).

[26] U. K. De and A. K. Raychaudhuri, *Proc. R. Soc. Ser. A* **303**, 97 (1968).

[27] T. Gronwall, *Ann. of Math.* **20**, 292 (1919).

[28] A. Melfo and H. Rago, *Astrophys. Space Sci.* **193**, 9 (1992).

[29] W. C. Saslaw, S. D. Maharaj and N. K. Dadhich, *Astrophys. J* **471**, 571 (1996).

[30] N. Dadhich , S. Hansraj and S. D. Maharaj, *Phys. Rev. D* **93**, 044072 (2016).

[31] P. C. Vaidya and R. Tikekar, *J. Astrophys. Astron.* **3**, 325, (1982).

[32] K. R. Karmarkar, *Proc. Ind. Acad. Sci. A* **27**, 56 (1948).

[33] S. N. Pandey and S. P. Sharma, *Gen. Rel. Grav.* **14**, 113 (1982).

[34] F. Rahaman, *et al*, *Int. J. Mod. Phys. D* **23**, 1450042 (2014).

[35] S. Ray, A. A. Usmani, F. Rahaman, M. Kalam, and K. Chakraborty, *Ind. J. Phys.* **82**, 1191 (2008).

[36] P. Bhar, S. K. Maurya, Y. K. Gupta, and T. Manna, *Eur. Phys. J. A* **52**, 312 (2016).

[37] S. K. Maurya, Y. K. Gupta, B. Dayanand, and S. Ray, *Eur. Phys. J. C* **76**, 266 (2016).

[38] S. K. Maurya, Y. K. Gupta, S. Ray, and D. Deb, *Eur. Phys. J. C* **76**, 693 (2016).

[39] S. K. Maurya, Y. K. Gupta, T. T. Smith, and F. Rahaman, *Eur. Phys. J. A* **52**, 191 (2016).

[40] S. K. Maurya, Y. K. Gupta, S. Ray, and D. Deb, *Eur. Phys. J. C* **77**, 45 (2017).

[41] K. N. Singh, P. Bhar, and N. Pant, *Astrophys. Space Sci.* **361**, 339 (2016).

[42] K. N. Singh and N. Pant, *Eur. Phys. J. C* **76**, 524 (2016).

[43] M. Kohler and K. L. Chao, *Z. Naturforchg* **27**, 1537 (1965).

[44] A. G. Riess *et al.*, *Astron. J.* **116**, 1009 (1998).

[45] S. Perlmutter *et al.*, *Astrophys. J.* **517**, 565 (1999).

[46] G. W. Horndeski, *Int. J. Theor. Phys.* **10**, 363 (1974).

[47] D. Gross, *Nucl. Phys. Proc. Suppl.* **74**, 426 (1999).

[48] S. G. Ghosh, S. Jhingan, and D. W. Deshkar, *J. Phys.: Conf. Series* **484**, 012013 (2014).

[49] D. G. Boulware and S. Deser, *Phys. Rev. Lett.* **55**, 2656 (1985).

[50] F. R. Tangherlini, *Il Nuovo Cimento* **27**, 636 (1963).

[51] R. C. Myers and M. J. Perry, *Ann. Phys.* **172**, 304 (1986).

[52] J. T. Wheeler, *Nucl. Phys. B* **268**, 737 (1986).

[53] T. Torii and H. Maeda, *Phys. Rev. D* **71**, 124002 (2005).

[54] R. C. Myers and J. Z. Simons, *Phys. Rev. D* **38**, 2434 (1988).

[55] H. Maeda, *Phys. Rev. D* **73**, 104004 (2006).

[56] S. Jhingan and S. G. Ghosh, *Phys. Rev. D* **81**, 024010 (2010).

[57] N. K. Dadhich, A. Molina, and A. Khugaev, *Phys. Rev. D* **81**, 104026 (2010).

[58] R. Casadio and J. Ovalle, *Gen. Rel. Grav.* **46**, 1669 (2014).

[59] T. Clifton, P. Dunsby, R. Goswami, and A. M. Nzioki, *Phys. Rev. D* **87**, 063517 (2013).

[60] Z. Kang, Y. Zhan–Ying, Z. De–Cheng, and Y. Rui–Hong, *Chin. Phys. B* **21**, 020401 (2012).

[61] S. C. Davis, *Phys. Rev. D* **67**, 024030 (2003).

[62] S. Hansraj, B. Chilambwe, and S. D. Maharaj, *Eur. Phys. J. C* **27**, 277 (2015).

[63] S. D. Maharaj, B. Chilambwe, and S. Hansraj, *Phys. Rev. D* **91**, 084049 (2015).

[64] B. Chilambwe, S. Hansraj, and S. D. Maharaj, *Int. J. Mod. Phys. D* **24**, 1550051 (2015).

[65] M. Govender and S. Thirukkanesh, *Astrophys. Space Sci.* **358**, 8 (2015).

[66] S. K. Maurya, B. S. Ratanpal and M. Govender, *Ann. Phys.* **382**, 36 (2017).

[67] S. K. Maurya and M. Govender, *Eur. Phys. J. C* **77**, 420 (2017).

[68] S. K. Maurya, A. Banerjee, M. K. Jasim, J. Kumar, A. K. Prasad, and A. Pradhan, *Phys. Rev. D* **99**, 044029 (2019).

[69] K. R. Karmarkar, *Proc. Ind. Acad. Sci. A* **27**, 56 (1948).

[70] R. L. Bowers and E. P. T. Liang, *Astrophys. J.* **188**, 657 (1974).

[71] S. K. Maurya, A. Banerjee, and S. Hansraj, *Phys. Rev. D* **97**, 044022 (2018).

[72] L. Herrera, G. Le Denmat, and N. O. Santos, *Mon. Not. R. Astron. Soc.* **237**, 257 (1989).

[73] R. Chan, L. Herrera, and N. O. Santos *Mon. Not. R. Astron. Soc.* **265**, 533 (1993).

[74] L. Herrera, G. Le Denmat, and N. O. Santos, *Gen. Rel. Grav.* **44**, 1143 (2012).

[75] M. Govender, N. Mewelal, and S. Hansraj, *Eur. Phys. J. C* **79**, 24 (2019).

[76] M. Govender, A. Maharaj, D. Lortan, and D. Day, *Astrophys. Space. Sci.*, **363**, 165 (2018).

[77] C. Bogdanos, C. Charmousis, B. Goutraux, and R. Zegers, *J. High Energy Phys.* **0910**, 37 (2009).

[78] M. Wright, *Gen. Rel. Grav.* **48**, 93 (2016).

[79] P. Mafa Takisa and S. D. Maharaj, *Astrophys. Space. Sci.* **343**, 569 (2013).

[80] S. D. Maharaj, J. Sunzu, and S. Ray, *Eur. Phys. J. Plus* **129**, 3 (2014).

[81] H. L. Duorah and R. Ray, *Class. Quant. Grav.* **4**, 1691 (1987).

[82] H. A. Buchdahl, *Class. Quant. Grav.* **1**, 301 (1984).

[83] A. Molina, N. K. Dadhich, and A. Khugaev, *Gen. Rel. Grav.* **49**, 96 (2017).

[84] J. D. Walecka, *Phys. Lett.* **59**, 109 (1975).

[85] S. D. Maharaj and R. Maartens, *Gen. Rel. Grav.* **21**, 899 (1989).

[86] G. Caporaso and K. Brecher, *Phys. Rev. D* **20**, 1823 (1979).

[87] P. S. Koliogiannis and C. C. Moustakidis, *Astrophys. Space. Sci.* **364**, 52 (2019).

[88] Z. Xian-Feng and J. Huan-Yu, *Revista Mexicana de Astronomia y Astrofisica* **50**, 103 (2014).